

Boundary Element Analysis of Non-Prismatic Beams and Plates

by

Mohammad Shebdar Khan

A Thesis Presented to the

FACULTY OF THE COLLEGE OF GRADUATE STUDIES

KING FAHD UNIVERSITY OF PETROLEUM & MINERALS

DHAHRAN, SAUDI ARABIA

In Partial Fulfillment of the
Requirements for the Degree of

MASTER OF SCIENCE

In

CIVIL ENGINEERING

June, 1995

INFORMATION TO USERS

This manuscript has been reproduced from the microfilm master. UMI films the text directly from the original or copy submitted. Thus, some thesis and dissertation copies are in typewriter face, while others may be from any type of computer printer.

The quality of this reproduction is dependent upon the quality of the copy submitted. Broken or indistinct print, colored or poor quality illustrations and photographs, print bleedthrough, substandard margins, and improper alignment can adversely affect reproduction.

In the unlikely event that the author did not send UMI a complete manuscript and there are missing pages, these will be noted. Also, if unauthorized copyright material had to be removed, a note will indicate the deletion.

Oversize materials (e.g., maps, drawings, charts) are reproduced by sectioning the original, beginning at the upper left-hand corner and continuing from left to right in equal sections with small overlaps. Each original is also photographed in one exposure and is included in reduced form at the back of the book.

Photographs included in the original manuscript have been reproduced xerographically in this copy. Higher quality 6" x 9" black and white photographic prints are available for any photographs or illustrations appearing in this copy for an additional charge. Contact UMI directly to order.

UMI

**A Bell & Howell Information Company
300 North Zeeb Road, Ann Arbor, MI 48106-1346 USA
313/761-4700 800/521-0600**



BOUNDARY ELEMENT ANALYSIS OF NON-PRISMATIC BEAMS AND PLATES

BY

MOHAMMAD SHEBDER KHAN

A Thesis Presented to the
FACULTY OF THE COLLEGE OF GRADUATE STUDIES
KING FAHD UNIVERSITY OF PETROLEUM & MINERALS
DHAHRAN, SAUDI ARABIA

In Partial Fulfillment of the
Requirements for the Degree of

MASTER OF SCIENCE

In

CIVIL ENGINEERING

June 1995

UMI Number: 1377134

UMI Microform 1377134
Copyright 1996, by UMI Company. All rights reserved.

**This microform edition is protected against unauthorized
copying under Title 17, United States Code.**

UMI

**300 North Zeeb Road
Ann Arbor, MI 48103**

**KING FAHD UNIVERSITY OF PETROLEUM & MINERALS
DHAHRAN, SAUDI ARABIA**

COLLEGE OF GRADUATE STUDIES

This thesis, written by

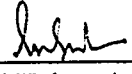
Mohammad Shebder Khan

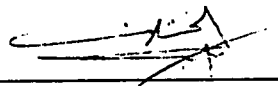
under the direction of his thesis committee and approved by all its members, has been presented to and accepted by the Dean, College of Graduate Studies, in partial fulfillment of the requirements for the degree of

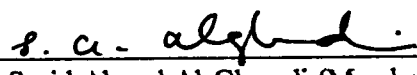
Master of Science in Civil Engineering

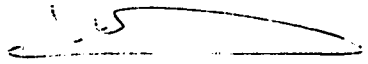
Thesis Committee :



Dr. Husain Jubran Al-Gahtani (Chairman)

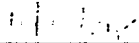

Prof. Abul Kalam Azad (Member)


Dr. Abdulrahman Khathlan (Member)

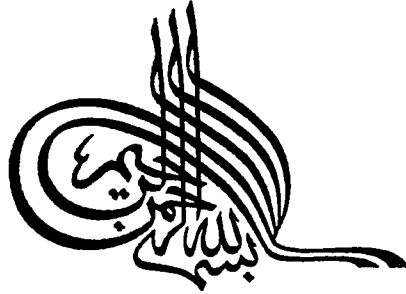

Dr. Saeid Aboud Al-Ghamdi (Member)


Dr. Alfarabi M. Sharif
Chairman, Department of Civil Engineering


Dr. Ala H. Al-Rabeh
Dean, College of Graduate Studies

Date : 





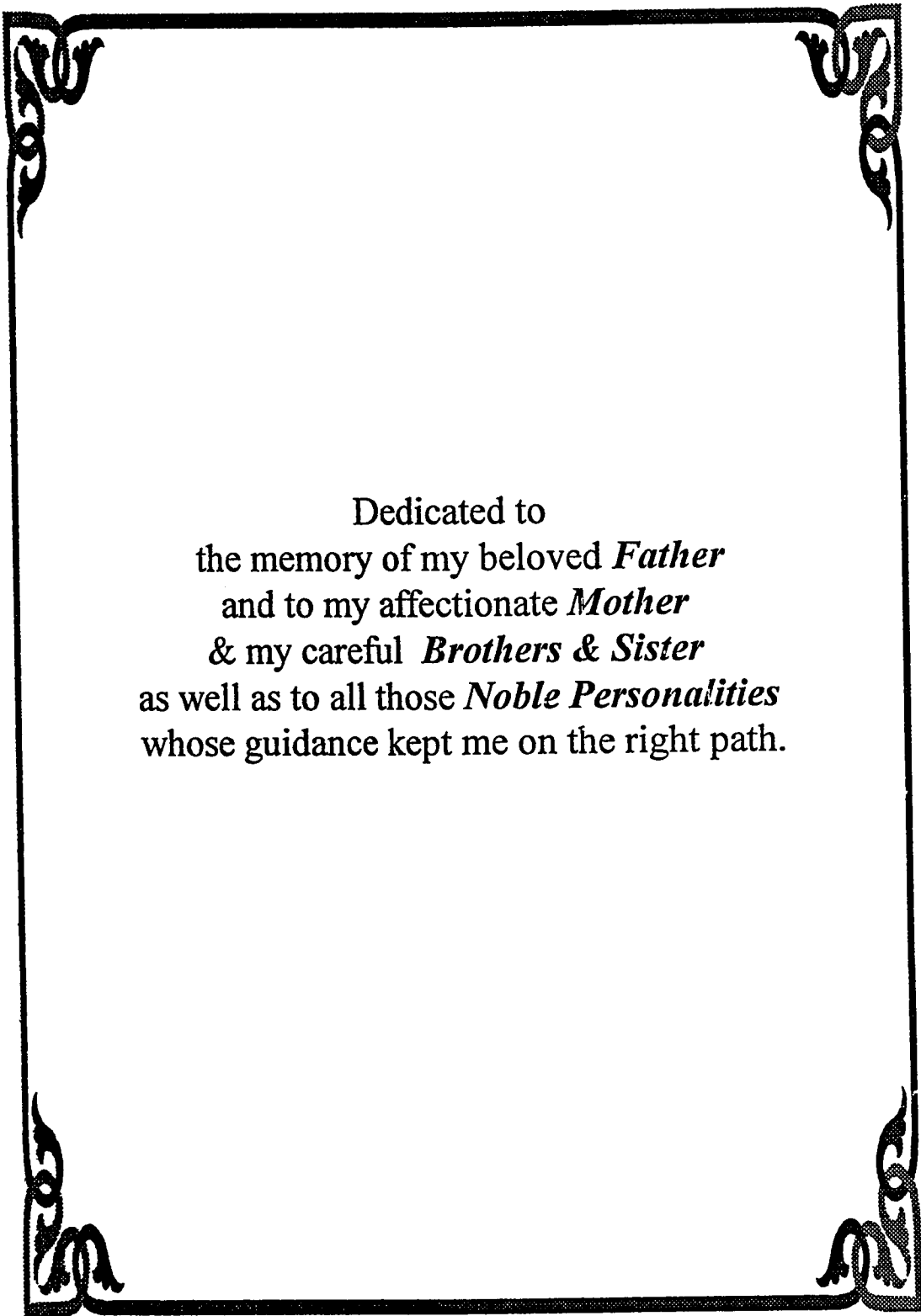
(In the name of Allah the Most Beneficent, The Most Merciful)

سبحنك لا علم لنا إلا ما علمتنا انك أنت

العليم الحكيم

Glory be to You, We have no knowledge except what you have taught us. Verily, It's You, The all Knower, The all Wise. (Holy Qura'n 2:32)

بسم الله الرحمن الرحيم



Dedicated to
the memory of my beloved *Father*
and to my affectionate *Mother*
& my careful *Brothers & Sister*
as well as to all those *Noble Personalities*
whose guidance kept me on the right path.

ACKNOWLEDGMENTS

First, I thank Allah, the Almighty, All praise is for Him for bestowing me the health, power and patience to complete this research.

I would like to acknowledge the support provided by King Fahd University of Petroleum and Minerals for the completion of this research. I would like to acknowledge with deep gratitude and sincere appreciation, the continuous assistance, constant inspiration and professional guidance given to me by the chairman of the thesis committee Dr. Husain J. Al-Gahtani and other members of the thesis committee Prof. A. K. Azad, Dr. Abdulrahman Khatlan and Dr. Saeid A. Al-Ghamdi, who have taken care and showed great interest in the work by assisting and giving invaluable suggestions.

My sincere thanks to Dr. Al-Farabi M. Sharief, Chairman, Department of Civil Engineering for all the help provided. I also thank all my teachers, friends and colleagues for their help and moral support during my stay at KFUPM. I also thank Br. Mahmood Sharief for typing most of this manuscript.

Finally, I thank all my family members for their continuous encouragement and moral support.

M. S. Khan

TABLE OF CONTENTS

LIST OF TABLES.....	xi
LIST OF FIGURES.....	xii
ABSTRACT (ENGLISH).....	xiv
ABSTRACT (ARABIC).....	xv
 CHAPTER 1	
INTRODUCTION	1
1.1 GENERAL	1
1.2 LITERATURE SURVEY	3
<i>1.2.1 Non- Prismatic Beams.....</i>	<i>3</i>
<i>1.2.2 Non- prismatic Plates.....</i>	<i>8</i>
1.3 SCOPE AND OBJECTIVES	12
 CHAPTER 2	
BOUNDARY ELEMENT METHOD	14
2.1 GENERAL	14
2.2 HISTORICAL DEVELOPMENT.....	15

2.3 BASIC CONCEPT	16
2.4 ADVANTAGES OVER OTHER NUMERICAL METHODS	18

CHAPTER 3

BEAMS	21
3.1 PRISMATIC BEAMS	21
3.2 FUNDAMENTAL SOLUTION FOR PRISMATIC BEAMS.....	29
3.3 NON - PRISMATIC BEAMS	33
3.4 DERIVATION OF FUNDAMENTAL SOLUTION	37
3.4.1 <i>Linear variation</i>	37
3.4.2 <i>Parabolic variation</i>	41
3.5 CONTINUOUS NON-PRISMATIC BEAMS	43

CHAPTER 4

PLATES	46
4.1 INTRODUCTION.....	46
4.2 GOVERNING EQUATIONS.....	48
4.3 REDUCTION OF THE PLATE BENDING DIFFERENTIAL EQUATION TO TWO POISSON'S EQUATIONS.....	52
4.4 BOUNDARY ELEMENT FORMULATION FOR POISSON'S EQUATION	53
4.4.1 <i>Boundary Integral Equations</i>	56

4.4.2 Boundary Element Equations.....	59
4.4.3 Computation of Vector $\{B\}$:	66
4.4.3.1 Distributed loads :	66
4.4.3.2 Concentrated loads :	69
4.4.4 Computation of singular integrals.....	69
4.4.4.1 Computation of H^i :	69
4.4.3.2 Computation of $G^{(2i-1)}$	70
4.4.5 Numerical Integration.....	74

CHAPTER 5

APPLICATIONS	76
5.1 BE FORMULATION FOR SIMPLY SUPPORTED PLATES	76
5.1.1 Boundary element equations.....	77
5.1.2 Computation of Stresses.....	79
5.2 OTHER BOUNDARY CONDITIONS.....	80
5.3 NUMERICAL EXAMPLES.....	81
5.3.1 Program NPBEAM.....	81
5.3.1.1 Example 1 : Symmetrical non-prismatic beam with linearly varying depth...	82
5.3.1.2 Example 2 : Symmetrical non-prismatic beam with parabolically varying depth.....	85

5.3.1.3 Example 3 : Genration of PCA Table for a non-prismatic beam with linearly varying section	88
5.3.1.4 Example 4 : Continuous bridge girder of variable depth.....	93
5.3.2 Program <i>NPLATE</i>	96
5.3.2.1 Example 1 : Simply supported square plate carrying a concentrated load at the center	96
5.3.2.2 Example 2 : Simply supported plate with linearly varying thickness carrying inearly varying load.....	99
5.3.2.3 Example 3 : Simply supported plate with linearly varying stiffness in both direction.....	106
5.3.2.4 Example 4 : Plate with linearly varying stiffness, simply supported on 3 sides and fixed on the fourth side.....	110

CHAPTER 6

SUMMARY AND CONCLUSIONS.....	115
------------------------------	-----

APPENDIX A

DESCRIPTION OF THE PROGRAMS NPBEAM & NPLATE	118
DESCRIPTION OF THE PROGRAM NPBEAM.....	120
DESCRIPTION OF THE PROGRAM NPLATE.....	123

EXAMPLE PROBLEM : CONTINUOUS NON-PRISMATIC BRIDGE GIRDER.....	125
EXAMPLE PROBLEM : SIMPLY SUPPORTED PLATE WITH VARYING RIGIDITY IN X & Y DIRECTIONS.....	127
REFERENCES	132

Vita

LIST OF TABLES

Table	Page
TABLE 4-1 LOCATION OF THE GAUSS POINTS AND THEIR WEIGHTS	75
TABLE 5-1 FIXED END MOMENTS OF THE BEAM SHOWN IN FIGURE 5-1	84
TABLE 5-2 FIXED END MOMENTS OF THE BEAM SHOWN IN FIGURE 5-2	87
TABLE 5-3 FIXED END MOMENT COEFFICIENT FOR THE BEAM SHOWN IN FIGURE 5-3A	91
TABLE 5-4 FIXED END MOMENT COEFFICIENT FOR THE BEAM SHOWN IN FIGURE 5-3 B.....	92
TABLE 5-5 BENDING MOMENTS, SLOPES AND SUPPORT REACTIONS OF THE BEAM SHOWN IN FIGURE 5-4.....	95
TABLE 5-6 VALUES OF THE DEFLECTION COEFFICIENT K OF THE PLATE SHOWN IN FIGURE 5-7	103
TABLE 5-7 VALUES OF THE COEFFICIENT K OF M_x OF THE PLATE SHOWN IN FIGURE 5-7 .	104
TABLE 5-8 VALUES OF THE COEFFICIENT K OF M_y OF THE PLATE SHOWN IN FIGURE 5-7 .	105
TABLE 5-9 DEFLECTION AND M_x ALONG THE CENTER LINE $x = a/2$ OF THE PLATE	109
TABLE 5-10 MOMENT M_x ALONG THE FIXED EDGE OF THE PLATE SHOWN IN FIGURE 5-1	112
TABLE 5-11 MOMENT M_x ALONG THE FIXED EDGE OF THE PLATE SHOWN IN FIGURE 5-17.....	114

LIST OF FIGURES

Figure	Page
FIGURE 3-1 BEAM WITH UNIFORM SECTION	22
FIGURE 3-2 POSITIVE SENSE FOR FORCES AND DISPLACEMENTS	24
FIGURE 3-3 THE FUNCTION, V^*	30
FIGURE 3-4 BEAM WITH VARYING RIGIDITY	35
FIGURE 3-5 LINEAR VARIATION.....	38
FIGURE 3-6 PARABOLIC VARIATION.....	40
FIGURE 3-7 CONTINUOUS BEAM WITH VARYING FLEXURAL RIGIDITY	44
FIGURE 4-1 COORDINATE SYSTEM.....	49
FIGURE 4-2 PLATE ELEMENT	50
FIGURE 4-3 NOTATION FOR POISSON'S EQUATION.....	54
FIGURE 4-4 NOTATION FOR SOURCE AND FIELD POINTS.....	58
FIGURE 4-5 BOUNDARY DISCRETIZATION.....	61
FIGURE 4-6 LINEAR ELEMENT	64
FIGURE 4-7 BOUNDARY ELEMENTS AND INTERNAL CELLS FOR NUMERICAL INTEGRATION.....	65
FIGURE 4-8 FOUR - NODED RECTANGULAR ELEMENT	68
FIGURE 4-9 THREE - NODED TRIANGULAR ELEMENT.....	68
FIGURE 4-10 COMPUTATION OF SINGULAR ELEMENTS $G^{(2l-1)}$	71

FIGURE 5-1 BEAM WITH LINEARLY VARYING THICKNESS CARRYING UDL.....	83
FIGURE 5-2 BEAM WITH PARABOLIC VARYING THICKNESS CARRYING UDL.....	86
FIGURE 5-3 UNSYMMETRICAL HAUNCH BEAM WITH PARABOLICALLY VARYING DEPTH.	89
FIGURE 5-4 CONTINUOUS BRIDGE GIRDER WITH PARABOLICALLY VARYING DEPTH.....	94
FIGURE 5-5 SIMPLY SUPPORTED SQUARE PLATE OF UNIFORM THICKNESS CARRYING A CENTRAL CONCENTRATED LOAD	97
FIGURE 5-6 PROFILE OF M_x ALONG THE CENTER LINE OF THE PLATE PARALLEL TO X-AXIS	98
FIGURE 5-7 SIMPLY SUPPORTED PLATE WITH LINEARLY VARYING THICKNESS.....	100
FIGURE 5-8 BOUNDARY DISCRETIZATION OF THE PLATE SHOWN IN FIGURE 5-7	101
FIGURE 5-9 FINITE ELEMENT MESH FOR THE HALF OF THE PLATE SHOWN IN FIGURE 5-7..	102
FIGURE 5-10 SIMPLY SUPPORTED PLATE WITH VARYING RIGIDITY IN BOTH X AND Y DIRECTIONS.	107
FIGURE 5-11 FINITE ELEMENT MESH FOR THE PLATE SHOWN IN FIGURE 5-10.	108
FIGURE 5-12 PLATE WITH LINEARLY VARYING STIFFNESS, THREE SIDES SIMPLY SUPPORTED, THE FOURTH SIDE FIXED	111
FIGURE 5-13 SQUARE PLATE OF SIDE A WITH UNIFORM STIFFNESS THREE SIDES SIMPLY SUPPORTED, THE FOURTH SIDE FIXED	113
FIGURE A-1 FLOW CHART OF THE PROGRAM NPBEAM.....	119
FIGURE A-2 FLOW CHART OF THE PROGRAM NPLATE	122

ABSTRACT

Name : Mohammad Shebder Khan

**Title : Boundary Element Analysis of Non-Prismatic
Beams and Plates**

Major Field : Civil Engineering (Structures)

Date of Degree : June 1995

Boundary element solutions for the bending of non-prismatic beams and plates are presented. The boundary integral formulation is developed for the analysis of non-prismatic beams. The required fundamental solutions for non-prismatic beams of linear and parabolic profiles are derived and exact relations are obtained among the variables over the nodes (beam supports). The method is then extended for the analysis of continuous beams with varying depth. The problem of a plate with linearly varying rigidity is solved by splitting the equation governing the transverse deflection of the plate into two Poisson's equations, for which, fundamental solutions are available. Finally, the proposed formulations for both beams and plates are tested through several numerical examples.

Master of Science Degree

King Fahd University of Petroleum and Minerals

Dhahran, Saudi Arabia

June 1995

خلاصة الرسالة

- اسم الطالب الكامل : محمد شبير خان
- عنوان الدراسة : تحليل العتبات والصفائح الغير منتظمة باستخدام طريقة التفاضل المحيط
- التخصص : هندسة مدنية (انشاءات)
- تاريخ الشهادة : محرم 1416 هـ

تقدم هذه الدراسة حلاً لانتشاء العتبات والصفائح ذوات العمق المتغير. وتستند هذه الدراسة الى طريقة التكامل المحيط حيث يتم تحقيق المعادلة التفاضلية التي تحكم انحراف العتبه ثم الحصول على علاقات دقيقة بين المتغيرات عند مواقع الدعامات. كما تم تطوير الطريقه لتشمل العتبات المتواصله. أما بالنسبة للصفائح ذوات العمق المتغير خطياً فقد تم استبدال المعادلة التي تحكم انحراف الصفيحة بمعادلتين من نوع "بويسون". وقد تم اختبار الحل المقترح بواسطة أمثلة عديدة تثبت تطابق النتائج الحالية مع نتائج الحلول التحليلية والعديدية.

درجة الماجستير في العلوم

جامعة الملك فهد للبترول والمعادن

الظهران، المملكة العربية السعودية

محرم 1416 هـ

CHAPTER 1

INTRODUCTION

1.1 General

Non-prismatic members are commonly used in many engineering structures, such as highway bridges, buildings, space and air-craft structures, as well as in many mechanical components and machines. They have some structural advantages over the prismatic members. The major advantages are :

1. The sharp reentrant corner that otherwise occurs at the junction of a beam with a column can be avoided.
2. The support moment capacity can be increased which results in considerable reduction of the span moment. Consequently, mid span depth of the beam or plate can be reduced.
3. Better distribution of the internal stresses can be achieved which reduces and may even cancel the shear stresses.

4. Over long spans, savings in material may be considerable both by virtue of the better distribution of stresses and reduction of dead load.
5. Since the cross-section of the non-uniform beam or plate will take a shape corresponding to the stress distribution under any loading condition, variable section beams and plates can be designed to have improved dynamic performance.

Since the members of variable cross section are involved in many important structures, it is necessary to analyze this kind of members with a greater precision. In the case of beams and plates of variable depth, the governing differential equation is found to have variable coefficients and this fact increases the difficulty of the solution. Analytical methods of solutions for the analysis of non-prismatic beams are available [1,2], but they involve lengthy calculations. To simplify the method, tables and charts for beam constants are prepared and published by Portland Cement Association (PCA)[5]. However, these tables have the following limitations:

- a) They can give the constants only for straight and parabolic haunches
- b) They are applicable for two types of loading, i.e. concentrated and uniformly distributed loading. Partial loading cases are not considered.
- c) They cannot be used directly for multi-span continuous beam.

Prior to the advent of the computer, plates of variable thickness could be analyzed for certain types of thickness profiles. Analytical solutions for the bending of non-prismatic plates are available for only limited number of cases involving , simple plate geometries, linear variation of flexural rigidity and simple types of loading [30, 31 and 32].

1.2 Literature Survey

1.2.1 Non- Prismatic Beams

A considerable amount of research has been done in analyzing non-prismatic beams and girders. The analysis of non-prismatic beams is covered in many classical textbooks on structural analysis [1, 2, 3]. The most popular analytical technique for analyzing non-prismatic beams is the slope-deflection method. The procedure involves lengthy calculation of many constants, to compute the angular coefficients. The effected angles of rotation of the ends of the beam are calculated using these angular coefficients. Finally, using these angles of rotation end moments are calculated. In the case of beams having linear or parabolic haunches (both symmetrical and Unsymmetrical) the integrations have to be made rigorously. However the calculations are tedious and time consuming. To simplify the analysis, special tables [1] have been prepared giving the

numerical values of the angular coefficients for calculating effected angles of rotation for parabolic and linear haunches.

Another alternative procedure is to use moment distribution method [1] if appropriate values for the stiffness, carry over factors and fixed end moments are available. In this method also, in order to obtain fixed end moments, many integration of complex form have to be carried out, which is very difficult to integrate using the exact integration. Therefore numerical integration has to be applied. The procedure is to divide beam into a number of segments and calculate the numerical values of the required quantities for each segment and summing up these individual segment constants to give the constant thickness of the whole beam. In 1958, Cross presented stiffness and carry over factors of non-prismatic members to be used in the moment distribution method [4].

More extensive tables and charts are given in the booklet published by Portland Cement Association (PCA) for the computation of beams constants necessary for the analysis of structures having non-prismatic members[5].

In 1958, the concept of the method of the equivalent systems was initiated and developed by Fertis [6,7]. This method is further developed by Fertis and Keene [8] and Fertis and Rajesh Taneja [9] . The method of equivalent systems is similar to the moment area method in some way. This method is based on the theorem of the equivalent systems by which, a member of variable stiffness $EI(x)$, can be replaced by any number of equivalent systems of uniform stiffness EI , where the deflection curve of each one of the equivalent system is everywhere identical to the deflection curve of the original variable

stiffness member. Using this principle, in this method, the original member of variable stiffness $EI(x)$ is replaced by a uniform stiffness EI whose elastic line is identical to that of the original variable stiffness member. The mathematical derivation of the equivalent system of constant stiffness EI that replaces the original system of variable stiffness $EI(x)$ begins by considering the second order differential equation for the elastic curve of the member. By integrating this differential equation, the identical elastic line for the equivalent system of constant stiffness is obtained. Moment diagram for this equivalent system is drawn. The expressions for the shear force and the applied load for the equivalent system are derived and the problem becomes a problem with constant stiffness. Although this method simplifies the mathematical complexities of the problem, it involves the approximations of using the equivalent system of constant stiffness.

In 1963, Boley [10] obtained the stresses and deflection of thin rectangular beams of variable depth in the form of series. In 1977, Just [11] developed exact stiffness matrices for linearly tapered beams of rectangular, box and I-section. In 1981, Rutledge and Beskos [12] proposed a method of obtaining stiffness coefficients for a beam with constant width and linearly varying depth.

Resende, Doyle and Mumuni [13,14] have independently developed finite element models for non-prismatic beams with a 3-node straight line element with six degrees of freedom at each node. Kosko [15] applied the method of substituting two or three prismatic elements for a tapered member to tapered frame members whose cross-sectional size vary in a smooth fashion, while the centroids all lie on a straight line. The

flexibility parameters which represent the elastic behavior of such members are calculated by simple quadrature. In 1983, Karabalis and Beskos [16] presented a numerical method based on finite element method for the static, dynamic and stability analysis of linear elastic plane structures consisting of beams with constant width and variable depth.

In 1985, Banerjee and Williams [17] obtained explicit expressions for the dynamic stiffness for axial, torsional and flexural vibrations of a tapered beam using Bernoulli-Euler theory and Bessel functions. Arvind [18] obtained stiffness and consistent mass matrices for linearly tapered beam element in explicit form using exact expressions for the displacement functions.

In 1986, Hota and Spyrakos [19] presented a Fourier-cum-polynomial series solution for the boundary value problems with variable properties. Miyamoto, Iwasaki and Deto [20] presented an iterative boundary element approach to analyze continuous beams with varying cross section. The method uses the fundamental solution of an infinite beam with a uniform section. The remaining part of the equation is treated as fictitious body force that can be calculated by discretizing the beam into number of elements and this can be updated in each iteration. Since the domain is discretized, obviously such procedure shares the same disadvantages of the domain discretization methods as larger number of algebraic equations are to be solved. In 1987, Karamanlidis and Jasti [21] developed a novel finite element methodology for analyzing the frame structures composed of non-prismatic members. The formulation was based on a modified version of the variational theorem of Hellinger and Reissner.

Raymond and Wang [22] reported a numerical technique for the calculation of the stiffness matrix of non-prismatic members. The procedure is to divide the member into number of elements, choose four or five sections along the member and calculate cross sectional area and moment of inertia at each section. Then cross sectional areas and moments of inertia of all the sections are generated using Gregory-Newton interpolation method. Finally, stiffness of the entire member is calculated by adding the stiffness of all elements.

In 1990, Lee *et al.* [23] developed a solution of the static deflection of a non-uniform Bernoulli-Euler beam in closed integral form with the assumption that the bending rigidity of a non-uniform beam is second-order differentiable with respect to the axial coordinate variable. In 1991, Naseruddin El-Mezaini et al. [24] investigated the behavior of beams of variable depth based on finite element method using the isoparametric plane stress finite elements in the modeling.

In 1992, Lee and Lin [25] presented the exact solution for the free vibration of a symmetric non-uniform Timoshenko beam with tip mass at one end elastically restrained at the other end of the beam. Kathnelson [26] obtained an asymptotic frequency equation for beams elastically restrained at the edges. In 1993, Aristizabal-Ochoa [27] presented an algorithm that evaluates the static, stability and vibration response of non-prismatic beams and columns. Recently, in 1994, Lee [28], using the Green's function, obtained the static deflection of general elastically end restrained non-uniform beams resting on a non-linear elastic foundation subjected to axial and transverse forces,

governed by a non-linear fourth order non-homogeneous ordinary differential equation with variable coefficients.

1.2.2 Non- prismatic Plates

The solution of rectangular plates with variable thickness has been of great concern to many investigators during the past decades. The old literature shows that the solution of the plate problem via the classical route is, in general, limited to relatively simple plate geometry, loading and boundary conditions. [29, 30, 31, 32]. Conway [33] also obtained solutions for symmetrically loaded circular plates with a wide variety of radial thickness variations. In 1962, Mansfield [34] expressed the governing differential equations of a plate with variable thickness in terms of the Laplacian operator, and then obtained solutions for a rectangular plate whose thickness varies exponentially along the length. In addition he obtained solutions for a circular plate whose thickness varies as a power of the radius. Then the method of equivalent systems was used to solve static, dynamics and vibration problems associated with plates of variable stiffness by Fertis and Kozama [35] and Fertis and Cunningham [36]. The method was further extended in 1988 by Fertis and Mijatov [37] for the solution of various types of beam-like structures with members of variable stiffness and for the solution of rectangular plates of variable thickness. In this method, in order to determine the deflection of the rectangular

plates with variable thickness in one dimension, the original variable thickness plate is transformed into an equivalent system of uniform plates subjected to new loading.

In 1965, Appl and Byers [38] obtained upper and lower bounds for fundamental frequency of a simply supported rectangular plate with linearly varying thickness. In 1968, Cheung Y.K. [39] used the finite strip method in the analysis of elastic slabs [40] and elastic plates with two opposite simply supported ends. In this method, the plate is discretized into a small number of strips and potential energy of each strip is calculated. Final equations are obtained by adding the contribution from each strip. Then the principle of minimum potential energy is applied. After the boundary conditions have been introduced, equations can be solved to yield the displacement. In 1970, Lord and Yousef [41] developed a finite element for the analysis of circular plates by considering the plate to be composed of concentric rings of uniform thickness.

In 1978, Mukhopadhyay [42] presented a semi-analytical solution for rectangular plate bending using a method similar to finite strip method. In this method, a displacement function satisfying the boundary conditions along two opposite edges is assumed. This displacement function is then substituted in the differential equation of the plate by certain transformation to obtain the governing differential equation with constant coefficients. Then finite difference technique is used for the solution.

In 1988 Uko and Cusens [43] presented a spline finite strip method for analyzing variable thickness solid slab bridges. This method utilizes cubic B-splines as displacement functions and numerical integration to take account of variable thickness. In 1989,

Fariborz and Pourbohloul [44] applied the extended Kantorovich method to the bending analysis of the plate variable thickness. The extended Kantorovich method is an iterative procedure and was originally devised by Kerr [45]. This technique has an advantage over other weighted residual methods in the sense that the final result is independent of the initial guess for the solution. But as far as the computation is concerned, it is more involved because the solution of a system of differential equations rather than algebraic equations is required in every iteration. This technique allows the analysis of plates with constant as well as unidirectional variable thickness. Azad *et al.* [46] proposed a method for the bending analysis of a radially tapered simply supported circular plate by using a Levy-type semi-inverse solution in conjunction with finite difference method. In 1990, Singh and Dey [47] presented the finite difference energy method for buckling of the plates with varying thickness. This method is an integral based finite difference approach using the principle of minimum potential energy.

Although there is considerable application of the boundary element method to the analysis of plates with constant thickness [48, 49, 50, 51, 52, 53, 54], its application to the case of plates with variable thickness is limited. This is obviously because the fundamental solution for the governing equation cannot be established, atleast, in a form that could be useful to develop a pure boundary element method solution. In 1988, Ohga *et al.* [55, 56] presented boundary element-transfer matrix method for bending analysis of plates with variable thickness. In this method, a transfer matrix is obtained from the system of equations derived by the procedure based on boundary element method. A

plate with variable thickness is considered as a combination of number of separate homogeneous sub-regions each having different plate thickness.

In 1991, Sapountzakis and Katsikadelis [57] developed an iterative mixed boundary element method for the analysis of plates of variable thickness. This method uses the fundamental solution of the plate with uniform thickness and the remaining part of the equation is treated as a fictitious body force which can be calculated by discretizing the plate domain and this can be updated in each iteration. Since this method also discretizes the domain, it also shares the same disadvantages of the domain discretization solutions. Jianqiao [58] presented an integral equation formulation for the finite deflection analysis of axi-symmetric circular plates with variable thickness based on the Karman equation and by means of Green identity.

In 1992, Cheung and Wenchang [59] came up with a new idea of combining the finite strip method with finite element and boundary element methods. Anant *et al.* [60] presented a differential quadrature method for computing the fundamental frequency of a thin rectangular plate with variable thickness. In this method, a partial derivative of a function with respect to a space variable at a discrete point is approximated as a weighted linear sum of the function values at all the discrete points in the region of that variable. Recently in 1993, Shahab [61] investigated the transverse vibration of variable thickness discs by using the Ritz method and the finite element technique. He has used a thin, two dimensional annular sector element with 12 degrees of freedom for the disc.

1.3 Scope and Objectives

The available literature indicates that there are three main approaches for the analysis of non-prismatic members :

1. Analytical methods such as slope deflection, Fourier series method etc.
2. Semi-analytical methods (e.g. method of equivalent systems)
3. Numerical methods such as finite difference and finite element methods

In most of the above approaches, the analysis is either tedious or time consuming. The broad objective of this study is to present an alternative boundary element method (BEM) for the bending analysis of non-prismatic beams and plates. The proposed method has the advantages of being simple, economical and accurate. The specific objectives of this study are:

- I. to develop an "exact" method of analysis of continuous non-prismatic beams using BEM. The stiffness of the beam can be assumed any general variation, provided that this variation is continuous and differentiable. Procedure, however, will be tested for linear and parabolic variations .
- II. to develop a BEM solution for plates with linear varying rigidity and general loading conditions.

The present study consists of two parts. In the first part, a boundary integral formulation is developed for the bending analysis of non-prismatic beams. Since it involves no approximations, it gives exact results. The method is then extended for the analysis of continuous beams with varying depth. In the second part, the problem of a plate with linearly varying rigidity is solved by splitting the biharmonic equation for transverse deflection of the plate into two Poisson's equations [34] . This method greatly simplifies the computational work required for the solution of the problem.

CHAPTER 2

BOUNDARY ELEMENT METHOD

2.1 General

The boundary element method (BEM) is a numerical technique for solving a wide range of boundary value problems in continuum mechanics. BEM offers important advantages over 'domain' type methods such as the finite difference (FDM) and finite element method (FEM). The most important feature of the method is that it only requires the discretization of the surface rather than the volume. This results in much smaller system of equations and considerable reduction in the input data required to run a problem. In addition, the accuracy of the solution is enhanced since the only source of approximation errors comes from the boundary modelling.

2.2 Historical Development

Integral equation techniques were until recently considered to be a different type of analytical method in the solution of boundary value problems, somewhat unrelated to approximate methods. They became popular in Western Europe through the work of a series of Russian authors, such as Mukhelishvili, Mikhlin but they were not very popular among engineers. A predecessor of some of this work was Kellogg, who applied integral equations for the solution of Laplace type problems. Integral equation techniques were mainly used in fluid mechanics and general potential problems and known as the 'source' method which is an 'indirect' method of analysis, i.e. the unknowns are not the physical variables of the problem. However, due to difficulties in dealing with singular or weakly singular Kernels that arise in integral equations and also due to the lack of rigorous proofs of existence of solutions, the use of such technique was restricted to a limited number of problems. Furthermore, the technique of using integral equations as a tool for the solution of boundary value problems was not well known among engineers at that time and its potential for obtaining numerical solutions was not exploited until the advent of computers. In the sixties, as a consequence of the widespread use of the computers to solve problems of mathematical physics, some new and improved boundary integral formulations for potential theory and elasticity and also the corresponding numerical solutions were published. This fact can be considered as the beginning of the boundary

element method. Work on this method continued throughout the 1960 and 1970s in the pioneering work of Jaswon, Symm, Massonet and many others.

Since the early 1960s, a small research group started working at Southampton University on the application of integral equations to solve stress analysis problems. This work was continued through a series of theses dealing mainly with elastostatics problems. At the same time developments in finite elements had already started to find their way into formulation of boundary integral equations, specially in the idea of using general curved beam elements. Finally, in 1978 it was shown by Brebbia that direct boundary element method can also be formulated through weighted residual statements. The boundary element method was, therefore, shown to have a common basis with other numerical techniques. The work by the Southampton university group culminated in the first book in 1978 with the title "Boundary Elements" [62].

2.3 Basic concept :

The boundary element technique consists of transforming the governing partial differential equation, which involve the behavior of the unknown solution inside and on the surface of the domain, into an integral equation relating only boundary values. As a direct consequence, the dimension of problem is reduced by one. The boundary of the

domain is discretized into elements, and polynomial functions equivalent to those used in finite elements are then necessary to interpolate the values of approximated solution between nodal points. As the unknowns of the system are related only to the boundary, the domain does not need to be discretized. After performing the boundary integrals which are done mainly by some numerical process, smaller systems of equations are obtained compared to those achieved by domain type techniques. Then, other quantities at specified points inside the body or on the boundary can be evaluated after solving the system of equations. The method generally consists of the following steps :

1. Multiply the governing differential equation (with all non-zero terms on one side of the equality) with the 'fundamental solution' (to be defined later) and integrate over the domain a sufficient number of times, to get the so called 'domain integral equations'.
2. The boundary is discretized into a series of elements over which the primary variables and their normal derivatives are assumed to vary according to interpolation functions. The geometry of these elements can be modelled using straight lines, parabolas etc.;
3. The boundary integral equations are obtained by applying the domain integral equations at a number of particular nodes within each boundary element.

4. The integrals over each element are carried out by using, in general, a numerical quadrature scheme;
5. By imposing the prescribed boundary conditions of the problem, a system of linear algebraic equations is obtained. The solution of this system of equations, produces the boundary unknowns.
6. By using the boundary data obtained in the previous step, all the domain information in terms of primary variables and their derivatives can be obtained using the domain integral equations.

The above steps will be followed in obtaining the boundary element equations for beams and plates in chapter 3 and chapter 4 respectively. It should be noted that for the case of beams, the boundary elements are reduced to 'nodes' at the supports and therefore, step 4 is omitted from the procedure.

2.4 Advantages over other Numerical Methods

In recent years the boundary element techniques have been increasingly gaining popularity among the numerical methods, due to the following advantages :

Discretization : The most important feature of boundary elements is that it only requires discretization of the surface (boundary) rather than the volume, which always reduce the

problem by one dimension, e.g. if we are discretizing a two dimensional body, we need only line elements (one-dimension). Hence boundary element codes are easier to use with existing solid modellers and mesh generators. This advantage is particularly important for designing as the process usually involves a series of modifications which are more difficult to carry out using finite elements. Meshes can easily be generated and design changes do not require a complete remeshing.

Reduced set of equations : The boundary element method generally offers the advantage over 'domain' type methods, of working with smaller system of equations as a result of the discretization process.

Numerical accuracy : Since approximation is made only on the boundary, the boundary element method, in general, does not have any interpolation error inside the domain.

Stress concentration problems : Unlike the displacement-based FEM procedure of obtaining the stresses indirectly from the domain nodal displacements, the BEM offers a direct way of stress computation via its integral equations. Such advantage is more marked in stress concentration and high gradients problems.

Despite the above important advantages, the method has some limitations. The method requires a 'fundamental solution' of the given differential equation. This is a difficult task which shows up in the case of non-linear or non-homogeneous problems where obtaining the fundamental solution is almost impossible. Such a difficulty can,

however, be overcome by considering the part of differential equation, for which we have a fundamental solution and treating the remaining part as a fictitious body force to be computed iteratively [Ref. 20 and 60].

CHAPTER 3

BEAMS

3.1 Prismatic Beams

Consider a uniform Bernoulli-Euler beam element 1-2 of length L and subjected to lateral loading as shown in Figure 3-1. The governing differential equation for transverse deflection of the beam is

$$EI \frac{d^4 w}{dx^4} + f(x) = 0 \quad 0 < x < L \quad (3.1)$$

where w = transverse deflection of the beam;

EI = flexural rigidity;

$f(x)$ = distributed load.

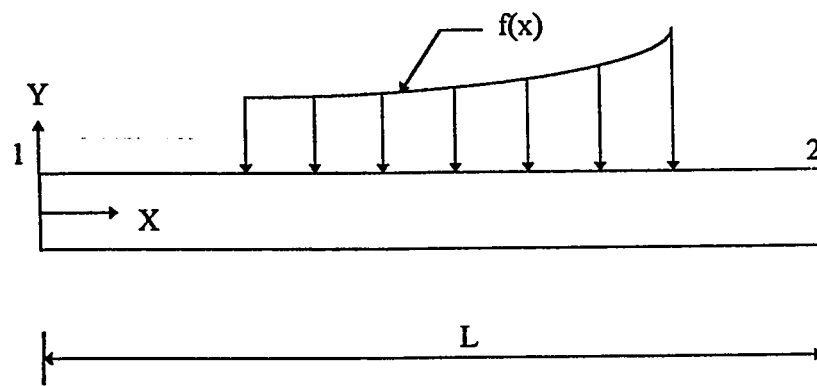


Figure 3-1 Beam with uniform section

The boundary element method begins by considering the domain of the problem in its entirety without subdivisions. All the discretization is performed on the boundary. In this case, there are only two "nodes" involved, regardless of the complexity of the problem. The two nodes are placed, respectively at $x=0$ and at $x = L$ as shown in Figure 3-1. The slope $\theta(x)$, moment $M(x)$ and shear $V(x)$ are related to the primary variable, deflection $w(x)$ by :

$$\theta(x) = \frac{dw}{dx}; \quad (3.2)$$

$$M(x) = EI \frac{d^2w}{dx^2}; \quad (3.3)$$

$$V(x) = EI \frac{d^3w}{dx^3} \quad (3.4)$$

The above variables are shown in Figure in their positive sense. In order to derive the boundary integral equations, multiply the left hand side of equation (3.1) by a weighting function w^* and integrate over the domain of the beam, i.e.

$$\int_0^L \left(EI \frac{d^4w}{dx^4} + f(x) \right) w^* dx = 0 \quad (3.5)$$

Integrating eqn. (3.5) once by parts, we get

$$\int_0^L \left(-EI \frac{d^3w}{dx^3} \frac{dw^*}{dx} + f(x) w^* \right) dx + [V w^*]_{x=0}^{x=L} = 0 \quad (3.5a)$$

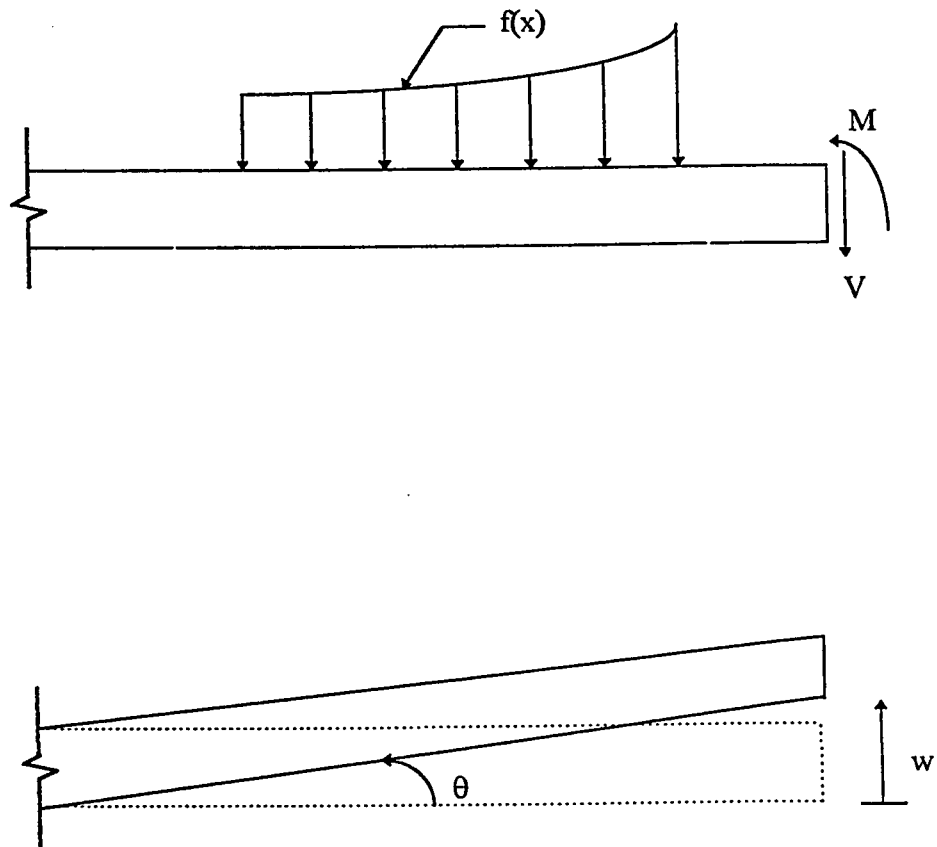


Figure 3-2 Positive sense for forces and displacements

And two more integrations give

$$\int_0^L \left(EI \frac{d^2 w}{dx^2} \frac{d^2 w^*}{dx^2} + f(x) w^* \right) dx + \left[V w^* - M \frac{dw^*}{dx} \right]_{x=0}^{x=L} = 0 \quad (3.5b)$$

$$\int_0^L \left(-EI \frac{dw}{dx} \frac{d^3 w^*}{dx^3} + f(x) w^* \right) dx + \left[V w^* - M \frac{dw^*}{dx} + \theta EI \frac{d^2 w^*}{dx^2} \right]_{x=0}^{x=L} = 0 \quad (3.5c)$$

The fourth integration gives

$$\int_0^L \left(w EI \frac{d^4 w^*}{dx^4} + f(x) w^* \right) dx + \left[V w^* - M \frac{dw^*}{dx} + \theta EI \frac{d^2 w^*}{dx^2} - w EI \frac{d^3 w^*}{dx^3} \right]_{x=0}^{x=L} = 0 \quad (3.5d)$$

If we define

$$\theta^* = \frac{dw^*}{dx},$$

$$M^* = EI \frac{d^2 w^*}{dx^2} \text{ and}$$

$$V^* = EI \frac{d^3 w^*}{dx^3}, \text{ equation (3.5d) becomes}$$

$$\int_0^L w \left(EI \frac{d^4 w^*}{dx^4} \right) dx + \int_0^L f(x) w^* dx - \left[-Vw^* + M\theta^* - \theta M^* + wV^* \right]_{x=0}^{x=L} = 0 \quad (3.5e)$$

As a particular choice for the auxiliary function $w^*(x, \xi)$ we introduce the idea of *fundamental solution*. Let us choose $w^*(x, \xi)$ such that it satisfies the following differential equation

$$EI \frac{d^4 w^*}{dx^4} + \delta(x - \xi) = 0 \quad (3.6)$$

where δ is Dirac delta function, which has the following properties

$$\delta(x - \xi) = \begin{cases} 0 & x \neq \xi \\ \infty & x = \xi \end{cases} \quad (3.6a)$$

$$\int_0^L g(x) \delta(x - \xi) dx = g(\xi) \quad (3.6b)$$

Then equation (3.5e) becomes

$$w(\xi) = \left[V w^* - M \theta^* + \theta M^* - w V^* \right]_{x=0}^{x=L} + \int_0^L f(x) w^* dx \quad (3.7)$$

Furthermore, equation (3.7) may be differentiated with respect to ξ to produce representation for slope, moment and shear at any point ξ on the beam.

$$\theta(\xi) = \left[V \frac{dw^*}{d\xi} - M \frac{d\theta^*}{d\xi} + \theta \frac{dM^*}{d\xi} - w \frac{dV^*}{d\xi} \right]_{x=0}^{x=L} + \int_0^L f(x) \frac{dw^*}{d\xi} dx \quad (3.8)$$

The boundary element model consists of the entire beam demarked by nodes at its two ends. In order to have a well-posed problem, it is necessary to have a certain number of boundary conditions specified. The boundary conditions are of two types. Specified values of the displacements (w) and slope (θ) are known as "forced" or "essential" boundary conditions. Specified values of the shearing forces (V) and the bending moment (M) are known as "natural" boundary conditions. A well-posed problem specifies either a shearing force or displacement at a boundary point; and either a bending moment or slope at the point. It is important to understand that both a shearing force and a displacement cannot be prescribed at the same point; neither can both a bending moment and a slope specified. However, one or the other of each of these boundary conditions must be specified for a unique solution to exist. Note that there are always four known boundary conditions and four unknown boundary conditions in a well-posed problem.

The boundary element method proceeds from this point by first solving for the unknown boundary data (that has not been specified) in terms of those which have been specified. To successfully implement this procedure, four simultaneous equations in the four unknown quantities must be obtained. These equations can be obtained in the

following matrix form by applying equation(3.7) and equation (3.8) at the boundary points i.e. $\xi \rightarrow 0$ and $\xi \rightarrow L$ corresponding to subscripts 1 and 2 such that

$$\begin{bmatrix} 1 - V^*(0,0) & M^*(0,0) & V^*(L,0) & -M^*(L,0) \\ -V^*(0,0) & 1 + M^*(0,0) & V^*(L,0) & -M^*(L,0) \\ -V^*(0,L) & M^*(0,L) & 1 + V^*(L,L) & -M^*(L,L) \\ -V^*(0,L) & M^*(0,L) & V^*(L,L) & 1 - M^*(L,L) \end{bmatrix} \begin{Bmatrix} w_1 \\ \theta_1 \\ w_2 \\ \theta_2 \end{Bmatrix} =$$

$$\begin{bmatrix} -w^*(0,0) & \theta^*(0,0) & w^*(L,0) & -\theta^*(L,0) \\ -w^*(0,0) & \theta^*(0,0) & w^*(L,0) & -\theta^*(L,0) \\ -w^*(0,L) & \theta^*(0,L) & w^*(L,L) & -\theta^*(L,L) \\ -w^*(0,L) & \theta^*(0,L) & w^*(L,L) & -\theta^*(L,L) \end{bmatrix} \begin{Bmatrix} V_1 \\ M_1 \\ V_2 \\ M_2 \end{Bmatrix} + \begin{Bmatrix} \int_0^L f(x) w^*(x,0) dx \\ \int_0^L f(x) w^{*'}(x,0) dx \\ \int_0^L f(x) w^*(x,L) dx \\ \int_0^L f(x) w^{*'}(x,L) dx \end{Bmatrix} \quad (3.9)$$

where ' implies the differentiation with respect to ξ i.e. $\frac{\partial}{\partial \xi}$,

w_1 = deflection at node 1 and w_2 = deflection at node 2

θ_1 = rotation at node 1 and θ_2 = rotation at node 2

M_1 = moment at node 1 and M_2 = moment at node 2

V_1 = shear at node 1 and V_2 = shear at node 2.

Thus, once the fundamental solution is known, equation (3.7) furnishes a complete representation of the solution of the original boundary value problem in terms of the values of deflection, slope, moment, shear at the beam ends and the given load function $f(x)$.

3.2 Fundamental Solution for Prismatic Beam

The fundamental solution, w^* of the equation (3.7), if EI is taken to be constant i.e. prismatic beam, can be derived as follows :

Consider the differential equation (3.6)

$$EI \frac{d^4 w^*}{dx^4} + \delta(x - \xi) = 0$$

The integration of the above equation with respect to x , yields

$$EI \frac{d^3 w^*}{dx^3} = V^* = \begin{cases} C_1 & x < \xi \\ -(1 - C_1) & x > \xi \end{cases} \quad \text{where } 0 < C_1 < 1$$

The function V^* is plotted as shown in Figure 3-3 and it is clear from the figure that the slope of V^* is zero every where except at $x = \xi$ where it becomes $-\infty$ as it should be according to equation (3.6).

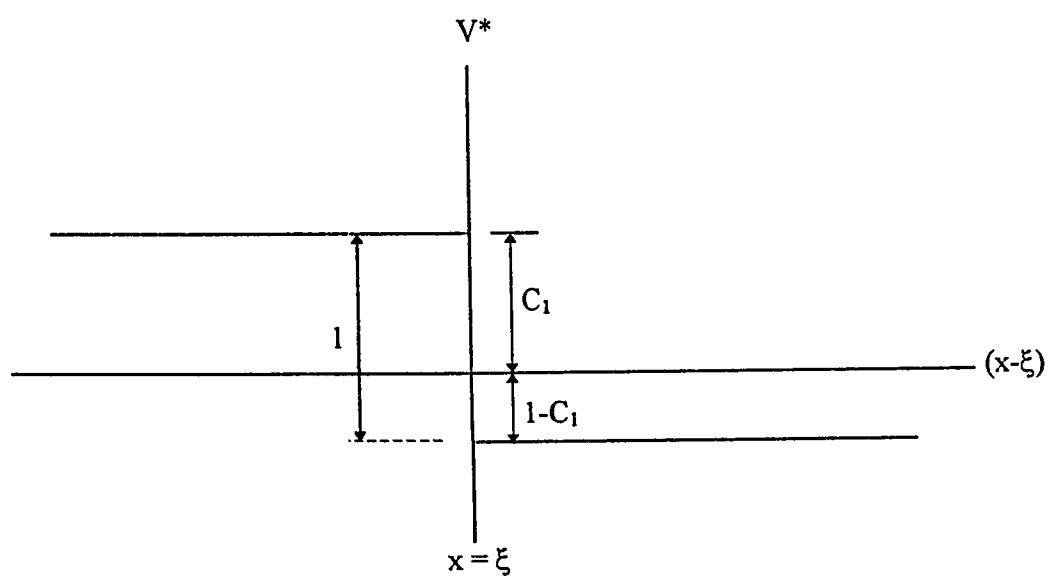


Figure 3-3 The function, V^*

For symmetry let us choose

$$C_1 = \frac{1}{2}$$

$$\text{Therefore } V^* = \begin{cases} \frac{1}{2} & x < \xi \\ -\frac{1}{2} & x > \xi \end{cases} \quad (3.10a)$$

Integrate V^* with respect to x to get M^*

$$EI \frac{d^2 w^*}{dx^2} = M^* = \begin{cases} \frac{1}{2}(x - \xi) & x < \xi \\ -\frac{1}{2}(x - \xi) & x > \xi \end{cases} \quad (3.10b)$$

Integrate M^* with respect to x to get θ^*

$$\frac{dw^*}{dx} = \theta^* = \begin{cases} \frac{(x - \xi)^2}{4EI} & x < \xi \\ -\frac{(x - \xi)^2}{4EI} & x > \xi \end{cases} \quad (3.10c)$$

and finally integrating θ^* with respect to x , we get

$$w^* = \begin{cases} \frac{(x - \xi)^3}{12EI} & x < \xi \\ -\frac{(x - \xi)^3}{12EI} & x > \xi \end{cases} \quad (3.10d)$$

Substituting the above fundamental solution in equation (3.9), we get the following equation

$$[H]\{\Delta\} = [G]\{F\} + \{B\} \quad (3.11)$$

where

$$[H] = \frac{1}{2} \begin{bmatrix} 1 & 0 & -1 & L \\ 0 & 1 & 0 & -1 \\ -1 & -L & 1 & 0 \\ 0 & -1 & 0 & 1 \end{bmatrix}, \quad [G] = \frac{1}{12 EI} \begin{bmatrix} 0 & 0 & -L^3 & 3L^2 \\ 0 & 0 & 3L^2 & -6L \\ L^3 & 3L^2 & 0 & 0 \\ 3L^2 & 6L & 0 & 0 \end{bmatrix}$$

$$\{\Delta\} = \begin{Bmatrix} w_1 \\ \theta_1 \\ w_2 \\ \theta_2 \end{Bmatrix}, \quad \{F\} = \begin{Bmatrix} V_1 \\ M_1 \\ V_2 \\ M_2 \end{Bmatrix} \text{ and } \{B\} = \frac{1}{12 EI_o} \begin{Bmatrix} \int_0^L x^3 f(x) dx \\ 0 \\ \int_0^L x^2 f(x) dx \\ 0 \\ \int_0^L (x-L)^3 f(x) dx \\ 0 \\ \int_0^L (x-L)^2 f(x) dx \\ 0 \end{Bmatrix}$$

Equation (3.11) is the usual form for boundary element matrices. Since unknown values of $\{\Delta\}$ align with known values of $\{F\}$ in equation (3.11) and vice-versa, the system of equations may be rearranged into form :

$$[A]\{X\} = \{Z\} \quad (3.12)$$

where $\{X\}$ contains all the unknown boundary data, and $\{Z\}$ contains the algebraic sum of the products of all known boundary values with their corresponding columns of $[G]$ or $[H]$ as the case may be. It should be noted that neither $[H]$ nor $[G]$ are symmetric. It should also be noted that none of these matrices is a "stiffness" matrix in the usual structures sense.

Once the system (3.12) is solved, all the unknown boundary values of forces and displacements will be known. These are substituted in to the domain equation for deflection i.e. equation (3.7) and the resulting equation can be evaluated at any point ξ . The same is true for the domain equation for slope i.e. equation (3.8). Also equation (3.8) may be differentiated further to obtain the shearing force and the bending moment at any point ξ .

3.3 Non - Prismatic Beams

Consider the beam shown in Figure 3-4, whose depth is a function of x . The governing differential equation(GDE) for transverse deflection of the beam is given by

$$\frac{d^2}{dx^2} \left(EI(x) \frac{d^2 w}{dx^2} \right) + f(x) = 0 \quad 0 \leq x \leq L, \quad (3.13)$$

Let w_1 , θ_1 , M_1 and V_1 be the deflection, slope, moment and shear respectively at the left end of the beam, w_2 , θ_2 , M_2 and V_2 be the deflection, slope, moment and shear respectively at the right end of the beam. Multiply equation (3.13) by a weighting function w^* and integrate over the length of the beam to get :

$$\int_0^L \left[\frac{d^2}{dx^2} \left(EI(x) \frac{d^2 w}{dx^2} \right) + f(x) \right] w^* dx = 0. \quad (3.13a)$$

Integrate by parts four times, we get

$$\begin{aligned} & \int_0^L w \frac{d^2}{dx^2} \left(EI(x) \frac{d^2 w^*}{dx^2} \right) dx - \left[w \frac{d}{dx} \left(EI(x) \frac{d^2 w^*}{dx^2} \right) \right]_0^L + \left[\frac{dw}{dx} EI(x) \frac{d^2 w^*}{dx^2} \right]_0^L \\ & - \left[EI(x) \frac{d^2 w}{dx^2} \frac{dw^*}{dx} \right]_0^L - \left[w^* \frac{d}{dx} \left(EI(x) \frac{d^2 w}{dx^2} \right) \right]_0^L + \int_0^L f(x) w^* dx = 0 \end{aligned} \quad (3.14)$$

If w^* (derived in the next section) is chosen to be the fundamental solution (as defined in section 3.1) of equation (3.13a) i.e.

$$\frac{d^2}{dx^2} \left(EI(x) \frac{d^2 w^*}{dx^2} \right) + \delta(x - \xi) = 0 \quad (3.15)$$

where $\delta(x - \xi)$ is the Dirac delta.

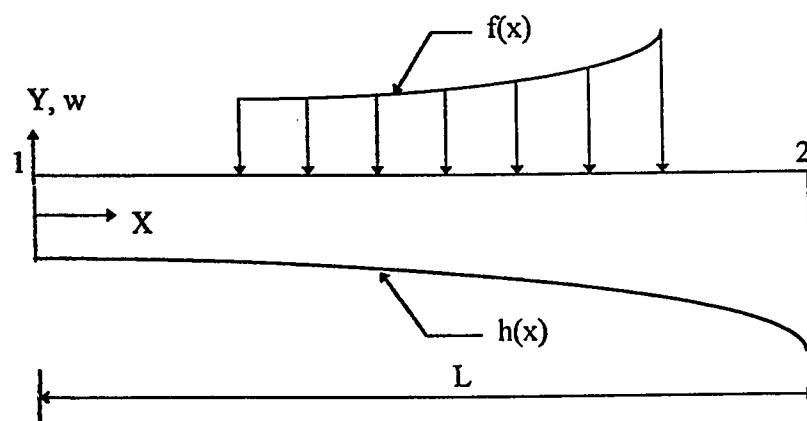


Figure 3-4 Beam with varying rigidity

then equation (3.14) becomes :

$$w(\xi) = \left[V w^* - M \theta^* + \theta M^* - w V^* \right]_{x=0}^{x=L} + \int_0^L f(x) w^* dx \quad (3.16)$$

Eqn.(3.16) computes the deflection w at any point inside the domain $(0, L)$ in terms of boundary values of w , θ , M , V and the given function of the load $f(x)$. Apply eqn.(3.16) and its derivatives with respect to ξ at the boundary points i.e. $\xi \rightarrow 0$ and $\xi \rightarrow L$ to get the boundary equations similar to equation (3.11)

$$[H]\{\Delta\} = [G]\{F\} + \{B\} \quad (3.17)$$

The explicit expressions of the elements of $[H]$ and $[G]$ matrices can be obtained by using the fundamental solution and after applying the boundary conditions and rearranging the known and the unknown variables, we get an equation similar to equation (3.12), written as

$$[A]\{X\} = \{Z\} \quad (3.18)$$

where $\{X\}$ contains all the unknown boundary data, and $\{Z\}$ contains the algebraic sum of the products of all known boundary values with their corresponding columns of $[G]$ or $[H]$ as the case may be.

3.4 Derivation of Fundamental Solution Non-Prismatic Sections

3.4.1 Linear variation

The fundamental solution of the differential equation governing the beams of variable thickness can be derived using the available fundamental solution of the beam with uniform depth. For instance, if the depth, $h(x)$ of the beam varies linearly such as $h(x) = h_0(1+bx)$ as shown in Figure 3-5, the governing differential equation becomes

$$\frac{d^2}{dx^2}(EI_0(1+bx)^3 \frac{d^2 w}{dx^2}) + f(x) = 0 \quad 0 \leq x \leq L \quad (3.19)$$

where h_0 and I_0 are the depth and moment of inertia at the origin and b is a constant. Since the change in stiffness will not effect V^* and M^* of prismatic beams i.e. Equations (3.10a) and (3.10b). Therefore they can also be used for non-prismatic beams.

$$M^* = -\text{Sgn}(x-\xi) \frac{(x-\xi)}{2} \quad (3.20a)$$

$$V^* = -\frac{1}{2} \text{Sgn}(x-\xi) \quad (3.20b)$$

$$\text{where } \text{Sgn}(x-\xi) = \begin{cases} 1 & x > \xi \\ -1 & x < \xi \end{cases}$$

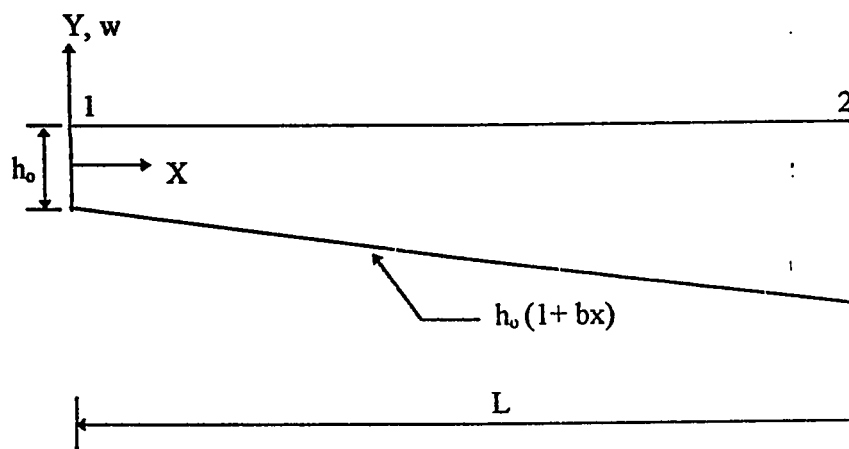


Figure 3-5 Linear variation

Integrate M^* with respect to x , between x and ξ to get θ^*

$$\begin{aligned}
 \theta^* &= \int_{\xi}^x \frac{M^*}{EI} dx = \int_{\xi}^x -\text{Sgn}(x-\xi) \frac{(x-\xi)}{2EI_0(1+bx)^3} dx \\
 &= -\text{Sgn}(x-\xi) \frac{1}{2EI_0} \left[\frac{1}{b^2} \left(\frac{-1}{(1+bx)} + \frac{1}{2(1+bx)^2} \right) + \frac{\xi}{2b(1+bx)^2} \right]_{\xi}^x \\
 &= -\text{Sgn}(x-\xi) \frac{1}{4EI_0b^2} \left[\frac{1+b\xi}{(1+bx)^2} - \frac{2}{(1+bx)} + \frac{1}{(1+b\xi)} \right] \quad (3.20c)
 \end{aligned}$$

integrate θ^* with respect to x , between x and ξ to get w^*

$$\begin{aligned}
 w^* &= \int_{\xi}^x \theta^* dx = -\text{Sgn}(x-\xi) \frac{1}{2EI_0} \left[\frac{-(1+b\xi)}{2b^3(1+bx)} - \frac{1}{b^3} \text{Log}(1+bx) + \frac{x}{2b^2(1+bx)} \right]_{\xi}^x \\
 w^* &= -\text{Sgn}(x-\xi) \frac{1}{4EI_0b^2} \left[(x-\xi) \left\{ \frac{1}{1+bx} + \frac{1}{1+b\xi} \right\} - \frac{2}{b} \log \frac{1+bx}{1+b\xi} \right] \quad (3.20d)
 \end{aligned}$$

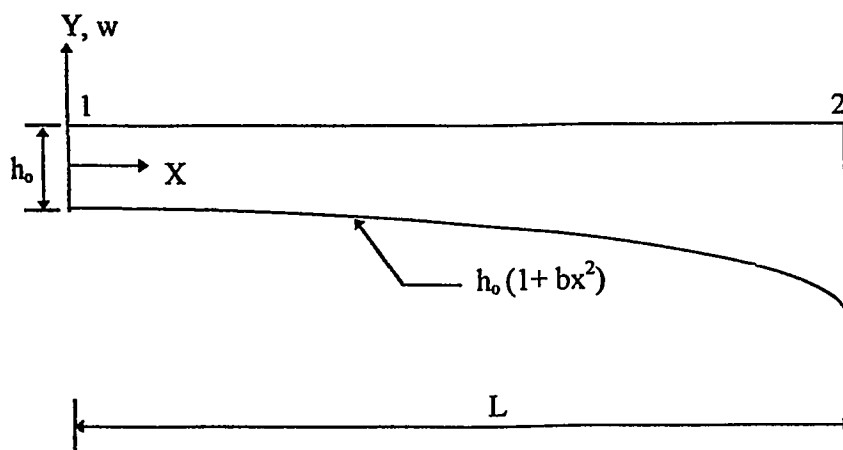


Figure 3-6 Parabolic Variation

3.4.2 Parabolic variation

If the depth of beam varies parabolically i.e. $h(x) = h_0(1 + bx^2)$ as shown in

Figure 3-6, the governing differential equation becomes

$$\frac{d^2}{dx^2}(EI_0(1 + bx^2)^3 \frac{d^2 w}{dx^2}) + f(x) = 0 \quad 0 \leq x \leq L \quad (3.21)$$

Again, V^* and M^* are same as before and θ^* can be obtained by integrating M^*

$$\begin{aligned} \theta^* &= \int_{\xi}^x -\text{Sgn}(x - \xi) \frac{(x - \xi)}{2EI_0(1 + bx^2)^3} dx \\ &= -\text{Sgn}(x - \xi) \frac{1}{EI_0} \left[\frac{-(1 + bx\xi)}{8b(1 + bx^2)^2} - \frac{3x\xi}{16(1 + bx^2)} - \frac{3\xi \tan^{-1}(x\sqrt{b})}{16\sqrt{b}} \right]_x^{\xi} \\ &= -\text{Sgn}(x - \xi) \frac{1}{EI_0} \left[\frac{-(1 + bx\xi)}{8b(1 + bx^2)^2} - \frac{3x\xi}{16(1 + bx^2)} - \frac{3\xi \tan^{-1}(x\sqrt{b})}{16\sqrt{b}} + \frac{-1}{8b(1 + b\xi^2)} \right. \\ &\quad \left. + \frac{3\xi^2}{16(1 + b\xi^2)} + \frac{3\xi \tan^{-1}(\xi\sqrt{b})}{16\sqrt{b}} \right] \quad (3.22a) \end{aligned}$$

$$\begin{aligned}
 w^* = \int_{\xi}^x \theta^* dx = & -\text{Sgn}(x-\xi) \frac{1}{EI_0} \left[\frac{-x}{16b(1+bx^2)} - \frac{\tan^{-1}(x\sqrt{b})}{16b^{\frac{3}{2}}} + \frac{\xi}{16b(1+b\xi^2)} - \frac{3\xi \log\left(\frac{(1+b\xi^2)}{b}\right)}{32b} \right. \\
 & \left. - \frac{3x\xi \tan^{-1}(x\sqrt{b})}{16\sqrt{b}} + \frac{3\xi \log(1+b\xi^2)}{32b} \right. \\
 & \left. + x \left(\frac{1}{8b(1+b\xi^2)} + \frac{3\xi^2}{16b(1+b\xi^2)} + \frac{3\xi \tan^{-1}(\xi\sqrt{b})}{16\sqrt{b}} \right) \right]_{\xi}^x
 \end{aligned}$$

$$\begin{aligned}
 w^* = & -\text{Sgn}(x-\xi) \frac{1}{EI_0} \left[\frac{\xi-x}{16b(1+bx^2)} + \frac{\tan^{-1}(\xi\sqrt{b}) - \tan^{-1}(x\sqrt{b})}{16b^{\frac{3}{2}}} + \right. \\
 & \left. + \frac{3x\xi}{16\sqrt{b}} (\tan^{-1}(\xi\sqrt{b}) - \tan^{-1}(x\sqrt{b})) - \frac{(x-\xi)}{8b(1+b\xi^2)} + \frac{3(x\xi^2 - \xi^3)}{16b(1+b\xi^2)} \right] \\
 & (3.22b)
 \end{aligned}$$

Similarly, fundamental solutions can be derived for other types of variations in depth of the beam. On substitution of the fundamental solutions derived in this section in to equation (3.16), we get the exact expressions for elements of the matrices [H] and [G].

3.5 Continuous Non-Prismatic Beams

The above formulation can be extended to the analysis of continuous beams with varying flexural rigidity. In continuous beams, the procedure is basically the same as for single span beams taking into consideration the connectivity between the spans. To explain this, let us Consider a two-span continuous beam with arbitrary boundary condition as shown in Figure 3-7. Let us first define the variables, w_1 , θ_1 , M_1 , and V_1 as the deflection, slope, moment and shear respectively at support 1, w_2 is the deflection at support 2, θ_{21} , M_{21} , and V_{21} are the slope, moment and shear respectively just before the support 2 and θ_{23} , M_{23} , and V_{23} are the slope, moment and shear respectively just after the support 2 and finally w_3 , θ_3 , M_3 , and V_3 are the deflection, slope, moment and shear respectively at support 3. The total number of unknowns in the beam is 10 (i.e. 2 at support 1, 6 at support 2 and 2 at support 3). The application of equation (3.17) to both span yields 8 equations. The remaining two equations can be obtained by satisfying the continuity and equilibrium at the intermediate support. i.e.

Moment before the support = - Moment after the support i.e.

$$M_{21} = - M_{23} = M_2 \quad (3.23a)$$

$$\text{Slope before the support} = -\text{Slope after the support i.e. } \theta_{21} = - \theta_{23} = \theta_2. \quad (3.23b)$$

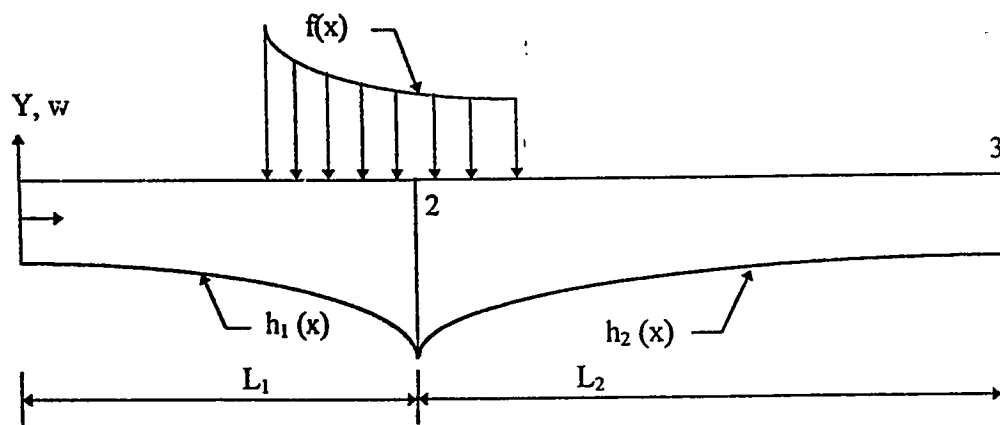


Figure 3-7 Continuous beam with varying flexural rigidity

After using the above two relations, the final equations become :

$$[H] \begin{Bmatrix} w_1 \\ \theta_1 \\ \theta_2 \\ w_3 \\ \theta_3 \end{Bmatrix} = [G] \begin{Bmatrix} V_1 \\ M_1 \\ V_{21} \\ V_{23} \\ M_2 \\ V_3 \\ M_3 \end{Bmatrix} + \{B\} \quad (3.24)$$

where $[H]$, $[G]$ and vector $\{B\}$ are as defined in equation (3.9). Then the boundary conditions are applied and the above system of equations is solved for the unknowns at the supports.

CHAPTER 4

PLATES

4.1 Introduction

The solution of plates with variable thickness has been of great interest to many investigators during the past decades. The literature review shows that analytical solutions of the plate problem, in general, limited to relatively simple plate geometry, loading and boundary conditions [Ref. 29, 30, 31, 32].

Although there is considerable application of the boundary element method to the analysis of plates with constant thickness [e.g. 50-55], its application to the case of plates with variable thickness is limited. This is obviously because the fundamental solution for the governing equation cannot be established, at least in a form that could be useful to develop a pure boundary element solution. This fact led to the investigation and

development of iterative techniques. In the cases where the fundamental solutions are not available, an iterative scheme has to be followed in which a fundamental solution to a part of the differential equation is used while the remaining part of the equation is treated as a fictitious unknown body force that can be updated in each iteration. Iterative methods for solving boundary element equations are discussed in detail in ref. [64]. This procedure is followed in reference [60] in which the fundamental solution of plate with uniform thickness is used and the remaining part of the equation is treated as a fictitious body force which can be calculated by discretizing the plate domains. Such procedure, however, loses the unique advantage of the boundary element method of dealing with unknowns over the boundary.

In the present work, the problem of a plate with linearly varying flexural rigidity is solved by splitting the biharmonic equation for transverse deflection of the plate into two Poisson's equations [34]. Each Poisson's equation has a known fundamental solution and therefore the BEM technique can be applied directly and the iterative procedure is avoided. This procedure greatly simplifies the computational work required for the solution of the problem and retains the advantage of the method mentioned above.

4.2 Governing Equations

In the plate bending, the plane $x_1 - x_2$ is taken to coincide with the mid plane of the plate as shown in Figure 4-1. The applied forces are per unit area inside the plate and per unit of length along Γ . The positive directions of the forces and moments are indicated in Figure 4-2. According to small deflection theory of thin non-prismatic plates, the governing differential equation is given [34] by :

$$D \nabla^2 \nabla^2 w + 2 \frac{\partial D}{\partial x_1} \frac{\partial}{\partial x_1} \nabla^2 w + 2 \frac{\partial D}{\partial x_2} \frac{\partial}{\partial x_2} \nabla^2 w + \nabla^2 D \nabla^2 w - (1-\nu) \left(\frac{\partial^2 D}{\partial x_1^2} \frac{\partial^2 w}{\partial x_2^2} - 2 \frac{\partial^2 D}{\partial x_1 \partial x_2} \frac{\partial^2 w}{\partial x_1 \partial x_2} + \frac{\partial^2 D}{\partial x_2^2} \frac{\partial^2 w}{\partial x_1^2} \right) = q \quad (4.1)$$

where w = deflection of the mid plane of the plate

$D(x_1, x_2)$ = flexural rigidity

$q(x_1, x_2)$ = distributed load

The bending moments and shearing forces are related to w as :

$$M_1 = -D \left(\frac{\partial^2 w}{\partial x_1^2} + \nu \frac{\partial^2 w}{\partial x_2^2} \right), \quad (4.2)$$

$$M_2 = -D \left(\frac{\partial^2 w}{\partial x_2^2} + \nu \frac{\partial^2 w}{\partial x_1^2} \right), \quad (4.3)$$

$$M_{12} = D(1-\nu) \frac{\partial^2 w}{\partial x_1 \partial x_2}, \quad (4.4)$$

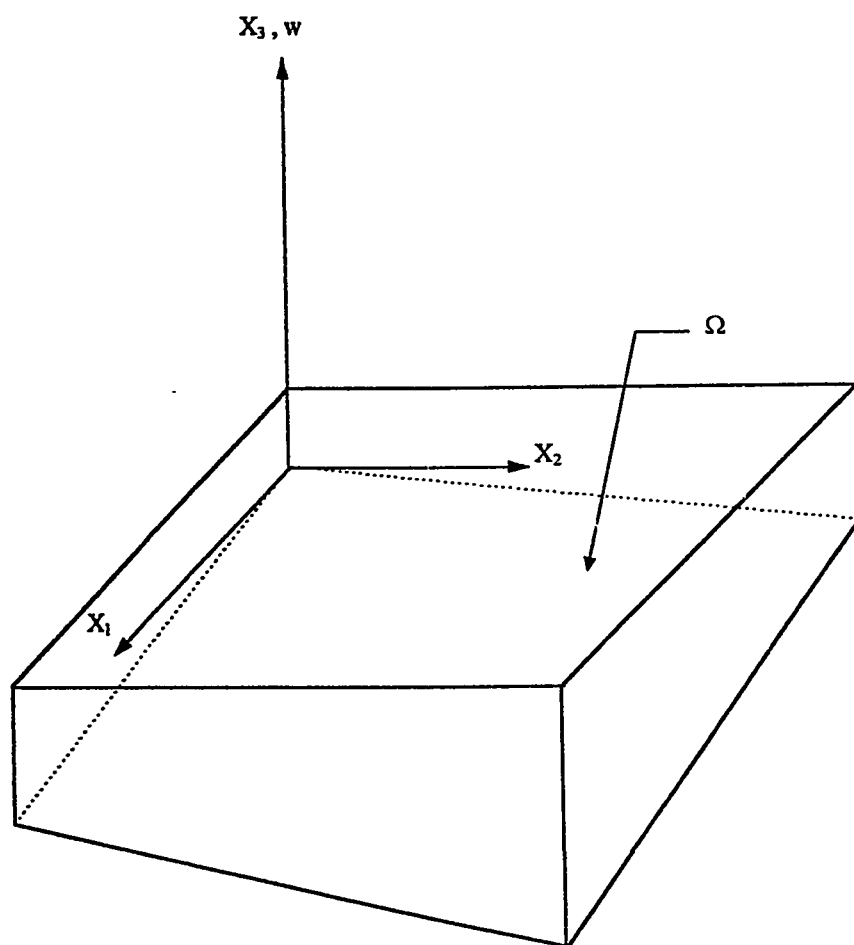


Figure 4-1 Coordinate System

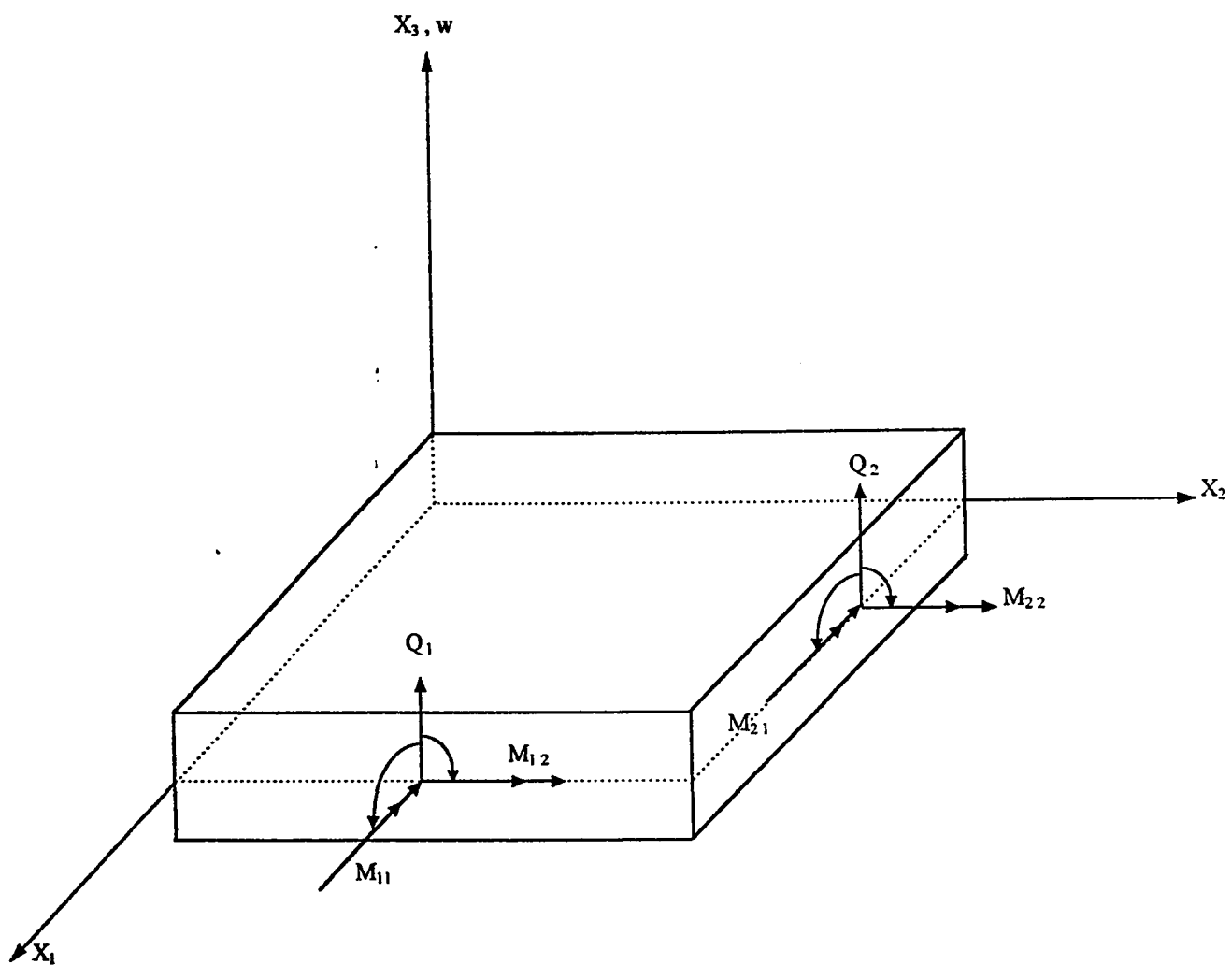


Figure 4-2 Plate element

$$Q_1 = -D \frac{\partial}{\partial x_1} \nabla^2 w - \frac{\partial D}{\partial x_2} (1-\nu) \frac{\partial^2 w}{\partial x_1 \partial x_2} - \frac{\partial D}{\partial x_1} \left(\frac{\partial^2 w}{\partial x_1^2} + \nu \frac{\partial^2 w}{\partial x_2^2} \right) \text{ and} \quad (4.5a)$$

$$Q_2 = -D \frac{\partial}{\partial x_2} \nabla^2 w - \frac{\partial D}{\partial x_1} (1-\nu) \frac{\partial^2 w}{\partial x_1 \partial x_2} - \frac{\partial D}{\partial x_2} \left(\frac{\partial^2 w}{\partial x_2^2} + \nu \frac{\partial^2 w}{\partial x_1^2} \right). \quad (4.5b)$$

effective shearing forces

$$V_1 = Q_1 - \frac{\partial M_{12}}{\partial x_2} \quad (4.5c)$$

$$V_2 = Q_2 - \frac{\partial M_{12}}{\partial x_1} \quad (4.5d)$$

Using equations (4.4, 4.5a, 4.5b) in equations (4.5c and 4.5d) we get

$$V_1 = - \frac{\partial}{\partial x_1} (D \nabla^2 w) - 2 \frac{\partial D}{\partial x_2} (1-\nu) \frac{\partial^2 w}{\partial x_1 \partial x_2} + \frac{\partial D}{\partial x_1} (1-\nu) \frac{\partial^2 w}{\partial x_2^2} - D(1-\nu) \frac{\partial^3 w}{\partial x_1 \partial x_2^2} \quad (4.6a)$$

$$V_2 = - \frac{\partial}{\partial x_2} (D \nabla^2 w) - 2 \frac{\partial D}{\partial x_1} (1-\nu) \frac{\partial^2 w}{\partial x_1 \partial x_2} + \frac{\partial D}{\partial x_2} (1-\nu) \frac{\partial^2 w}{\partial x_1^2} - D(1-\nu) \frac{\partial^3 w}{\partial x_2 \partial x_1^2} \quad (4.6b)$$

As a particular case of application of equation (4.1), let us consider the case in which the flexural rigidity D is linear function of x_1 and x_2 expressed in the form

$$D = D_0 + D_1 x_1 + D_2 x_2 \quad (4.7)$$

where D_0 , D_1 and D_2 are constants. In such case, equation (4.1) becomes

$$(D_0 + D_1 x_1 + D_2 x_2) \nabla^2 \nabla^2 w + 2 D_1 \frac{\partial}{\partial x_1} \nabla^2 w + 2 D_2 \frac{\partial}{\partial x_2} \nabla^2 w = q \quad (4.8)$$

which can be written as

$$\nabla^2 [(D_0 + D_1 x_1 + D_2 x_2) \nabla^2 w] = q$$

or simply

$$\nabla^2 [D \nabla^2 w] = q \quad (4.9)$$

4.3 Reduction of the plate bending differential equation to two

Poisson's equations

To make the solution of the plate bending problem easier, let us replace the fourth order differential equation (4.9) of the plate bending problem by two equations of the second order which represent the deflections of a membrane or Poisson's equation [34].

Let us now introduce a new notation which is defined as

$$M = \frac{M_1 + M_2}{(1+\nu)} = -D \left(\frac{\partial^2 w}{\partial x_1^2} + \frac{\partial^2 w}{\partial x_2^2} \right) \quad (4.10)$$

Therefore

$$\nabla^2 w = -\frac{M}{D} \quad (4.11)$$

Substituting equation (4.11) into equation (4.9)

$$\nabla^2 M = -q \quad (4.12)$$

Now the fourth order differential equation (4.9) is transformed into two second order Poisson's equations (4.11) & (4.12) which can be solved through the following two steps:

- Step I: Solve equation (4.12) and get the solution of 'M' inside the domain.

- **Step II :** Solve equation (4.11) for deflection 'w' using the values 'M' inside the domain obtained in step I and the corresponding rigidity D.

In both steps the equation dealt with is Poisson's equation. The boundary element solution for such equation is discussed in the following section.

4.4 Boundary Element Formulation for Poisson's Equation

Consider, the following general two-dimensional Poisson's equation in Ω .

$$a_o \nabla^2 u + f = 0 \quad (4.13)$$

and a_o is a specified coefficient and f is a specified function of x_1 and x_2 . In addition to the primary variable u , we also seek

$$\begin{aligned} q_1 &= a_o \frac{\partial u}{\partial x_1} \\ q_2 &= a_o \frac{\partial u}{\partial x_2} \end{aligned} \quad (4.14)$$

The boundary conditions considered here are such that at each point on the boundary Γ either the potential u or the flux $q_n = q_1 n_1 + q_2 n_2$ is prescribed, where n_i are the unit normals to the boundary. Multiplying equation (4.13) by a weighting function u^* and integrating by parts using divergence theorem, we get the following variational formulation,

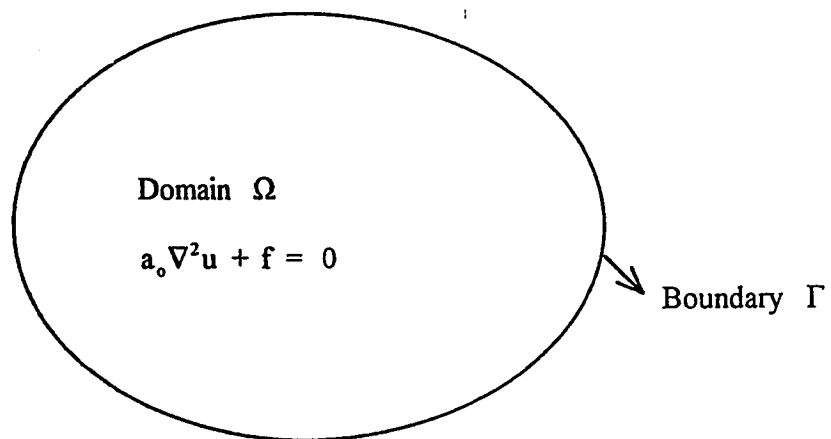


Figure 4-3 Notation for Poisson's equation

$$\begin{aligned}
& - \int_{\Omega} \frac{\partial u^*}{\partial x_1} \left(a_o \frac{\partial u}{\partial x_1} \right) + \frac{\partial u^*}{\partial x_2} \left(a_o \frac{\partial u}{\partial x_2} \right) d\Omega \\
& + \int_{\Gamma} u^* \left[\left(a_o \frac{\partial u}{\partial x_1} \right) n_1 + \left(a_o \frac{\partial u}{\partial x_2} \right) n_2 \right] ds + \int_{\Omega} u^* f d\Omega = 0
\end{aligned} \tag{4.15}$$

Integrating by parts once again, we get the following inverse formulation,

$$\begin{aligned}
& \int_{\Omega} u \left[\frac{\partial}{\partial x_1} \left(a_o \frac{\partial u^*}{\partial x_1} \right) + \frac{\partial}{\partial x_2} \left(a_o \frac{\partial u^*}{\partial x_2} \right) \right] d\Omega + \int_{\Gamma} u^* q_n ds \\
& - \int_{\Gamma} u \left[\left(a_o \frac{\partial u^*}{\partial x_1} \right) n_1 + \left(a_o \frac{\partial u^*}{\partial x_2} \right) n_2 \right] ds + \int_{\Omega} u^* f d\Omega = 0
\end{aligned} \tag{4.16}$$

In short equation (4.16) can be written as

$$\int_{\Omega} u (\nabla^2 u^*) d\Omega = - \int_{\Gamma} u^* q_n ds + \int_{\Gamma} u q_n^* ds - \int_{\Omega} u^* f d\Omega \tag{4.17}$$

$$\text{where } q_n^* = a_o \left[\frac{\partial u^*}{\partial x_1} n_1 + \frac{\partial u^*}{\partial x_2} n_2 \right] \tag{4.18}$$

4.4.1 Boundary Integral Equations

Our aim is now to find a solution satisfying the Poisson's equation. If we assume that u^* satisfies equation (4.13) with f being a concentrated charge acting at a point $\tilde{\xi}$, i.e.

$$\nabla^2 u^* + \delta(\tilde{x} - \tilde{\xi}) = 0 \quad (4.19)$$

where δ is a Dirac delta function which has the following two properties :

$$\delta(\tilde{x} - \tilde{\xi}) = \begin{cases} 0 & \tilde{x} \neq \tilde{\xi} \\ \infty & \tilde{x} = \tilde{\xi} \end{cases} \quad (4.20)$$

$$\int_{\Omega} g(\tilde{x}) \delta(\tilde{x} - \tilde{\xi}) d\Omega = g(\tilde{\xi}) \quad (4.21)$$

The solution of equation (4.19) is called the 'fundamental solution'. If equation (4.19) is used in equation (4.17) we get

$$\int_{\Omega} u \delta(\tilde{x} - \tilde{\xi}) d\Omega = \int_{\Gamma} u^* q_n ds - \int_{\Gamma} u q_n^* ds + \int_{\Omega} u^* f d\Omega \quad (4.22a)$$

Using equation (4.21) in equation (4.22a) we get

$$u(\tilde{\xi}) = \int_{\Gamma} u^* q_n ds - \int_{\Gamma} u q_n^* ds + \int_{\Omega} u^* f d\Omega \quad (4.22b)$$

Assuming that we have the fundamental solution u^* , equation (4.22b) gives us the solution of the primary variable u at any point $\tilde{\xi}$ in terms of the boundary values of u and q_n . For an isotropic two dimensional medium the fundamental solution [65] of equation (4.19) is

$$u^* = \frac{1}{2\pi a_0} \ln \frac{1}{r} \quad (4.23a)$$

Where r is the distance from the source point of application of the unit potential (ξ_1, ξ_2) to the field point under consideration as shown in Figure 4-4, i.e.

$$r = \sqrt{(x_1 - \xi_1)^2 + (x_2 - \xi_2)^2} \quad (4.23b)$$

$$\text{and } q_n^* = -\frac{1}{2\pi} (\rho_1 n_1 + \rho_2 n_2) \quad (4.24)$$

$$\begin{aligned} \text{Where } \rho_1 &= \frac{x_1 - \xi_1}{r} \\ \rho_2 &= \frac{x_2 - \xi_2}{r} \end{aligned} \quad (4.25)$$

Use equations (4.23a) & (4.24) in equation (4.22b)

$$\begin{aligned} u(\tilde{\xi}) = \frac{1}{2\pi} \left[\int_{\Gamma} u \frac{\rho_1 n_1 + \rho_2 n_2}{r} ds + \frac{1}{a_0} \int_{\Gamma} q_n \ln \left(\frac{1}{r} \right) ds \right. \\ \left. + \frac{1}{a_0} \int_{\Omega} f \ln \left(\frac{1}{r} \right) d\Omega \right]; \quad \tilde{\xi} \in \Omega \end{aligned} \quad (4.26)$$

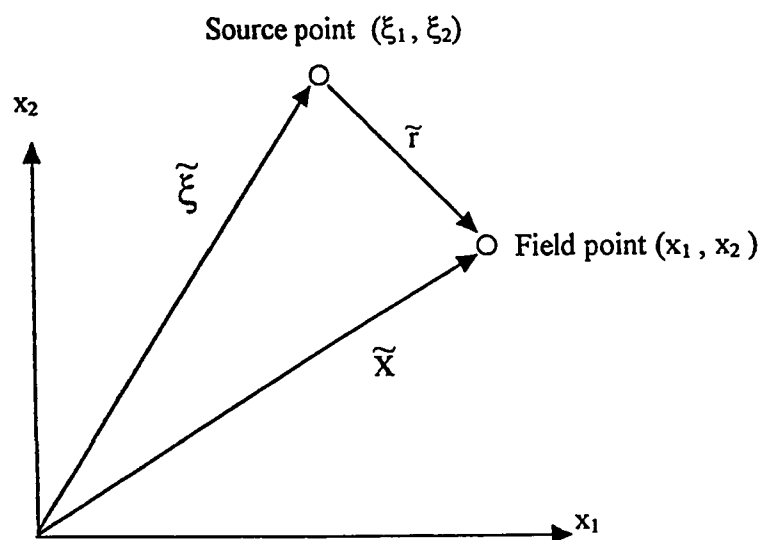


Figure 4-4 Notation for source and field points

Equation (4.26) is called the domain integral equation and it enables us to calculate the primary variable u at any point $\tilde{\xi}$ inside the domain Ω , by using both the primary and secondary variables over the boundary and the specified function, f , over the domain.

The secondary variables such as the fluxes can also be obtained directly by taking proper derivatives of equation (4.26) i.e.

$$q_1(\tilde{\xi}) = \frac{1}{2\pi} \left[-a_0 \int_{\Gamma} u \frac{(1-2\rho_1^2)n_1 - 2\rho_1\rho_2 n_2}{r^2} ds + \int_{\Gamma} q_n \frac{\rho_1}{r} ds + \int_{\Omega} f \frac{\rho_1}{r} d\Omega \right] \quad (4.27)$$

$$q_2(\tilde{\xi}) = \frac{1}{2\pi} \left[-a_0 \int_{\Gamma} u \frac{(1-2\rho_2^2)n_2 - 2\rho_1\rho_2 n_1}{r^2} ds + \int_{\Gamma} q_n \frac{\rho_2}{r} ds + \int_{\Omega} f \frac{\rho_2}{r} d\Omega \right] \quad (4.28)$$

where $\tilde{\xi}$ in Ω .

4.4.2 Boundary Element Equations

Equation (4.26) is also applicable as $\tilde{\xi} \rightarrow \Gamma$, but as $\tilde{\xi} \rightarrow \Gamma$, at some point on the boundary when $\tilde{x} \rightarrow \tilde{\xi}$, $r \rightarrow 0$, the integrands of equation (4.26) become singular.

The integral containing $\ln\left(\frac{1}{r}\right)$ is not a problem because the function is integrable but the

one containing $\left(\frac{1}{r}\right)$ needs special treatment. The treatment of singular integrals is discussed in section 4.4.4. When equation (4.26) is applied on the boundary, we get the boundary integral equation which has the following form

$$u(\tilde{\xi}) = \frac{1}{2\pi} \left[\oint_{\Gamma} u \frac{\rho_1 n_1 + \rho_2 n_2}{r} ds + \frac{1}{a_0} \int_{\Gamma} q_n \ln\left(\frac{1}{r}\right) ds \right. \\ \left. + \frac{1}{a_0} \int_{\Omega} f \ln\left(\frac{1}{r}\right) d\Omega \right] \quad \tilde{\xi} \in \Gamma \quad (4.29)$$

where the notation \oint is used to indicate the singularity of the integral.

The boundary element equations can be obtained by discretizing the boundary (integrals containing the boundary unknowns) and the domain (integrals containing the known body force). Let us divide Γ into N elements as shown in Figure 4-5, then equation (4.26) becomes

$$2\pi u(\tilde{\xi}_i) - \sum_{j=1}^N \int_{\Gamma_j} u \frac{\rho_1 n_1 + \rho_2 n_2}{r} ds = \frac{1}{a_0} \sum_{j=1}^N \int_{\Gamma_j} q_n \ln\left(\frac{1}{r}\right) ds + B_i \quad \tilde{\xi} \text{ on } \Gamma \quad (4.30)$$

where $i = 1, N$ and B_i is a vector representing the domain integral in equation (4.26)

which will be discussed in section 4.4.3

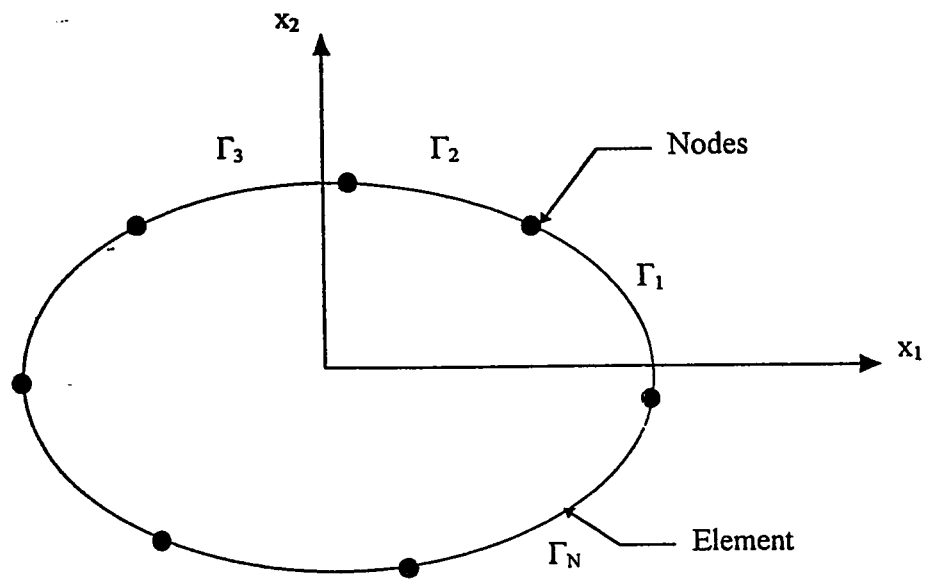


Figure 4-5 Boundary discretization

Let us approximate u and q_n on the boundary by assuming linear variation over each boundary element, i.e.

$$u = u^{(j-1)}\phi_1(\eta) + u^{(j)}\phi_2(\eta) \quad (4.31)$$

$$q_n = q_n^{(2j-1)}\phi_1(\eta) + q_n^{(2j)}\phi_2(\eta) \quad (4.32)$$

where $u^{(j)}$ is the potential at node j , $q_n^{(2j-1)}$ is flux after node $j-1$, and $q_n^{(2j)}$ is flux before node j , and ϕ_1 and ϕ_2 are the linear interpolation functions which can be written in terms of a local coordinates η as

$$\phi_1(\eta) = \frac{1}{2}(1-\eta) \quad (4.33)$$

$$\phi_2(\eta) = \frac{1}{2}(1+\eta) \quad (4.34)$$

where η ranges from -1 to 1. The global coordinate system \tilde{x} is transformed linearly to the local coordinates $\tilde{\eta}$ using the same interpolation functions

$$\tilde{x} = \tilde{x}^{(j-1)}\phi_1(\eta) + \tilde{x}^{(j)}\phi_2(\eta) \quad (4.35)$$

So that $n_1 ds = dx_2 = \frac{dx_2}{d\eta} d\eta$, and

$$n_2 ds = -dx_1 = -\frac{dx_1}{d\eta} d\eta$$

After using the above definitions in boundary integral equation (4.30) we get

$$\begin{aligned}
2\pi u(\tilde{\xi}_i) - \sum_{j=1}^N u^{(j)} \left[\int_{\Gamma_j} \phi_2 \left(\frac{\rho_1 n_1 + \rho_2 n_2}{r} \right) ds + \int_{\Gamma_{j+1}} \phi_1 \left(\frac{\rho_1 n_1 + \rho_2 n_2}{r} \right) ds \right] \\
= \frac{1}{a_0} \sum_{j=1}^N q_n^{(2j)} \int_{\Gamma_j} \phi_2 \ln \left(\frac{1}{r} \right) ds + q_n^{(2j+1)} \int_{\Gamma_{j+1}} \phi_1 \ln \left(\frac{1}{r} \right) ds + B_i
\end{aligned} \quad (4.36)$$

Applying Equation (4.36) at the N boundary nodes, we get the following boundary element equation written in matrix form :

$$\sum_{j=1}^N H^{ij} u^j = \sum_{j=1}^{2N} G^{ij} q_n^j + B_i \quad i = 1, N \quad (4.36a)$$

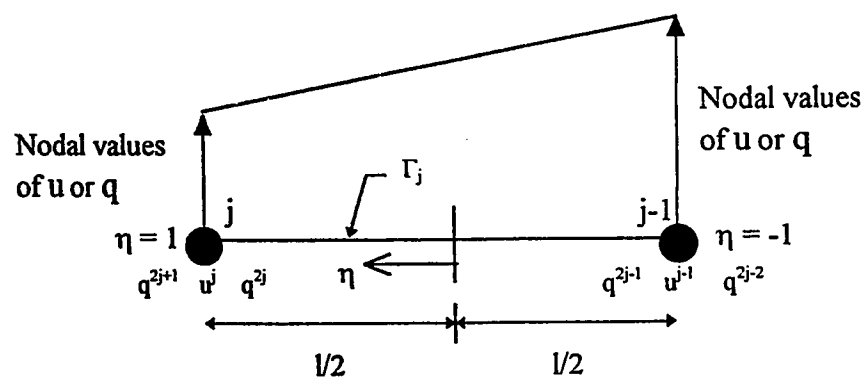


Figure 4-6 Linear element

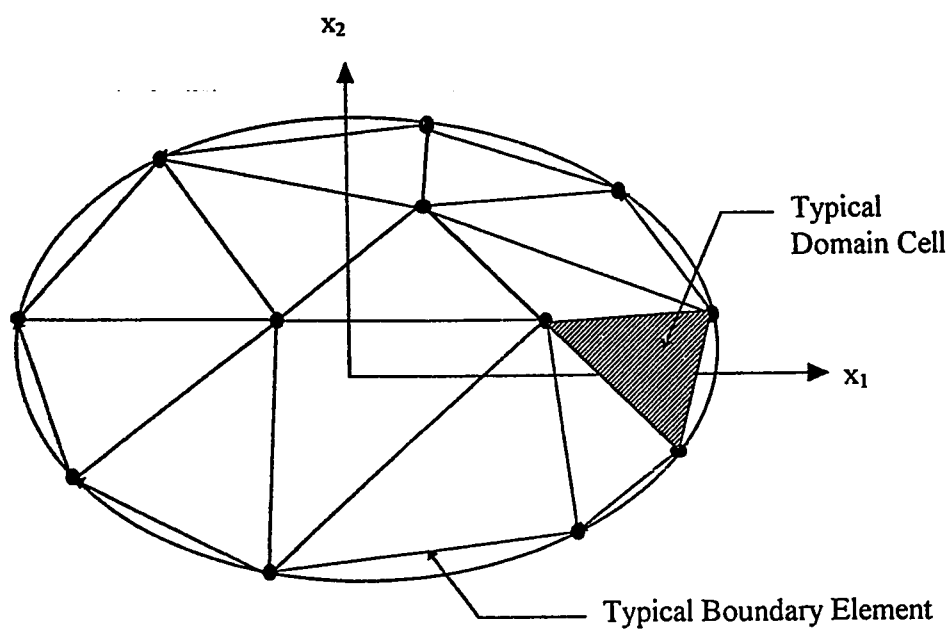


Figure 4-7 Boundary elements and internal cells for numerical integration

4.4.3 Computation of Vector {B}

4.4.3.1 Distributed loads

$$B_i = \int_{\Omega} f u^*(\tilde{x}, \tilde{\xi}_i) d\Omega = \frac{1}{2\pi a_0} \int_{\Omega} f \ln \frac{1}{r(\tilde{x}, \tilde{\xi}_i)} d\Omega \quad (4.37)$$

Let us divide the domain Ω into M number of cells as shown in Figure 4 -7. and integrate numerically over each cell.

$$B_i = \frac{1}{2\pi a_0} \sum_{e=1}^M \int_{\Omega_e} f \ln \frac{1}{r(\tilde{x}, \tilde{\xi}_i)} d\Omega_e \quad (4.38)$$

Let us approximate the function, f and the coordinates \tilde{x} over each cell

$$f = \sum_{l=1}^m f^l \phi_l(\eta_1, \eta_2) , \quad (4.39)$$

$$x_1 = \sum_{l=1}^m x_1^l \phi_l(\eta_1, \eta_2) , \quad (4.40)$$

$$x_2 = \sum_{l=1}^m x_2^l \phi_l(\eta_1, \eta_2) \quad \text{and} \quad (4.41)$$

$$dx_1 dx_2 = J d\eta_1 d\eta_2 \quad (4.42)$$

where ϕ_l are interpolation functions, m is the number of nodes associated with each cell e and J is Jacobean which is given by

$$J = \begin{vmatrix} \sum_{l=1}^m x_1^l \frac{\partial \phi_l}{\partial \eta_1} & \sum_{l=1}^m x_2^l \frac{\partial \phi_l}{\partial \eta_1} \\ \sum_{l=1}^m x_1^l \frac{\partial \phi_l}{\partial \eta_2} & \sum_{l=1}^m x_2^l \frac{\partial \phi_l}{\partial \eta_2} \end{vmatrix} \quad (4.43)$$

For a four noded rectangular element as shown in Figure 4-8 the interpolation functions are

$$\begin{aligned} \phi_1 &= \frac{1}{4}(1-\eta_1)(1-\eta_2) \\ \phi_2 &= \frac{1}{4}(1+\eta_1)(1-\eta_2) \\ \phi_3 &= \frac{1}{4}(1-\eta_1)(1+\eta_2) \\ \phi_4 &= \frac{1}{4}(1+\eta_1)(1+\eta_2) \end{aligned} \quad (4.44)$$

where $-1 \leq \eta_1 \leq 1$ and $-1 \leq \eta_2 \leq 1$

For a 3-noded triangular element as shown in Figure 4-9, the interpolation functions are

$$\begin{aligned} \phi_1 &= \eta_1 \\ \phi_2 &= \eta_2 \\ \phi_3 &= 1 - \eta_1 - \eta_2 \end{aligned} \quad (4.45)$$

where $0 \leq \eta_1 \leq 1$ and $0 \leq \eta_2 \leq 1$

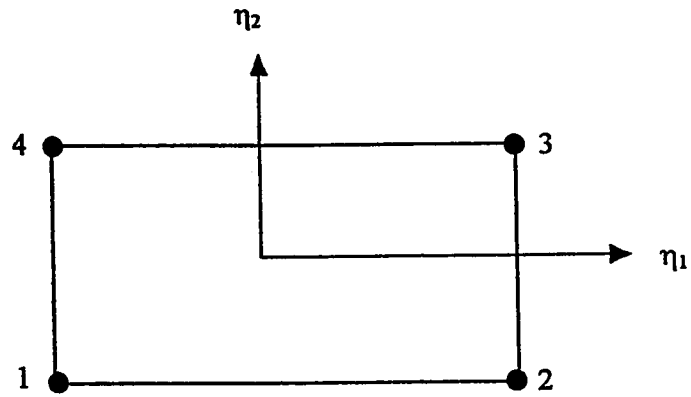


Figure 4-8 Four - Noded rectangular element

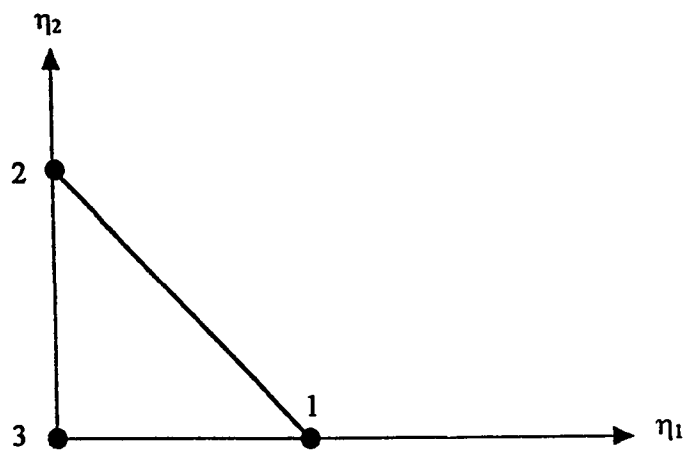


Figure 4-9 Three - Noded triangular element

The integral over each cell can be written as

$$\int_{\Omega_i} F(\eta_1, \eta_2) d\eta_1 d\eta_2. \quad (4.46)$$

4.4.3.2 Concentrated loads

In the case of concentrated loads, Problem becomes very simple, the domain does not need to be discretized. The load vector B_i in equation (4.37) becomes :

$$B_i = \int_{\Omega} Q \delta(\tilde{x} - \tilde{x}_c) u^*(\tilde{x}, \tilde{\xi}_i) d\Omega \quad (4.47)$$

where Q is the concentrated load applied at \tilde{x}_c . Using the property of Dirac delta function, the equation (4.47) reduces to

$$B_i = Q u^*(\tilde{x}_c, \tilde{\xi}_i)$$

4.4.4 Computation of singular integrals

4.4.4.1 Computation of H^{ii} :

Consider the special boundary condition of $u = u_0 = \text{constant}$, then its derivative q_n

becomes zero. i.e. $[H] \{u\} = [G] \{q_n\}$

$$u_o [H] \{I\} = \{0\}$$

$$\text{so that } [H]\{I\} = 0$$

$$\text{i.e. } H^{ii} = - \sum_{\substack{j=1 \\ j \neq i}}^N H^{ij} \quad (4.48)$$

But $[H]$ depends only on the geometry of the boundary. Therefore equation (4.48) is also true for general boundary conditions.

4.4.4.2 Computation of $G^{(2i-1)}$:

Consider the integral $\int_{\Gamma_i} \phi_2 \ln \left(\frac{1}{r} \right) ds$ for $\tilde{\xi}$ is at node i

$r = l_i - s$ and $ds = -dr$ and $\phi_2(r) = (1-r/l_i)$ as shown in Figure 4-10a, where l_i is the length of Γ_i . Then

$$\int_{\Gamma_i} \phi_2 \ln \left(\frac{1}{r} \right) ds = - \int_{l_i}^0 \left(1 - \frac{r}{l_i} \right) \ln \left(\frac{1}{r} \right) dr = - \frac{l_i}{2} [\ln(l_i) - 1.5] \quad (4.49)$$

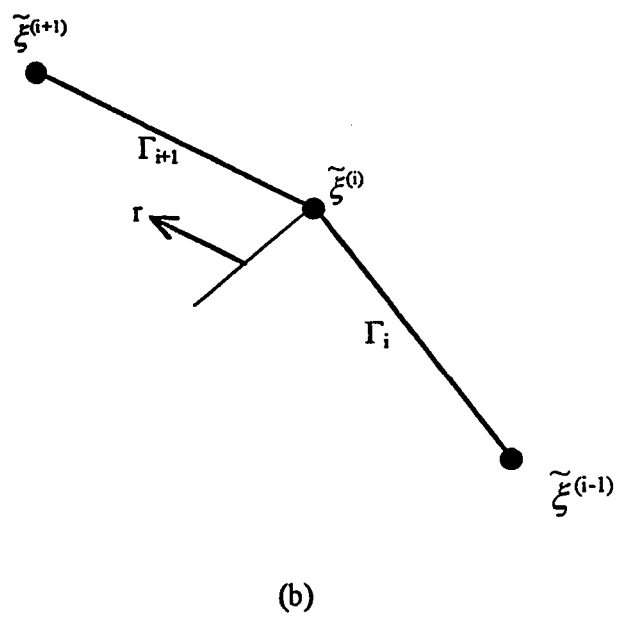
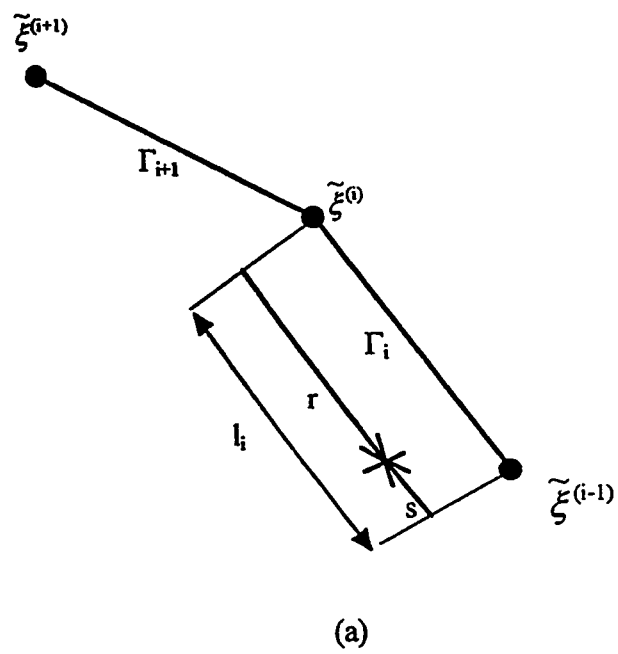


Figure 4-10 Computation of singular elements $G^{(2i-1)}$

Similarly for the integral $\int_{\Gamma_{j+1}} \phi_1 \ln\left(\frac{1}{r}\right) ds$ when $\tilde{\xi}$ is at node i

$r = s$ and $ds = dr$ as shown in Figure 4-10b

$$\phi_1(r) = \left(1 - \frac{r}{l_{i+1}}\right)$$

$$\int_{\Gamma_{i+1}} \phi_1 \ln\left(\frac{1}{r}\right) ds = - \int_0^{l_{i+1}} \left(1 - \frac{r}{l_{i+1}}\right) \ln\left(\frac{1}{r}\right) dr = \frac{l_{i+1}}{2} [\ln(l_{i+1}) - 1.5] \quad (4.50)$$

Therefore boundary equation can be written in matrix form as

$$[H] \{u\} = [G] \{q_n\} + \{B\} \quad (4.51)$$

$$\text{where } H^{ij} = \begin{cases} - \int_{\Gamma_j} \phi_2 \left(\frac{\rho_1 n_1 + \rho_2 n_2}{r} \right) ds - \int_{\Gamma_{j+1}} \phi_1 \left(\frac{\rho_1 n_1 + \rho_2 n_2}{r} \right) ds & i \neq j \\ 1 - \int_{\Gamma_i} \phi_2 \left(\frac{\rho_1 n_1 + \rho_2 n_2}{r} \right) ds + \int_{\Gamma_i} \phi_1 \left(\frac{\rho_1 n_1 + \rho_2 n_2}{r} \right) ds & i = j \end{cases} \quad (4.52)$$

$$G^{i(2i-1)} = \begin{cases} \int_{\Gamma_j} \phi_2 \ln\left(\frac{1}{r}\right) ds & i \neq j \\ \frac{l_i}{2} [\ln(l_i) - 1.5] & i = j \end{cases} \quad (4.53)$$

$$G^{i(2i)} = \begin{cases} \frac{1}{a_0 r_{j+1}} \int \phi_1 \ln\left(\frac{1}{r}\right) ds & i \neq j \\ \frac{l_{i+1}}{2} [\ln(l_{i+1}) - 1.5] & i = j \end{cases} \quad (4.54)$$

The boundary element method proceeds from this point by first solving for the unknown boundary data (that has not been specified) in terms of that which has been specified. Equation (4.51) is the usual form for boundary element matrices. Since unknown values of $\{u\}$ align with known values of $\{q_n\}$ in equation (4.51) and vice-versa, the system of equations may be reordered into form :

$$[A] \{X\} = \{Z\} \quad (4.55)$$

where $\{X\}$ contains all the unknown boundary data, and $\{Z\}$ contains the algebraic sum of the products of all known boundary values with their corresponding columns of $[G]$ or $[H]$ as the case may be. Once we have solved the equation (4.55) for $\{u\}$ and $\{q_n\}$, we can determine u at any point $\tilde{\xi}$ in Ω using the following domain equation.

$$u(\tilde{\xi}) = u^i = -\frac{1}{2\pi} \left[\sum_{j=1}^N \bar{H}^{ij} u^j + \sum_{j=1}^N \bar{G}^{ij} q_n^j \right] \quad (4.56)$$

where u^j and q_n^j are boundary variables obtained from equation (4.55) , expressions for \bar{H}^{ij} and \bar{G}^{ij} are same as H^{ij} and G^{ij} given in equations (4.52 - 4.54) and 'bar' represents that the matrices are for domain equations.

4.4.5 Numerical Integration

Gauss quadrature method for numerical integration is one of the many schemes for numerical evaluation of definite integrals. All the boundary integrals can be written in the form $\int_{-1}^1 F(\eta) d\eta$. We can approximate these integrals using Gauss quadrature method i.e.

$$\int_{-1}^1 F(\eta) d\eta \cong \sum_{i=1}^n W_i F(\eta_i) \quad (4.58)$$

where n is the number of Gauss points in the interval $(-1, 1)$, η_i are the base points and w_i are the weight factors. Values for η_i and W_i are listed in *Table 4-1* for $n=2$ to $n=10$ [65].

Similarly a domain integral can be computed as

$$\int_{-1}^1 \int_{-1}^1 F(\eta_1, \eta_2) d\eta_1 d\eta_2 = \sum_{i=1}^n \sum_{j=1}^n W_i W_j F(\eta_{1i}, \eta_{2j}) \quad (4.59)$$

Table 4-1 Location of the Gauss points and their weights

$\pm\eta_i$	w_i
	n=2
0.5773 02691 89626	1.00000 00000 00000
	n=3
0.00000 00000 00000	0.88888 88888 88888
0.77459 66692 41483	0.55555 55555 55555
	n=4
0.33998 10435 84856	0.65214 51548 62546
0.56113 63115 94053	0.34785 48451 37454
	n=5
0.00000 00000 00000	0.56888 88888 88889
0.53846 93101 05683	0.47862 86704 99366
0.90617 98459 38664	0.23692 68850 56189
	n=6
0.23861 91860 83197	0.46791 39345 72691
0.66120 93864 66265	0.36076 15730 48139
0.93246 95142 03152	0.17132 44923 79170
	n=7
0.00000 00000 00000	0.41795 91836 73469
0.40584 51513 77397	0.38183 00505 05119
0.74153 11855 99394	0.27970 53914 89277
0.94910 79123 42759	0.12948 49661 68870
	n=8
0.18343 46424 95650	0.36268 37833 78362
0.52553 24099 16329	0.31370 66458 77887
0.79666 64774 13627	0.22238 10344 53374
0.96028 98564 97536	0.10122 85362 90376
	n=9
0.00000 00000 00000	0.33023 93550 01260
0.32425 34234 03809	0.31234 70770 40033
0.61337 14327 00590	0.26061 06964 02935
0.83603 11073 26636	0.18064 81606 94857
0.96816 02395 07626	0.08127 43883 61574
	n=10
0.14887 43389 81631	0.29552 42247 14753
0.43339 53941 29247	0.26926 67193 09936
0.67940 95682 99024	0.21908 63625 15982
0.86506 33666 88985	0.74945 13491 50581
0.97390 65285 17172	0.06667 13443 08688

CHAPTER 5

APPLICATIONS

5.1 BE Formulation for Simply Supported Plates

In the case of simply supported plates, the procedure discussed in the previous chapter can be applied directly. We start with the solution of the equation governing the variable M (as defined in equation 4.10), i.e.

$$\nabla^2 M + q = 0 \quad (5.1)$$

with boundary condition $M = 0$ on Γ .

From this solution we find the nodal values of M in the domain. Then we solve the following equation for deflection of the plate w .

$$\nabla^2 w + \frac{M}{D} = 0 \quad (5.2)$$

with the boundary condition $w = 0$ and the known body force M/D over the domain.

5.1.1 Boundary element equations

Boundary element formulation for Poisson's equation has already been discussed in detail in section 4.4. Consider equation (5.1), after the boundary discretization of equation (5.1), we get the following boundary element equations

$$[H] \{M\} = [G] \left\{ \frac{\partial M}{\partial n} \right\} + \{B\} \quad (5.3)$$

where $[H]$ and $[G]$ are as defined in chapter 4 equation (4.52 through 4.54) and

$$B = \int_{\Omega} q_n \ln \left(\frac{1}{r} \right) d\Omega \quad (5.4)$$

We solve equation (5.3) for the unknown boundary data, then using the following domain equation, we find the nodal values of M inside the domain

$$M(\xi) = -\frac{1}{2\pi} \left[\sum_{j=1}^N \bar{H}^{ij} M^j + \sum_{j=1}^N \bar{G}^{ij} \frac{\partial M^j}{\partial n} \right] \quad (5.5)$$

where the expressions for \bar{H}^{ij} and \bar{G}^{ij} are defined in equation (4.52 through 4.54). Then we consider the following equation

$$\nabla^2 w + \frac{M}{D} = 0 \quad (5.6)$$

which has the following integral solution (see equation 4.22)

$$w(\xi) = \int_{\Gamma} w^* \frac{\partial w}{\partial n} ds - \int_{\Gamma} w \frac{\partial w^*}{\partial n} ds + \int_{\Omega} w^* \frac{M}{D} d\Omega \quad (5.7)$$

which yields the following boundary element equation (after the discretization)

$$[H] \{w\} = [G] \{\theta_n\} + \{B\} \quad (5.8)$$

$$\text{where } \theta_n = \frac{\partial w}{\partial n} \quad \text{and} \quad B = \int_{\Omega} \frac{M}{D} \ln\left(\frac{1}{r}\right) d\Omega \quad (5.9)$$

On solving the boundary element equations i.e. equation (5.8) we obtain all the unknown boundary data, then the following domain equations can be used to calculate the deflection at any point $\tilde{\xi}$ inside the domain

$$w(\tilde{\xi}) = -\frac{1}{2\pi} \left[\sum_{j=1}^N \bar{H}^{ij} w^j + \sum_{j=1}^N \bar{G}^{ij} \frac{\partial w^j}{\partial n} \right] \quad (5.10)$$

5.1.2 Computation of Stresses

We know from equation (4.22) that the primary variable

$$w(\tilde{\xi}) = \int_{\Gamma} w^* \theta_n \, ds - \int_{\Gamma} w \theta_n^* \, ds + \int_{\Omega} w^* \frac{M}{D} \, d\Omega; \quad \tilde{\xi} \in \Omega \quad (5.11)$$

In order to compute stresses, the second derivatives of w are required.

$$\frac{\partial^2 w}{\partial \xi_1^2} = \int_{\Gamma} \frac{\partial^2 w^*}{\partial \xi_1^2} \theta_n \, ds - \int_{\Gamma} \frac{\partial^2 \theta_n^*}{\partial \xi_1^2} w \, ds + \int_{\Omega} \frac{\partial^2 w^*}{\partial \xi_1^2} \frac{M}{D} \, d\Omega \quad (5.12)$$

similarly

$$\frac{\partial^2 w}{\partial \xi_2^2} = \int_{\Gamma} \frac{\partial^2 w^*}{\partial \xi_2^2} \theta_n \, ds - \int_{\Gamma} \frac{\partial^2 \theta_n^*}{\partial \xi_2^2} w \, ds + \int_{\Omega} \frac{\partial^2 w^*}{\partial \xi_2^2} \frac{M}{D} \, d\Omega \quad (5.13)$$

We know that the fundamental solution of the Poisson's equation

$$w^* = \frac{1}{2\pi} \ln \frac{1}{r} \quad (5.14)$$

where r is as defined in equation (4.23a)

$$\frac{\partial^2 w^*}{\partial \xi_1^2} = -\frac{(1-2\rho_1^2)}{2\pi r^2} \text{ and} \quad (5.15)$$

$$\frac{\partial^2 w^*}{\partial \xi_2^2} = -\frac{(1-2\rho_2^2)}{2\pi r^2} \quad (5.16)$$

where ρ_1 and ρ_2 are as defined in equation (4.25)

Therefore

$$M_1 = -D \left(\frac{\partial^2 w}{\partial \xi_1^2} + \nu \frac{\partial^2 w}{\partial \xi_2^2} \right) \quad (5.17)$$

$$M_2 = -D \left(\frac{\partial^2 w}{\partial \xi_2^2} + \nu \frac{\partial^2 w}{\partial \xi_1^2} \right) \text{ and} \quad (5.18)$$

$$M_{12} = -M_{21} = D(1-\nu) \frac{\partial^2 w}{\partial \xi_1 \partial \xi_2} \quad (5.19)$$

Substituting equations(5.12) to (5.16)) into equations (5.17) to (5.19), we get the bending moments, from which stresses can be calculated directly.

5.2 Other Boundary Conditions

In the case of other boundary conditions, equation (5.1) and (5.2) cannot be solved independently of each other, since for each equation the number of boundary unknowns are either less or more than the available boundary element equations. For n boundary elements, equations (5.3) and (5.4) yields $2n$ equations and equation (5.5) yields another m equations for the domain nodal values of M . The total number of quantities is $2n+m$ which have to be solved simultaneously for $2n+m$ unknowns (i.e. $2n$ boundary values and m values of M).

5.3 Numerical Examples

Two generalized programs in FORTRAN 77 have been developed for the analysis of beams and plates of varying thickness based on the proposed method of analysis discussed in chapters 3 and 4.

1. NPBEAM

2. NPLATE

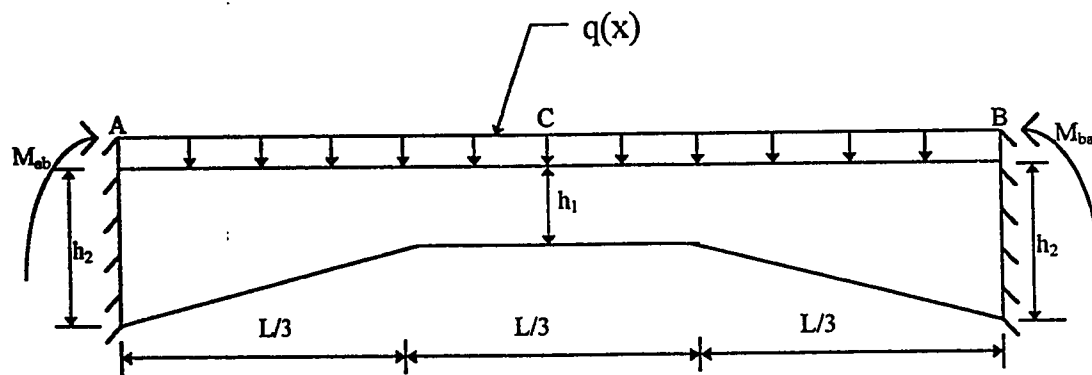
In order to investigate the capability and accuracy of the proposed method and programs, some numerical examples have been solved and the results are compared with the available analytical and numerical methods.

5.3.1 Program NPBEAM

The detail description of the program NPBEAM and its flow chart is given in Appendix A. This program is developed for the analysis of continuous non-prismatic beams based on the theory discussed in chapter 3. This program can be used for the analysis of beams with the linearly or parabolically varying depth and carrying any kind of loading, partial or entire span loading. To demonstrate the simplicity and accuracy of the procedure and to test the reliability of the program, four different examples have been solved. The results are compared with the available analytical and numerical solutions to demonstrate the efficiency and accuracy of the program.

5.3.1.1 Example 1 : A symmetrical non-prismatic beam with linearly varying depth

Consider a single span beam with linearly varying depth carrying uniformly distributed load and both edges are fixed as shown in Figure 5-1. This problem is solved by BEM, using the program NPBEAM. The results for the fixed end moments, deflection and moment at the mid span are given in Table 5-1. The second column shows the results obtained by NPBEAM, third column shows the results obtained from PCA Tables [5] and the last column shows the results obtained from STRUDL [66] by dividing the beam into 10 elements.



Where $L = 15$ units, $q = 1$ unit, $h_1 = 1$ unit and $h_2 = 2$ units

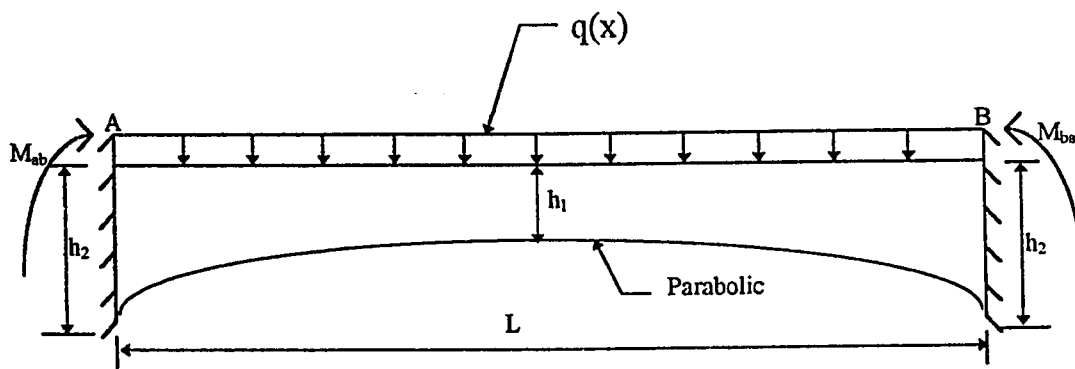
Figure 5-1 Beam with linearly varying thickness carrying uniformly distributed load

Table 5-1 Fixed end moments of the beam shown in Figure 5-1

Variable	BEM	PCA	STRUDL
M_{ab}	23.346	23.346	23.3818
M_c	4.807	4.779	4.895
w_c	372.80	-	372.798

5.3.1.2 Example 2 : A symmetrical non-prismatic beam with parabolically varying depth

Consider a single span symmetrical non-prismatic beam with parabolic varying depth carrying uniformly distributed load and both edges are fixed as shown in Figure 5-2. This problem is solved by BEM, using the program NPBEAM. The results are given in Table 5-2. The second column shows the results obtained by NPBEAM, third column shows the results obtained from PCA Tables [5] and the last column shows the results obtained from STRUDL by dividing the beam into 15 elements. From Table 5-2, we can see that the results are exactly the same as the results obtained from PCA.



Where $L = 10$ units, $q = 1$ unit, $h_1 = 1$ unit and $h_2 = 2$ units

Figure 5-2 Beam with parabolic varying thickness carrying uniformly distributed load

Table 5-2 Fixed end moments of the beam shown in Figure 5-2

Variable	BEM	PCA	STRUDL
M_{ab}	10.253	10.250	10.2025
M_c	2.74	2.74	2.69
w_c	110.75	-	110.23

5.3.1.3 Example 3 : Generation of PCA Tables for a non-prismatic beams

Consider the following problem of an un-symmetrical beam section with parabolic & straight haunch as shown in Figure 5-3a and 5-3b. Table 5-3 & Table 5.4, similar to PCA table 26 and table 52 respectively, for the fixed moments of the two different kinds of problems have been generated for illustration purpose. Fixed end moment coefficients for uniformly distributed load and concentrated loads are given for different members with parabolically and linearly varying depth. The left haunch of the beam shown in Figure 5-3a and 5-3b is kept constant while the right haunch is given 35 sets of dimensions. The lengths of the haunches in terms of the length of the member are 0.1, 0.2, 0.3, 0.4, 0.5, 0.75 and 1.00. Depth of the haunches are given by the ratio r and its values are 0.4, 0.6, 1.0, 1.5 and 2.0. Concentrated loads are placed at points 0.3, 0.5 and 0.7 of the length of the member. The following notations are used in Figure 5-3 and in Table 5-3 & Table 5-4.

a_A = ratio of the length of haunch at end A to the length of span

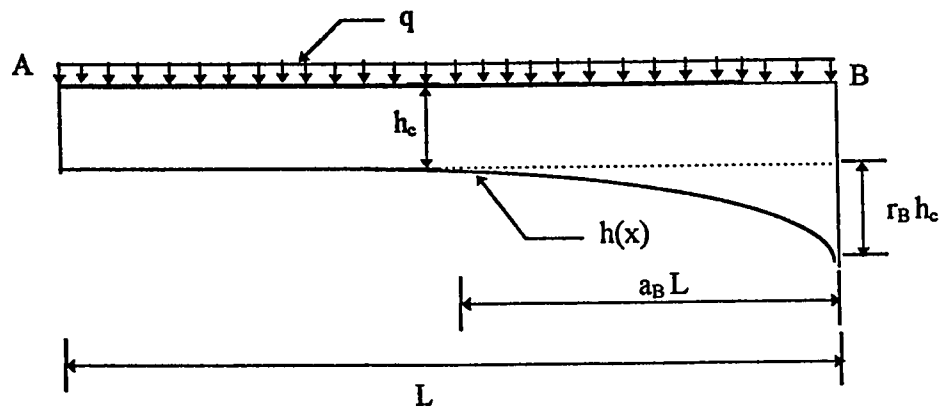
a_B = ratio of the length of haunch at end B to the length of span

b = ratio of the distance from loading point to end A to the length of span

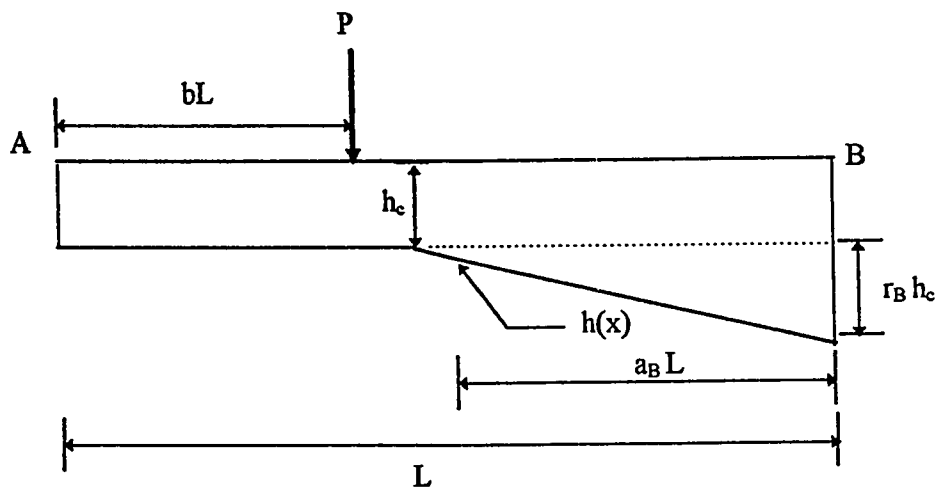
h_A = depth of the member at end A

h_B = depth of the member at end B

h_C = depth of the member at uniform section



(a) Parabolic haunch, Carrying uniformly distributed load



(b) Straight haunch, Carrying concentrated load

Figure 5-3 Unsymmetrical haunch beam

L = Total length of the member

M_{ab} = fixed end moment (F.E.M) at end A of the member

M_{ba} = fixed end moment (F.E.M) at end B of the member

P = concentrated load.

r_A = $\frac{h_A - h_C}{h_C}$ at end A

r_B = $\frac{h_B - h_C}{h_C}$ at end B

w = intensity of uniform load.

Table 5-3 Fixed end moment coefficient for the beam shown in Figure 5-3a
(Similar to PCA Table 26)

Right Hanuch		Moment coefficient	
a	r_B	M_{ab}	M_{ba}
0.1	0.40	0.0795	0.0914
	0.60	0.0782	0.0940
	1.00	0.0765	0.0976
	1.50	0.0751	0.1006
	2.00	0.0742	0.1025
0.2	0.40	0.0768	0.0975
	0.60	0.0745	0.1025
	1.00	0.0712	0.1098
	1.50	0.0684	0.1161
	2.00	0.0665	0.1205
0.3	0.40	0.0750	0.1018
	0.60	0.0720	0.1088
	1.00	0.0673	0.1196
	1.50	0.0633	0.1292
	2.00	0.0605	0.1362
0.4	0.40	0.0739	0.1045
	0.60	0.0703	0.1129
	1.00	0.0647	0.1266
	1.50	0.0596	0.1395
	2.00	0.0559	0.1491
0.5	0.40	0.0732	0.1058
	0.60	0.0693	0.1152
	1.00	0.0630	0.1310
	1.50	0.0571	0.1464
	2.00	0.0527	0.1586
0.75	0.40	0.0717	0.1059
	0.60	0.0672	0.1157
	1.00	0.0600	0.1331
	1.50	0.0533	0.1514
	2.00	0.0481	0.1668
1.00	0.40	0.0698	0.1045
	0.60	0.0648	0.1137
	1.00	0.0568	0.1300
	1.50	0.0492	0.1473
	2.00	0.0439	0.1622

Table 5-4 Fixed end moment coefficient for the beam shown in Figure 5-3 b
(Similar to PCA Table 52)

Right Haunch		Fixed end moment coefficient					
		b					
		0.3		0.5		0.7	
a	r _B	M _{ab}	M _{ba}	M _{ab}	M _{ba}	M _{ab}	M _{ba}
0.1	0.40	0.1426	0.0724	0.1164	0.1432	0.0534	0.1672
	0.60	0.1412	0.0753	0.1137	0.1489	0.0505	0.1734
	1.00	0.1393	0.0795	0.11	0.1568	0.0464	0.1821
	1.50	0.1378	0.0826	0.1072	0.1628	0.0434	0.1885
	2.00	0.1369	0.0847	0.1055	0.1669	0.0415	0.1931
0.2	0.40	0.1391	0.0806	0.1102	0.1585	0.0476	0.1809
	0.60	0.1363	0.0871	0.1049	0.1701	0.0423	0.1929
	1.00	0.1321	0.0968	0.0971	0.188	0.0346	0.2104
	1.50	0.1287	0.1049	0.0908	0.203	0.0285	0.2247
	2.00	0.1264	0.1104	0.0866	0.213	0.0246	0.2339
0.3	0.40	0.1368	0.087	0.1064	0.1684	0.0453	0.1865
	0.60	0.1327	0.097	0.099	0.1862	0.0387	0.2017
	1.00	0.1262	0.1134	0.0874	0.215	0.0289	0.2252
	1.50	0.1203	0.1286	0.0771	0.2412	0.0208	0.2452
	2.00	0.1161	0.1396	0.07	2599	0.0155	0.2586
0.4	0.40	0.1355	0.0911	0.1044	0.1734	0.0449	0.1849
	0.60	0.1305	0.1041	0.0958	0.195	0.0383	0.2001
	1.00	0.1219	0.1274	0.0815	0.2328	0.0283	0.2241
	1.50	0.1134	0.1513	0.1679	0.2704	0.0199	0.2453
	2.00	0.107	0.1702	0.0578	0.2994	0.0144	0.2597
0.5	0.40	0.1346	0.093	0.1032	0.1733	0.0448	0.1812
	0.60	0.1291	0.1079	0.0941	0.1958	0.0384	0.195
	1.00	0.1192	0.1364	0.1788	0.2371	0.0288	0.2175
	1.50	0.1087	0.1666	0.0636	0.2812	0.0020	0.2382
	2.00	0.1001	0.1969	0.0519	0.3174	0.0153	0.253
0.75	0.40	0.1297	0.0915	0.0972	0.1648	0.0432	0.1734
	0.60	0.1227	0.1058	0.0872	0.1823	0.0369	0.1837
	1.00	0.1108	0.1343	0.0717	0.2137	0.0281	0.2003
	1.50	0.0987	0.1694	0.058	0.2471	0.0212	0.216
	2.00	0.0886	0.2037	0.0748	0.2756	0.0167	0.2281
1.00	0.40	0.1243	0.0884	0.0954	0.1582	0.0436	0.1686
	0.60	0.1153	0.1002	0.0849	0.1718	0.0375	0.1667
	1.00	0.1004	0.1222	0.0691	0.1952	0.0288	0.1894
	1.50	0.0861	0.1468	0.0554	0.2185	0.022	0.201
	2.00	0.0751	0.1684	0.0459	0.2372	0.0176	0.2098

5.3.1.4 Example 4 : Continuous bridge girder of variable depth

Consider the following problem of a continuous bridge girder of variable depth as shown in Figure 5-4. The depth of the girder varies parabolically, Depth at the mid span and at both ends of the beam = 2.5 units and at the intermediate supports = 7.5 units. An analytical solution using slope deflection and PCA tables for this problem is available [1]. This problem has also been solved using STRUDL by dividing the beam into 20, 40, 60 and 80 elements and the results of bending moments, slopes and support reactions are given in Table 5-5. In this table, second column represents the analytical results, third column shows the results obtained by BEM and the last three columns show the results obtained by STRUDL. In the table, M stands for moment, θ stands for rotation and R stands for support reaction and subscripts for the support number i.e. M_2 means moment at support 2 and θ_1 means rotation at support 1 and so on.

Since the execution time of the computer mainly depends on the number of equations to be solved, It would be meaningful to compare BEM and FEM in this aspect. BEM does not require discretization of the beam therefore, it needs to solve four simultaneous equation for each span whereas in FEM, domain of the beam needs to be discretized, therefore, the number of equations to be solved increases as the number of elements increases.

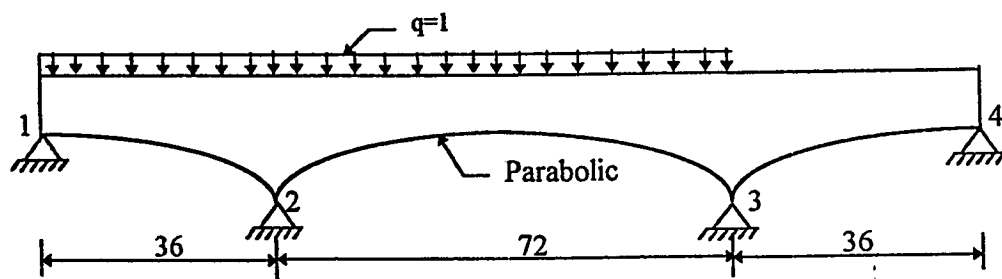


Figure 5-4 Continuous bridge girder with parabolically varying depth

Table 5-5 Bending moments, slopes and support reactions of the beam shown in Figure 5-4

Variable	Analytical	BEM	STRU DL		
		3 elements*	20 elem.*	40 elem.*	80 elem.*
M ₂	594.0	593.75	589.13	592.56	593.44
M ₃	453.0	452.81	450.39	452.18	452.64
θ ₁	289.20	290.25	288.56	289.20	290.0
θ ₂	423.84	423.92	426.12	425.58	424.66
θ ₃	614.89	615.50	618.35	617.85	616.39
θ ₄	772.76	775.54	776.80	776.24	775.51
R ₁	1.50	1.51	1.64	1.54	1.52
R ₂	72.85	72.45	72.29	72.41	72.44
R ₃	46.15	46.62	46.58	46.61	46.62
R ₄	-12.5	-12.58	-12.5	-12.6	-12.57
No. Eqns.	-	12	38	78	158

* Total number of elements for 3 spans.

5.3.2 Program NPLATE

The detailed description of the program NPLATE and its flow chart is given in Appendix A. This program is developed for the analysis of plates of linearly varying stiffness based on the theory discussed in the previous chapter. This program can be used for the analysis of plates with linearly varying stiffness and carrying any kind of loading, partial or entire span loading. To demonstrate the simplicity and capability of the procedure and to test the reliability of the program five different examples have been solved. The results are compared with the available analytical and numerical solutions to demonstrate the efficiency and accuracy of the program. The most distinguished feature of this program is that, it needs a simple 3 lines input file describing the dimensions of the plate, boundary conditions, type of loading and its value and the variation in thickness which can be seen in the sample input file for the program NPLATE in Appendix A.

5.3.2.1 *Example 1 : Simply supported square plate carrying a concentrated load at the center*

Consider a simply supported square plate of side a with uniform thickness carrying a concentrated load at the center as shown in Figure 5-5. This problem is solved just to demonstrate the accuracy of BEM when dealing with the problems involving singular solutions. Using the program NPLATE and dividing the plate into 60 boundary elements, bending moments along the center line parallel to X- axis are calculated.

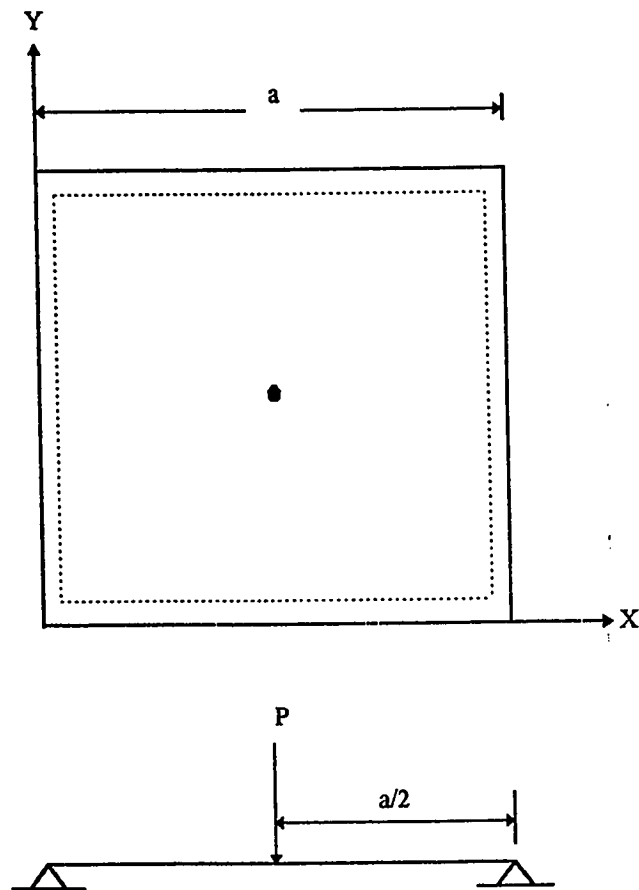


Figure 5-5 Simply Supported Square Plate of Uniform Thickness carrying a central Concentrated Load

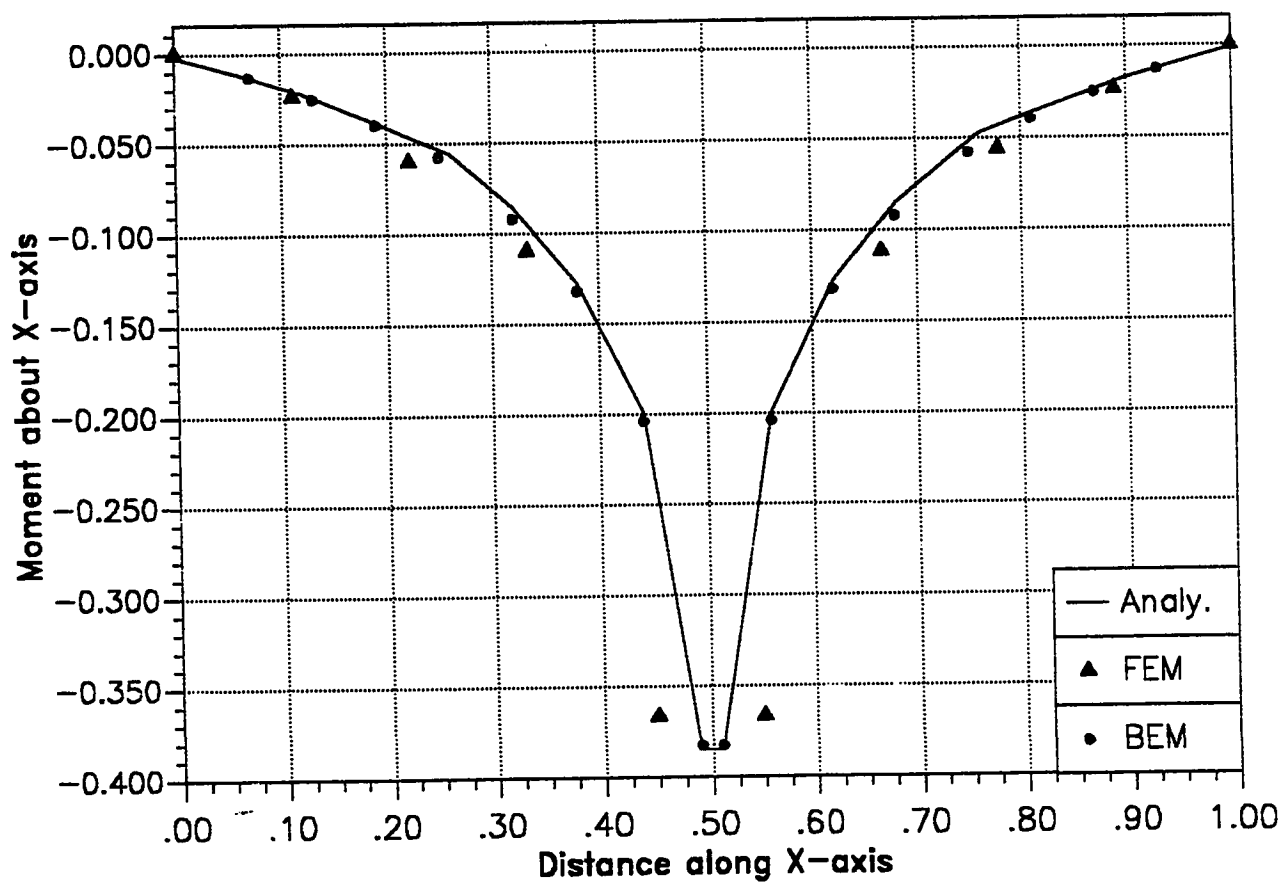


Figure 5-6 Profile of M_x along the center line of the plate parallel to X-axis
as shown in Figure 5-5

In order to compare the results, the problem is solved by finite element method by dividing a quadrant of plate into 16 nine-noded Lagrangian elements. The moment, M_x along the center line parallel to X-axis is calculated and plotted against the length of the plate as shown in Figure 5-6. From the plot one can easily see that the boundary element method could give the results more accurate than FEM near the center particularly.

5.3.2.2 Example 2 : Simply supported plate with linearly varying thickness carrying linearly varying load

Consider a simply supported square plate of side a with linearly varying thickness and carrying linearly varying load as shown in Figure 5-7. The analytical solution of this problem is available [30] and it was solved using the Levy's method. This problem is solved using program NPLATE by dividing the plate into 84 boundary elements as shown in Figure 5-8 and using FEM by dividing half of the plate into 32 nine-noded Lagrangian elements as shown in Figure 5-9. Deflection and moment about x and y axes are calculated along the center line of the plate parallel to y-axis. The results are shown in Table 5-6, Table 5-7 and Table 5-8.

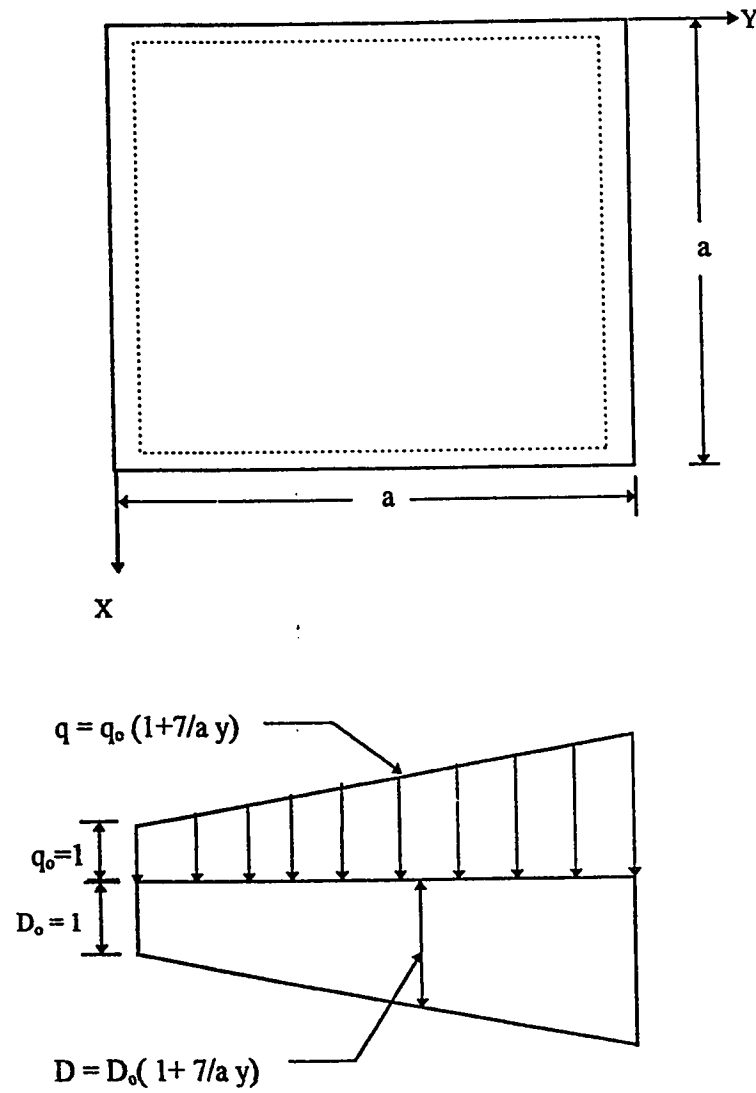


Figure 5-7 Simply supported plate with linearly varying thickness carrying linearly varying load.

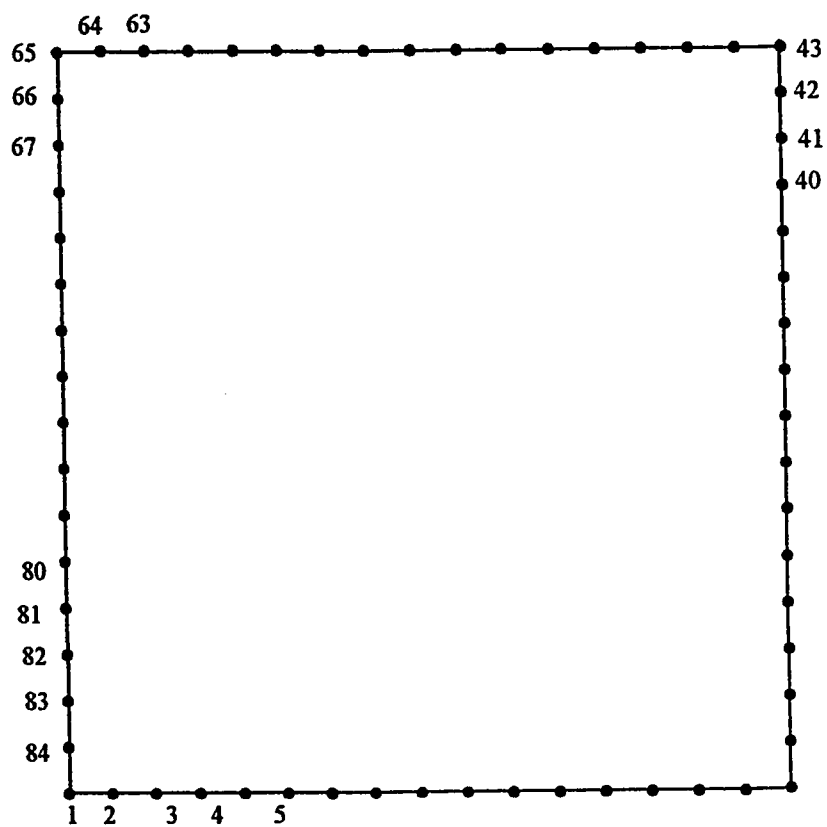


Figure 5-8 Boundary discretization of the plate shown in Figure 5-7

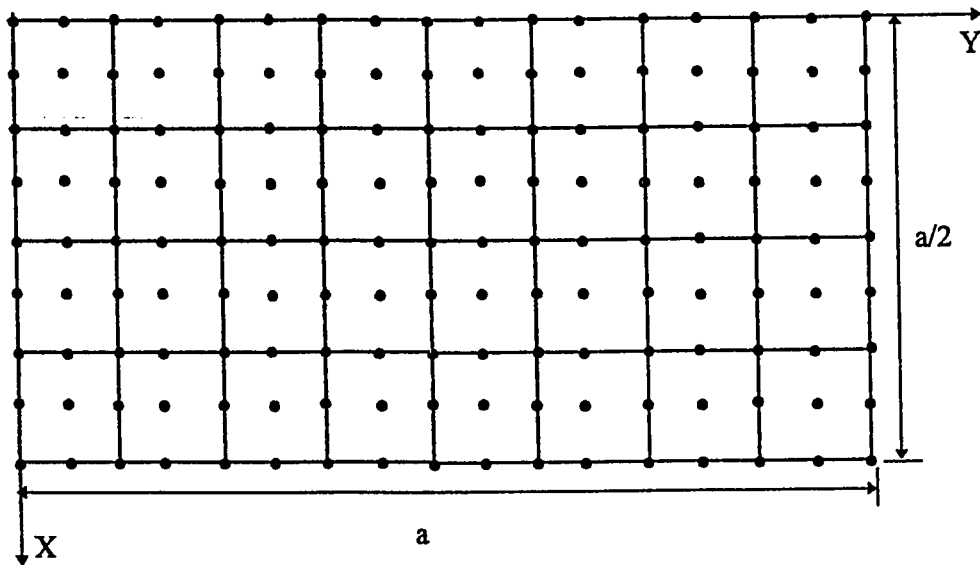


Figure 5-9 Finite Element mesh for the half of the plate shown in Figure 5-7

**Table 5-6 Values of the deflection coefficient k of the plate shown in Figure 5-7
along the line $x = a/2$ for $\nu = 0.16$**

$$w = k \frac{4q_0 a^4}{\pi^5 D_0}$$

Y/a	BEM	Analytical	FEM
0.0163	0.0215	0.0220	0.0210
0.1750	0.2050	0.2072	0.1990
0.3350	0.3070	0.3095	0.3000
0.4940	0.3270	0.3270	0.3210
0.6530	0.2762	0.2787	0.2730
0.8120	0.1725	0.1834	0.1690
0.9720	0.0284	0.0307	0.0270

**Table 5-7 Values of the coefficient k of M_x of the plate shown in Figure 5-7
along the line $x = a/2$ for $\nu = 0.16$**

$$M_x = k \frac{4q_0 a^2}{\pi^3}$$

Y/a	BEM	Analytical	FEM
0.0163	0.4080	0.4190	0.4000
0.1750	0.5920	0.5935	0.5300
0.3350	1.2137	1.2171	1.1100
0.4940	1.6600	1.6630	1.5300
0.6530	1.7584	1.7613	1.6000
0.8120	1.3855	1.3965	1.1900
0.9720	0.2658	0.2787	0.2200

**Table 5-8 Values of the coefficient k of M_y of the plate shown in Figure 5-7
along the line $x = a/2$ for $\nu = 0.16$**

$$M_y = k \frac{4q_0 a^2}{\pi^3}$$

Y/a	BEM	Analytical	FEM
0.0163	0.1050	0.1082	0.0900
0.1750	0.8650	0.8676	0.8100
0.3350	1.2548	1.2683	1.2300
0.4940	1.4773	1.4778	1.4400
0.6530	1.5098	1.5116	1.4900
0.8120	1.2155	1.2277	1.2500
0.9720	0.2678	0.2754	0.3000

5.3.2.3 Example 3 : Simply supported plate with linearly varying stiffness in both direction

Consider a simply supported plate with linearly varying rigidity in both directions along x and y axes and carrying uniformly distributed load as shown in Figure 5-10. This problem is solved using program NPLATE by dividing the plate into 84 boundary elements and using FEM by dividing the whole plate into 64 nine-noded Lagrangian elements as shown in Figure 5-11. Deflection and moment, M_x along the center line $x = a/2$ are calculated and the results are shown in Table 5-9. Since no analytical solution is available for this problem, the results are compared with FEM results only. The results of this problem obtained by program NPLATE are very close to the FEM results.

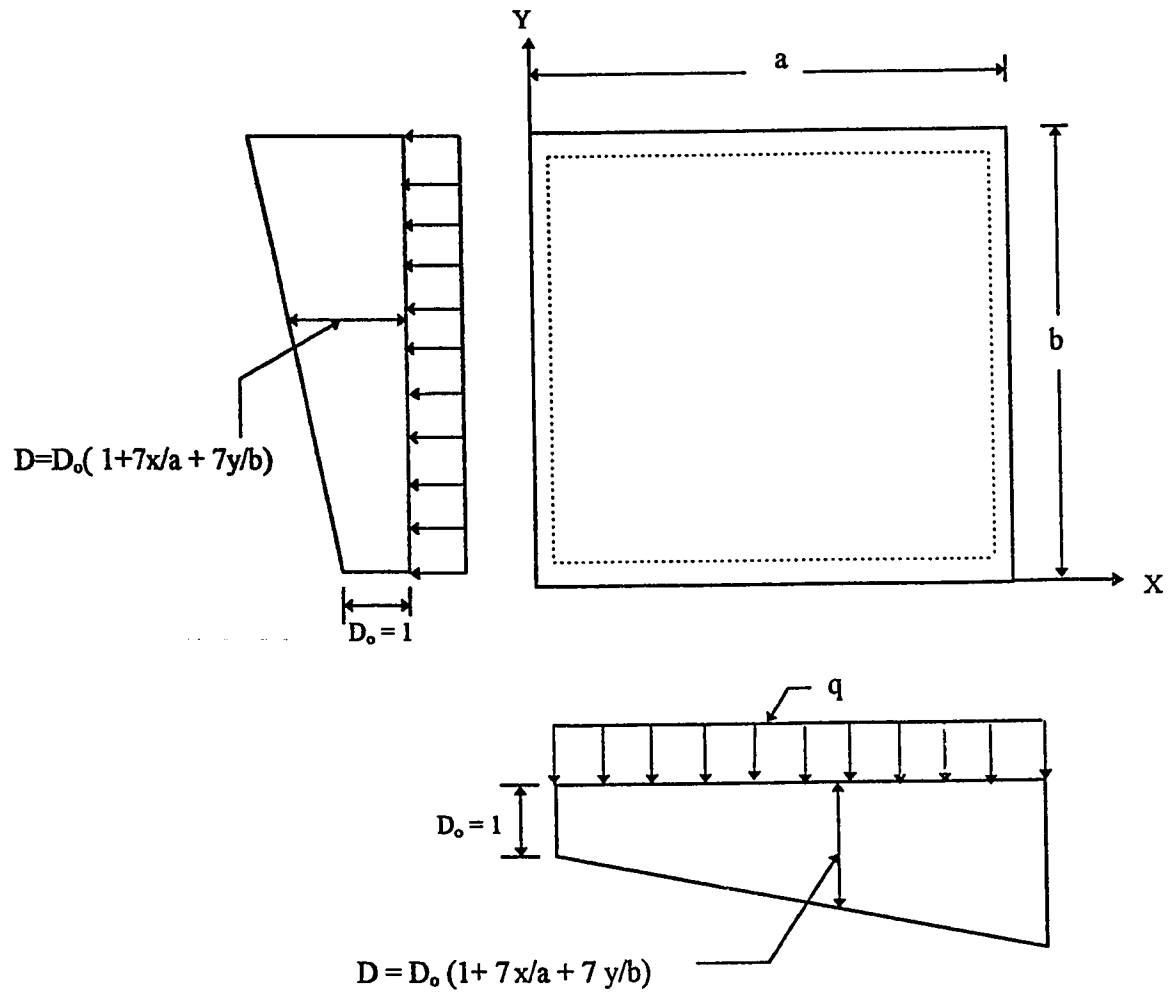


Figure 5-10 Simply supported plate with varying rigidity in both x and y directions.

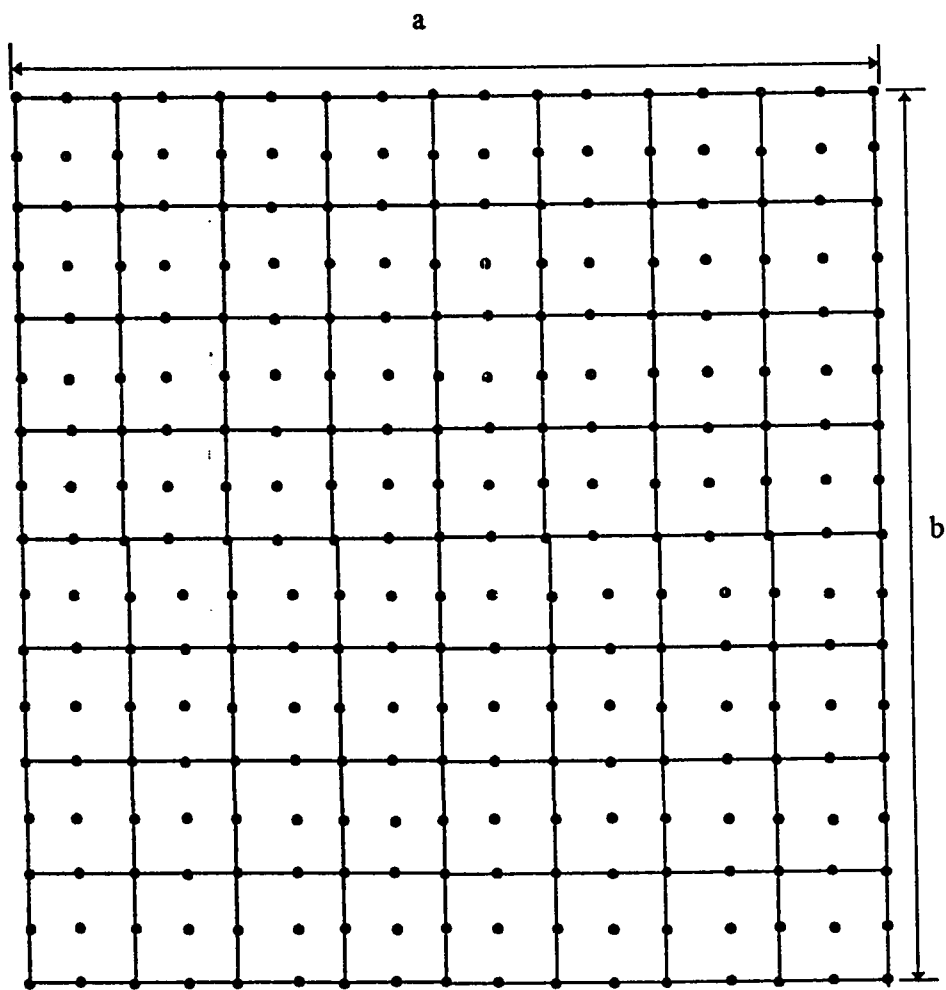


Figure 5-11 Finite element mesh for the plate shown in Figure 5-10.

Table 5-9 Deflection and M_x along the center line $x = a/2$ of the plate shown in Figure 5-10, for $a=b=1$, $\nu = 0.3$, $D_0 = 1$ and $q = 1$.

y	Deflection, w		M_x	
	BEM	FEM	BEM	FEM
0.125	0.01986	0.01850	0.2252	0.2207
0.250	0.03288	0.03155	0.3291	0.3185
0.500	0.04042	0.03890	0.3706	0.3670
0.750	0.02717	0.02670	0.2853	0.2771
0.875	0.01527	0.01485	0.187	0.1785

5.3.2.4 Example 4 :Plate with linearly varying stiffness, three sides simply supported and the fourth side fixed.

Consider a plate with linearly varying stiffness and carrying linearly varying load with the boundary conditions, three edges are simply supported and one edge is fixed as shown in Figure 5-12. This problem is solved using program NPLATE by dividing the plate boundary into 84 boundary elements. In the finite element solution the plate is divided into 64 nine-noded Lagrangian finite elements as shown in Figure 5-11. Bending moments at various points along the built in edge are calculated and are shown in Table 5-10. Since there is no analytical solution available for this particular problem, the results are compared with finite element results only. However, for the case of uniform rigidity, analytical solution is available [30]. For the testing purpose, the results of the uniform plate shown in Figure 5-13 are also compared in Table 5-11.

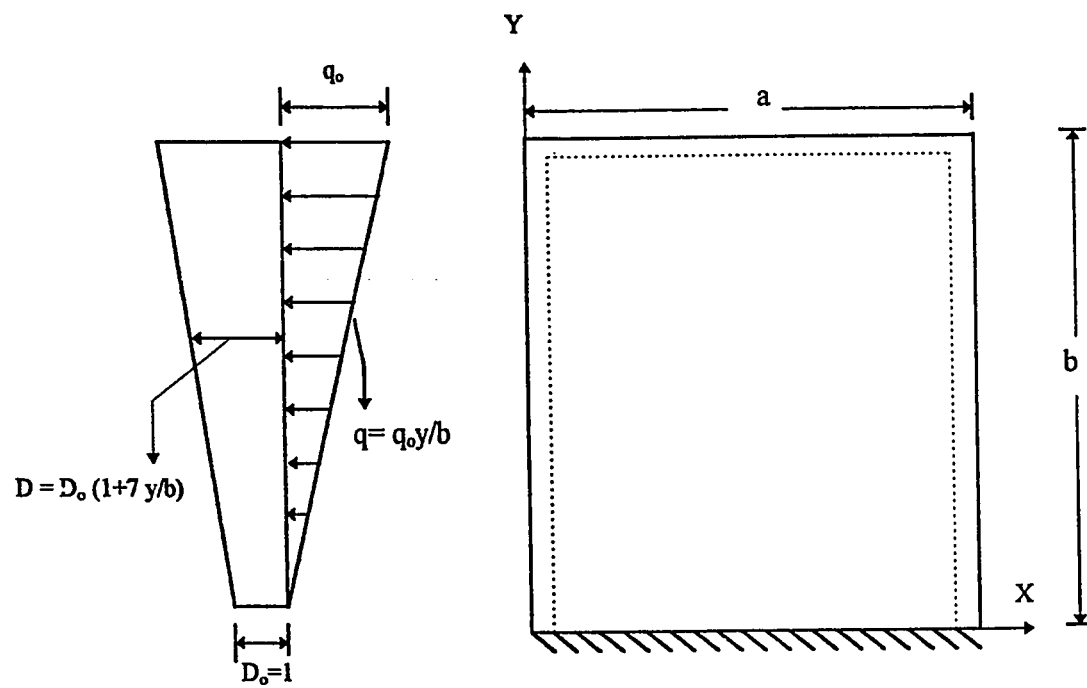


Figure 5-12 Plate with linearly varying thickness, three sides simply supported, the fourth side fixed and carrying linearly varying load

Table 5-10 Moment M_x along the fixed edge of the plate shown in Figure 5-12

for $a=b=1$, $\nu = 0.16$, $D_0 = 1$ and $q_0 = 1$

X/a	BEM	FEM
0.1250	0.0409	0.0349
0.2500	0.0644	0.0602
0.3750	0.0763	0.0751
0.5000	0.0982	0.0840
0.6250	0.0763	0.0751
0.7500	0.0644	0.0602
0.8750	0.0409	0.0349

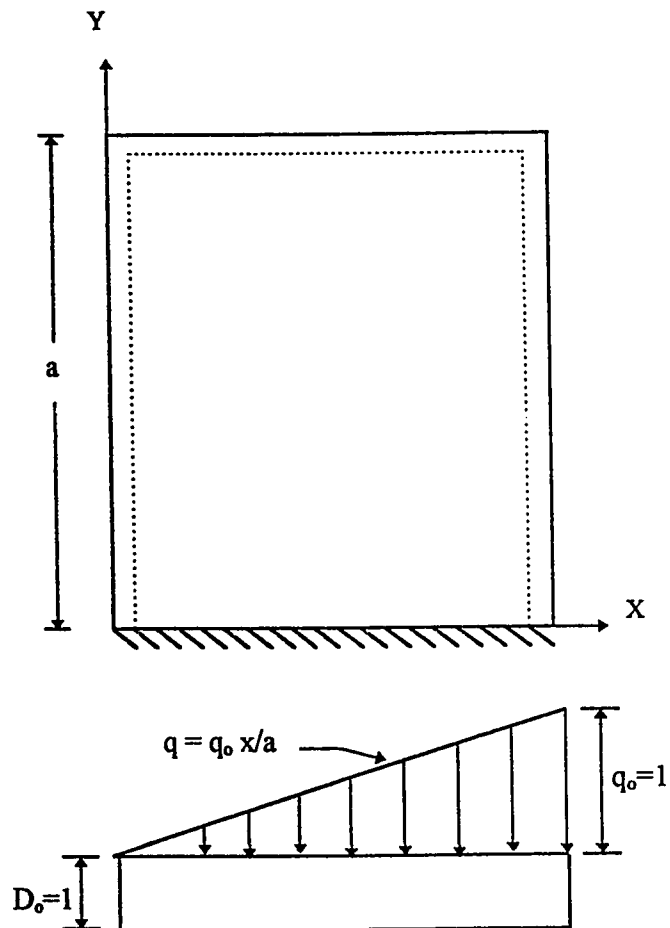


Figure 5-13 Square Plate with Uniform thickness three sides simply supported, the fourth side fixed and carrying linearly varying load .

Table 5-11 Moment, M_x along the fixed edge of the plate shown in Figure 5-13
for $a=b=1, \nu = 0.3, D_o = 1$ and $q_o = 1$

X/a	BEM	Analytical	FEM
0.1250	0.0135	0.0130	0.0130
0.2500	0.0248	0.0250	0.0239
0.3750	0.0347	0.0350	0.0338
0.5000	0.0420	0.0420	0.0415
0.6260	0.0440	0.0440	0.0429
0.7500	0.0413	0.0400	0.0402
0.8750	0.0300	0.0260	0.0280

CHAPTER 6

SUMMARY AND CONCLUSIONS

An exact method of analysis of non-prismatic beams and a simple method of analysis of plates with linearly varying stiffness is proposed. The fundamental solutions for non-prismatic beams of linear and parabolic depth profiles are derived and exact relations are obtained in terms of variables over the nodes. The method has also been extended to solve continuous non-prismatic beams carrying any kind of loading. A generalized computer program NPBEAM is developed in FORTRAN 77 to readily apply the proposed method. Several numerical examples are solved using this program and the results are compared with available numerical and analytical solutions. The accuracy of the method has also been verified by the standard PCA Tables .

In the case of plates, a simple method of analysis of plates with linearly varying stiffness is proposed incorporating the boundary element method. The method is to divide the biharmonic differential equation of transverse deflection of the plate into two

second order Poisson's equations and it greatly simplifies the complexities of the problem. A generalized computer program NPLATE is developed in FORTRAN 77 to readily apply the proposed method for the analysis of plate with linearly varying stiffness under any kind of loading, partial or entire span loading. Several numerical examples are solved using this program and the accuracy of the method has also been verified by comparing the results of the available analytical and numerical solutions.

Based on the theory developed and the results obtained for the numerical examples and the verification of the results by the standard methods, the following conclusions are drawn :

Non-Prismatic Beams :

1. For the case of beams, prismatic or non-prismatic, as the boundary conditions are satisfied exactly in the modelling., the BEM leads to exact solution. Comparison of the results obtained from BEM with those from classical analysis affirms the exactness of this method.
2. PCA Tables are available only for linearly and parabolic haunched beams fixed at both ends and carrying concentrated or full span uniformly distributed loading. The program NPBEAM can be used to generate similar tables for other cases.

3. The computer program NPBEAM is capable of analyzing beam with general stiffness variation. In view of its accuracy, it can be used as a reliable tool to check the accuracy of other methods.
4. In addition to the accuracy, the number of boundary element equations involved in the analysis of continuous non-prismatic beams are much less than those involved in other numerical methods such as finite difference and finite element methods.

Non-Prismatic Plates :

1. The proposed boundary element method provides a simple and reasonably accurate solution of plates with linearly varying stiffness. The method is particularly efficient for simply supported plates.
2. An important advantage of the BEM is its capability of dealing with problems which involves singular solutions as demonstrated by the example of a plate subjected to a central concentrated load.
3. The computer program NPLATE has been developed to readily analyze a plate. The program requires a simple input file which can be prepared with ease.

APPENDIX A

**DESCRIPTION OF THE PROGRAMS NPBEAM &
NPLATE**

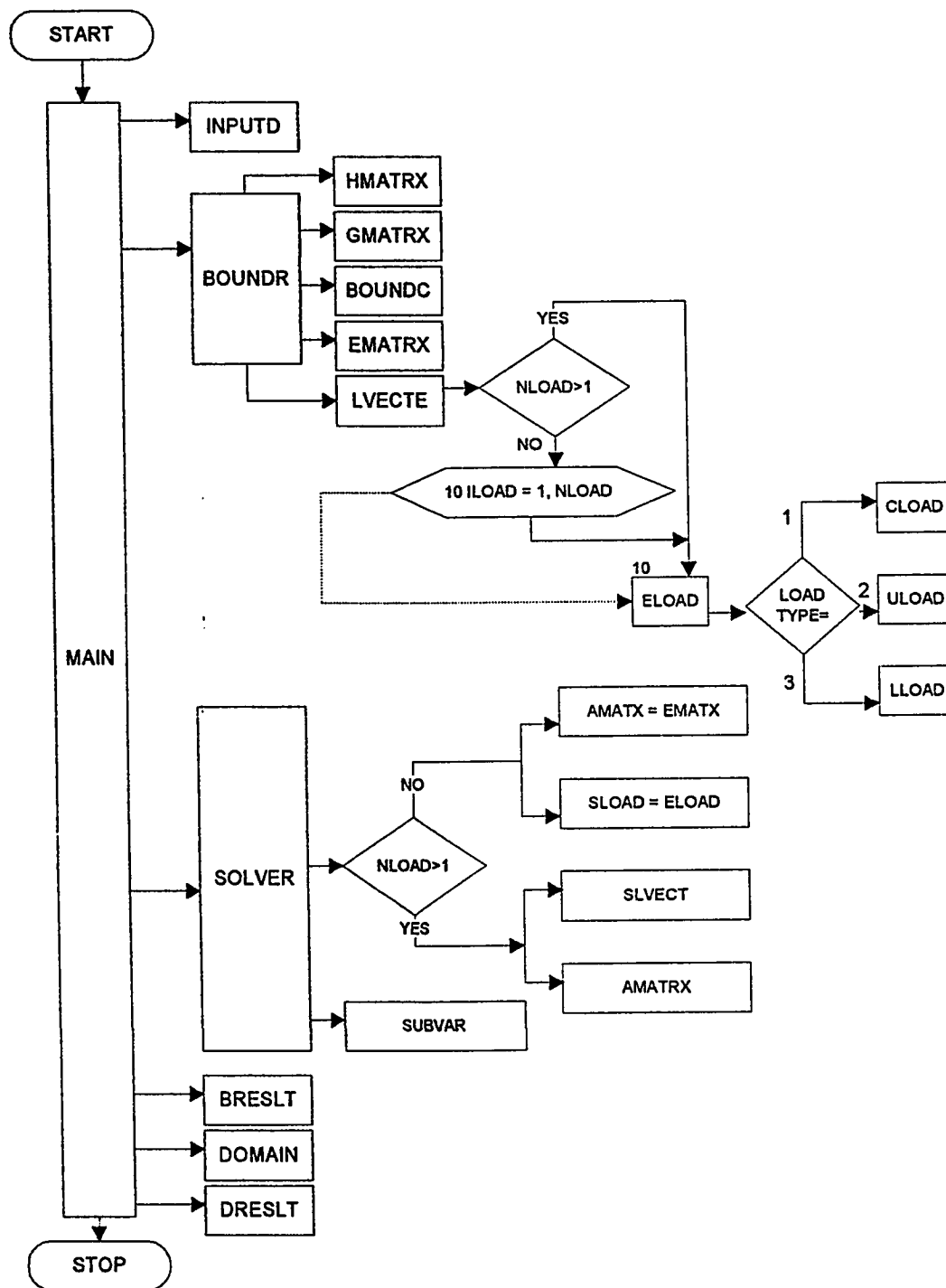


Figure A-1Flow chart of the program NPBEAM

A.1 Description of the program NPBEAM

The flow chart of the program NPBEAM is shown in the previous page. The main program consists of a series of call statements of subprograms.

- INPUTD** : This subroutine reads the required input data
- BOUNDR** : This is just a master-subroutine for the computation of the boundary details and forming the final boundary element equation i.e.
 $[A]\{X\}=\{Z\}.$
- HMATRX** : This subroutine computes the elements of H-matrix to calculate boundary variables.
- GMATRX** : This subroutine computes the elements of G-matrix to calculate boundary variables.
- BOUNDC** : This subroutine applies the boundary conditions of the beam ends for calculating the combined boundary element matrix for each span.
- EMATRX** : This subroutine calculates the combined boundary element matrix for each span.
- LVECTE** : This subroutine calculates the load vector i.e. $\{B\}$ for each span.
- CLOAD** : This subroutine calculates the elements of the load vector for concentrated load.

- ULOAD** : This subroutine calculates the elements of the load vector for uniformly distributed load.
- LLOAD** : This subroutine calculates the elements of the load vector for Varying load.
- SOLVER** : This subroutine calculates the combined boundary element matrix [A], load vector {Z} for the whole structure and solves for the boundary unknowns.
- BRESLT** : This subroutine prints the boundary results
- DOMAIN** : This subroutine calculates all the required variables at the domain points.
- DRESLT** : This subroutine prints the domain results.

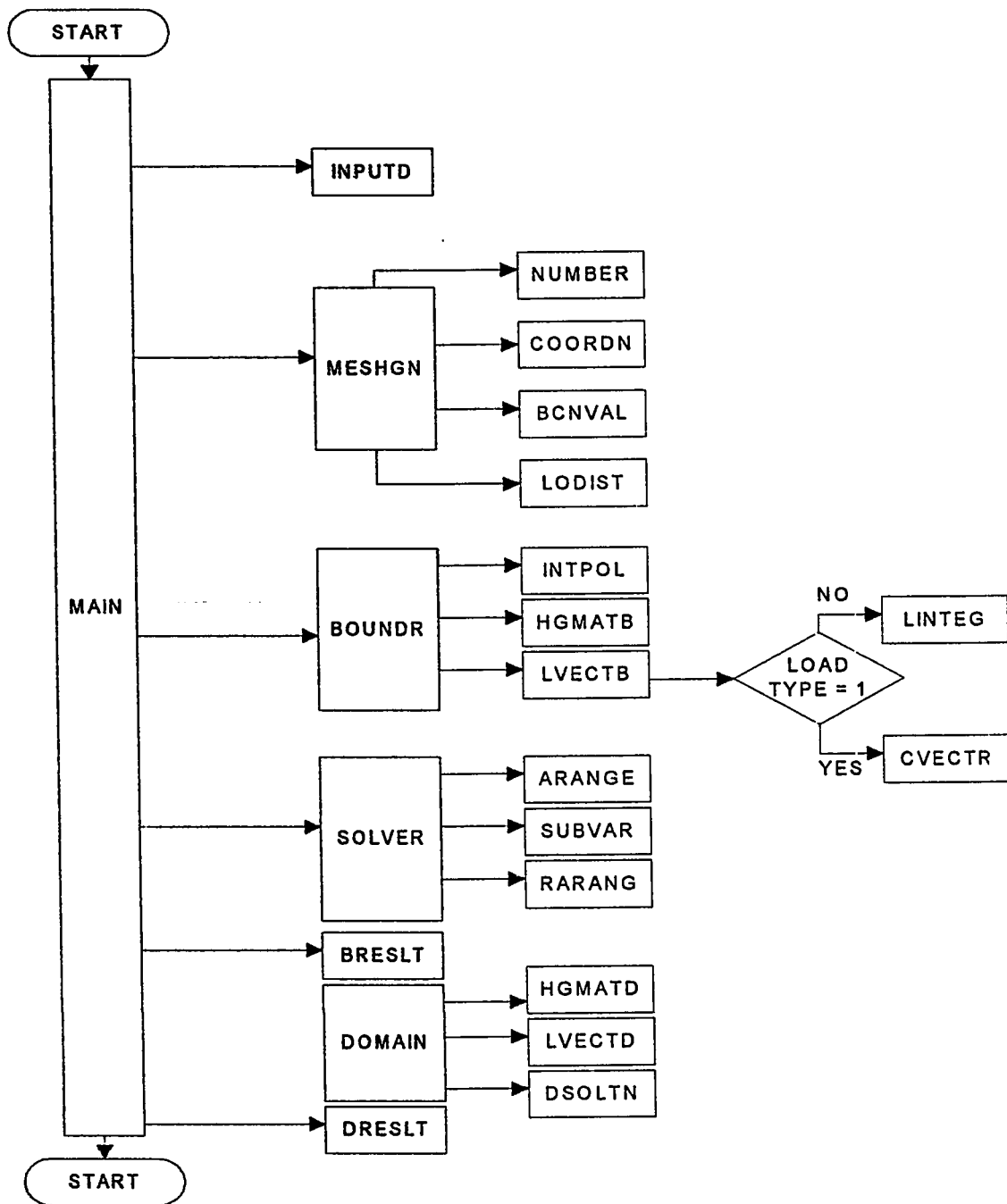


Figure A-2 Flow chart of the program NPLATE

A.2 Description of the program NPLATE

The flow chart of the program NPLATE is shown in the previous page. The main program consists of a series of call statements of subprograms.

INPUTD : This subroutine reads the required input data

MESHGN : This is just a master-subroutine for mesh generation, it calls the following four subroutines.

NUMBER : This subroutine generates the node numbers of all the boundary elements.

COORDN : This subroutine generates the nodal coordinates all the boundary elements.

BCNVAL : This subroutine assigns the boundary condition and its prescribed value from the input data, to each boundary node.

LODIST : This subroutine calculates intensity of the load at various points of the domain, if there is any distributed load.

BOUNDR : This is also a master-subroutine for the computation of the boundary details and forming the final boundary element equation i.e. $[A]\{X\} = \{Z\}$. it calls the following three subroutines.

INTPOL : This subroutine computes the interpolation functions.

- HGMATB** : This subroutine computes the elements of H and G matrices to calculate boundary variables.
- LVECTB** : This subroutine computes the elements of load vector {B}. It calls **LINTEG**, if there is any domain load and **CVECTR**, if there is any concentrated load.
- SOLVER** : This subroutine calculates the combined boundary element matrix [A], load vector {Z} for the whole structure and solves for the boundary unknowns.
- BRESLT** : This subroutine prints the boundary results
- DOMAIN** : This subroutine calculates all the required variables at the domain points. It calls **HGMATD** for computing the elements of H and G matrices for domain and **LVECTD** for computing elements of the load vector for domain.
- DRESLT** : This subroutine prints the domain results.

A.3 Example Problem

Following is the input file of program NPBEAM for the numerical example 5.3.1.3.

```

EXAMPLE PROBLEM OF 3-SPAN CONTINUOUS BRIDGE GIRDER
UNITS  FREE
3
1 0.0
2 36.0
3 108.0
4 144.0
1 2  2.5  7.5  1
1 1  1.0  0.0  36.0
2 2  2.5  7.5  1
1 1  1.0 -36.0  36.0
3 2  2.5  7.5  0
1 1

```


Following is the output file of program NPBEAM for the numerical example 5.3.1.3.

EXAMPLE PROBLEM OF 3-SPAN CONTINUOUS BRIDGE GIRDER
UNITS FREE

NUMBER OF SPANS..... = 3

NODE #	XCORD
1	0.0
2	36.0
3	108.0
4	144.0

ISPAN	TYPE	VARTN
1	PARABOLIC	0.00154
2	PARABOLIC	0.00154
3	PARABOLIC	0.00154

LOADING :

ISPAN	TYPE	VALUE	LENGTH
1	1	1.0	36
2	1	1.0	72

BOUNDARY CONDITIONS :

LEFT END	RIGHT END
HINGED	HINGED

BOUNDARY VARIABLES :

NODE	DEFL.	ROTATION	MOMENT	REACTION
1	0.000000E+00	0.290250E+03	0.000000E+00	-0.150679E+01
2	0.000000E+00	-0.423922E+03	0.593746E+03	0.724510E+02
3	0.000000E+00	0.615498E+03	0.452809E+03	0.466209E+02
4	0.000000E+00	-0.775545E+03	0.000000E+00	-0.125781E+02

A.4 Example Problem

Following is the input file of program NPLATE for the numerical example 5.3.2.2.

```
TEST PROBLEM-EXAMPLE 5.3.2.2
UNITS : FREE
1.0  1.0  21  21  0.3  3  1
1.0  0.0  7.0
1.0  0.0  7.0
1 1 1 1
0
```

Following is the output file of program NPLATE for the numerical example 5.3.2.2.

RESULTS OF THE PROGRAM NPLATE

PLATE TYPE : NON-PRISMATIC
 STIFFNESS VARIES LINEARLY ALONG Y-AXIS
 BOUNDARY CONDITIONS..: ALL SIMPLY SUPPORTED
 TYPE OF LOADING.....: LINEARLY VARYING LOAD ALONG Y-AXIS

STRUCTURAL DATA :

UNITS :FREE
 LENGTH OF THE PLATE ALONG X-AXIS ...: 1.000
 LENGTH OF THE PLATE ALONG Y-AXIS ...: 1.000
 INITIAL STIFFNESS OF THE PLATE.....: 1.000
 VARIATION OF STIFFNESS IN X-DIR....: 0.000
 VARIATION OF STIFFNESS IN Y-DIR....: 7.000
 VARIATION OF LOAD IN X-DIR: 0.000
 VARIATION OF LOAD IN Y-DIR: 7.000
 YOUNGS MODULUS, E: 1.000
 POISSONS RATIO: 0.160

NUMBER OF BOUNDARY ELEMENTS: 84

RESULTS OF THE PLATE ANALYSIS :

RESULTS ON THE BOUNDARY :

NODE#	X-CORD	Y-CORD	DEFLECTION	ROTATION
1	0.000E+00	0.000E+00	0.0000E+00	0.522E-05
2	0.323E-01	0.000E+00	0.0000E+00	-0.191E-02
3	0.968E-01	0.000E+00	0.0000E+00	-0.559E-02
4	0.129E+00	0.000E+00	0.0000E+00	-0.730E-02
5	0.194E+00	0.000E+00	0.0000E+00	-0.104E-01
6	0.226E+00	0.000E+00	0.0000E+00	-0.118E-01
7	0.290E+00	0.000E+00	0.0000E+00	-0.141E-01
8	0.323E+00	0.000E+00	0.0000E+00	-0.150E-01
9	0.387E+00	0.000E+00	0.0000E+00	-0.165E-01
10	0.419E+00	0.000E+00	0.0000E+00	-0.169E-01
11	0.484E+00	0.000E+00	0.0000E+00	-0.174E-01
12	0.516E+00	0.000E+00	0.0000E+00	-0.174E-01
13	0.581E+00	0.000E+00	0.0000E+00	-0.169E-01
14	0.613E+00	0.000E+00	0.0000E+00	-0.165E-01
15	0.677E+00	0.000E+00	0.0000E+00	-0.150E-01
16	0.710E+00	0.000E+00	0.0000E+00	-0.141E-01
17	0.774E+00	0.000E+00	0.0000E+00	-0.118E-01
18	0.806E+00	0.000E+00	0.0000E+00	-0.104E-01
19	0.871E+00	0.000E+00	0.0000E+00	-0.730E-02
20	0.903E+00	0.000E+00	0.0000E+00	-0.559E-02
21	0.968E+00	0.000E+00	0.0000E+00	-0.191E-02
22	0.100E+01	0.000E+00	0.0000E+00	0.644E-05
23	0.100E+01	0.645E-01	0.0000E+00	-0.373E-02
24	0.100E+01	0.968E-01	0.0000E+00	-0.543E-02

25	0.100E+01	0.161E+00	0.0000E+00	-0.838E-02
26	0.100E+01	0.194E+00	0.0000E+00	-0.962E-02
27	0.100E+01	0.258E+00	0.0000E+00	-0.116E-01
28	0.100E+01	0.290E+00	0.0000E+00	-0.124E-01
29	0.100E+01	0.355E+00	0.0000E+00	-0.135E-01
30	0.100E+01	0.387E+00	0.0000E+00	-0.138E-01
31	0.100E+01	0.452E+00	0.0000E+00	-0.141E-01
32	0.100E+01	0.484E+00	0.0000E+00	-0.141E-01
33	0.100E+01	0.548E+00	0.0000E+00	-0.136E-01
34	0.100E+01	0.581E+00	0.0000E+00	-0.132E-01
35	0.100E+01	0.645E+00	0.0000E+00	-0.121E-01
36	0.100E+01	0.677E+00	0.0000E+00	-0.114E-01
37	0.100E+01	0.742E+00	0.0000E+00	-0.971E-02
38	0.100E+01	0.774E+00	0.0000E+00	-0.873E-02
39	0.100E+01	0.839E+00	0.0000E+00	-0.654E-02
40	0.100E+01	0.871E+00	0.0000E+00	-0.534E-02
41	0.100E+01	0.935E+00	0.0000E+00	-0.275E-02
42	0.100E+01	0.968E+00	0.0000E+00	-0.139E-02
43	0.968E+00	0.100E+01	0.0000E+00	-0.139E-02
44	0.935E+00	0.100E+01	0.0000E+00	-0.274E-02
45	0.871E+00	0.100E+01	0.0000E+00	-0.528E-02
46	0.839E+00	0.100E+01	0.0000E+00	-0.644E-02
47	0.774E+00	0.100E+01	0.0000E+00	-0.850E-02
48	0.742E+00	0.100E+01	0.0000E+00	-0.938E-02
49	0.677E+00	0.100E+01	0.0000E+00	-0.108E-01
50	0.645E+00	0.100E+01	0.0000E+00	-0.114E-01
51	0.581E+00	0.100E+01	0.0000E+00	-0.122E-01
52	0.548E+00	0.100E+01	0.0000E+00	-0.124E-01
53	0.484E+00	0.100E+01	0.0000E+00	-0.125E-01
54	0.452E+00	0.100E+01	0.0000E+00	-0.124E-01
55	0.387E+00	0.100E+01	0.0000E+00	-0.118E-01
56	0.355E+00	0.100E+01	0.0000E+00	-0.114E-01
57	0.290E+00	0.100E+01	0.0000E+00	-0.102E-01
58	0.258E+00	0.100E+01	0.0000E+00	-0.938E-02
59	0.194E+00	0.100E+01	0.0000E+00	-0.752E-02
60	0.161E+00	0.100E+01	0.0000E+00	-0.644E-02
61	0.968E-01	0.100E+01	0.0000E+00	-0.405E-02
62	0.645E-01	0.100E+01	0.0000E+00	-0.274E-02
63	-0.173E-05	0.100E+01	0.0000E+00	0.119E-05
64	-0.173E-05	0.968E+00	0.0000E+00	-0.139E-02
65	-0.173E-05	0.903E+00	0.0000E+00	-0.407E-02
66	-0.173E-05	0.871E+00	0.0000E+00	-0.534E-02
67	-0.173E-05	0.806E+00	0.0000E+00	-0.768E-02
68	-0.173E-05	0.774E+00	0.0000E+00	-0.873E-02
69	-0.173E-05	0.710E+00	0.0000E+00	-0.106E-01
70	-0.173E-05	0.677E+00	0.0000E+00	-0.114E-01
71	-0.173E-05	0.613E+00	0.0000E+00	-0.127E-01
72	-0.173E-05	0.581E+00	0.0000E+00	-0.132E-01
73	-0.173E-05	0.516E+00	0.0000E+00	-0.139E-01
74	-0.173E-05	0.484E+00	0.0000E+00	-0.141E-01
75	-0.173E-05	0.419E+00	0.0000E+00	-0.140E-01
76	-0.173E-05	0.387E+00	0.0000E+00	-0.138E-01
77	-0.173E-05	0.323E+00	0.0000E+00	-0.130E-01
78	-0.173E-05	0.290E+00	0.0000E+00	-0.124E-01
79	-0.173E-05	0.226E+00	0.0000E+00	-0.107E-01

80	-0.173E-05	0.194E+00	0.0000E+00	-0.962E-02
81	-0.173E-05	0.129E+00	0.0000E+00	-0.699E-02
82	-0.173E-05	0.968E-01	0.0000E+00	-0.543E-02
83	-0.173E-05	0.645E-01	0.0000E+00	-0.373E-02
84	-0.173E-05	0.323E-01	0.0000E+00	-0.191E-02

SOLUTION AT DOMAIN POINTS :

X-CORD Y-CORD DEFLECTION ROTATION-X ROTATION-Y MOMENT-X MOMENT-Y

SOLUTION ALONG THE MID SPAN PARALLEL TO X-AXIS

0.50	0.02	0.2077E-01	0.1135E-06	0.1728E-01	-0.8992E-01	-0.3511E-01
0.50	0.05	0.6174E-01	0.6947E-07	0.1668E-01	-0.2806E+00	-0.1194E+00
0.50	0.08	0.1011E+00	0.7720E-07	0.1569E-01	-0.4494E+00	-0.2140E+00
0.50	0.11	0.1378E+00	0.8086E-07	0.1447E-01	-0.5984E+00	-0.3176E+00
0.50	0.15	0.1716E+00	0.9398E-07	0.1312E-01	-0.7298E+00	-0.4282E+00
0.50	0.18	0.2019E+00	0.1029E-06	0.1169E-01	-0.8453E+00	-0.5436E+00
0.50	0.21	0.2288E+00	0.1107E-06	0.1024E-01	-0.9470E+00	-0.6617E+00
0.50	0.24	0.2522E+00	0.1180E-06	0.8792E-02	-0.1036E+01	-0.7807E+00
0.50	0.27	0.2720E+00	0.1255E-06	0.7359E-02	-0.1115E+01	-0.8983E+00
0.50	0.31	0.2884E+00	0.1329E-06	0.5956E-02	-0.1183E+01	-0.1013E+01
0.50	0.34	0.3014E+00	0.1340E-06	0.4588E-02	-0.1244E+01	-0.1122E+01
0.50	0.37	0.3111E+00	0.1390E-06	0.3262E-02	-0.1296E+01	-0.1225E+01
0.50	0.40	0.3176E+00	0.1368E-06	0.1977E-02	-0.1342E+01	-0.1319E+01
0.50	0.44	0.3209E+00	0.1356E-06	0.7359E-03	-0.1381E+01	-0.1403E+01
0.50	0.47	0.3213E+00	0.1330E-06	-0.4623E-03	-0.1414E+01	-0.1476E+01
0.50	0.50	0.3188E+00	0.1381E-06	-0.1618E-02	-0.1441E+01	-0.1535E+01
0.50	0.53	0.3136E+00	0.1259E-06	-0.2729E-02	-0.1461E+01	-0.1580E+01
0.50	0.56	0.3056E+00	0.1288E-06	-0.3800E-02	-0.1474E+01	-0.1609E+01
0.50	0.60	0.2951E+00	0.1228E-06	-0.4826E-02	-0.1479E+01	-0.1621E+01
0.50	0.63	0.2821E+00	0.1233E-06	-0.5810E-02	-0.1475E+01	-0.1614E+01
0.50	0.66	0.2668E+00	0.1135E-06	-0.6748E-02	-0.1461E+01	-0.1588E+01
0.50	0.69	0.2492E+00	0.1053E-06	-0.7639E-02	-0.1435E+01	-0.1542E+01
0.50	0.73	0.2295E+00	0.9992E-07	-0.8478E-02	-0.1394E+01	-0.1475E+01
0.50	0.76	0.2078E+00	0.1001E-06	-0.9260E-02	-0.1336E+01	-0.1386E+01
0.50	0.79	0.1843E+00	0.9513E-07	-0.9982E-02	-0.1258E+01	-0.1275E+01
0.50	0.82	0.1591E+00	0.8897E-07	-0.1063E-01	-0.1157E+01	-0.1141E+01
0.50	0.85	0.1324E+00	0.8623E-07	-0.1121E-01	-0.1029E+01	-0.9837E+00
0.50	0.89	0.1044E+00	0.8475E-07	-0.1170E-01	-0.8696E+00	-0.8039E+00
0.50	0.92	0.7537E-01	0.8260E-07	-0.1208E-01	-0.6743E+00	-0.6015E+00
0.50	0.95	0.4555E-01	0.9632E-07	-0.1236E-01	-0.4382E+00	-0.3767E+00
0.50	0.98	0.1524E-01	0.2102E-06	-0.1250E-01	-0.1557E+00	-0.1305E+00

SOLUTION ALONG THE MID SPAN PARALLEL TO X-AXIS

0.02	0.50	0.1717E-01	0.1394E-01	-0.7928E-04	0.2260E-01	-0.2260E-01
0.05	0.50	0.5123E-01	0.1372E-01	-0.2373E-03	0.6171E-01	-0.6172E-01
0.08	0.50	0.8453E-01	0.1331E-01	-0.3943E-03	0.8833E-01	-0.8832E-01
0.11	0.50	0.1166E+00	0.1274E-01	-0.5474E-03	0.1047E+00	-0.1047E+00
0.15	0.50	0.1472E+00	0.1204E-01	-0.6944E-03	0.1129E+00	-0.1129E+00
0.18	0.50	0.1759E+00	0.1123E-01	-0.8333E-03	0.1145E+00	-0.1145E+00
0.21	0.50	0.2024E+00	0.1032E-01	-0.9623E-03	0.1112E+00	-0.1112E+00
0.24	0.50	0.2267E+00	0.9325E-02	-0.1080E-02	0.1044E+00	-0.1044E+00

0.27	0.50	0.2483E+00	0.8266E-02	-0.1184E-02	0.9541E-01	-0.9541E-01
0.31	0.50	0.2674E+00	0.7152E-02	-0.1272E-02	0.8542E-01	-0.8542E-01
0.34	0.50	0.2836E+00	0.5993E-02	-0.1344E-02	0.7538E-01	-0.7537E-01
0.37	0.50	0.2969E+00	0.4795E-02	-0.1395E-02	0.6608E-01	-0.6608E-01
0.40	0.50	0.3072E+00	0.3559E-02	-0.1418E-02	0.5821E-01	-0.5820E-01
0.44	0.50	0.3145E+00	0.2274E-02	-0.1394E-02	0.5220E-01	-0.5219E-01
0.47	0.50	0.3184E+00	0.8500E-03	-0.1226E-02	0.4826E-01	-0.4826E-01
0.50	0.50	0.3188E+00	0.1207E-06	-0.1618E-02	-0.1441E+01	-0.1535E+01
0.53	0.50	0.3185E+00	-0.8676E-03	-0.1984E-02	0.4886E-01	-0.4886E-01
0.56	0.50	0.3147E+00	-0.2292E-02	-0.1768E-02	0.5228E-01	-0.5227E-01
0.60	0.50	0.3075E+00	-0.3577E-02	-0.1664E-02	0.5823E-01	-0.5823E-01
0.63	0.50	0.2972E+00	-0.4813E-02	-0.1576E-02	0.6611E-01	-0.6611E-01
0.66	0.50	0.2839E+00	-0.6011E-02	-0.1486E-02	0.7540E-01	-0.7540E-01
0.69	0.50	0.2677E+00	-0.7170E-02	-0.1387E-02	0.8544E-01	-0.8544E-01
0.73	0.50	0.2487E+00	-0.8283E-02	-0.1278E-02	0.9543E-01	-0.9543E-01
0.76	0.50	0.2270E+00	-0.9342E-02	-0.1159E-02	0.1044E+00	-0.1044E+00
0.79	0.50	0.2028E+00	-0.1033E-01	-0.1028E-02	0.1112E+00	-0.1112E+00
0.82	0.50	0.1762E+00	-0.1124E-01	-0.8882E-03	0.1145E+00	-0.1145E+00
0.85	0.50	0.1475E+00	-0.1206E-01	-0.7393E-03	0.1129E+00	-0.1129E+00
0.89	0.50	0.1169E+00	-0.1276E-01	-0.5829E-03	0.1048E+00	-0.1048E+00
0.92	0.50	0.8472E-01	-0.1332E-01	-0.4205E-03	0.8836E-01	-0.8836E-01
0.95	0.50	0.5135E-01	-0.1373E-01	-0.2538E-03	0.6172E-01	-0.6172E-01
0.98	0.50	0.1721E-01	-0.1394E-01	-0.8468E-04	0.2254E-01	-0.2254E-01
0.50	0.50	0.3191E+00	-0.7005E-04	-0.1694E-02	-0.1436E+01	-0.1530E+01

REFERENCES

- [1] Timoshenko, S. P. & Young., D. H., "Theory of Structures" 2nd ed. McGraw-Hills, New York, 1965.
- [2] Hibbeler, R "Structural Analysis" 2nd ed. Macmillan publishing company, New York, 1990
- [3] Ghali, A & Neville., A. M., "Structural Analysis" McGraw-Hill book company, 1981.
- [4] Cross, H. and Morgan, N. "Continuous Frames of Reinforced Concrete" 14th ed. John wiley and sons, Inc. New York. 126-155, 1958.
- [5] Portland Cement Association, "Handbook of Frame constants". Beam factors and moment coefficients for variable sections PCA Chicago III, 1958.
- [6] Fertis, D.G. and Zobel, E., "Equivalent system for the deflection of variable stiffness members". Jr. Struct. Div., ASCE, 1958.
- [7] Fertis, D.G., "Dynamics and Vibration of Structures". John Wiley & Sons Inc. New York, 251-294, 1973
- [8] Fertis, D.G. and Michael E. Keene, "Elastic and Inelastic of Analysis of Non prismatic Members". Jr. Str. Eng. Vol. 116 No 2 Feb. 1990.
- [9] Fertis, D.G. and Rajesh Taneja, "Equivalent systems for inelastic analysis of prismatic and non-prismatic members". Jr. Str. Eng. Vol. 117 No 2 Feb. 1991.
- [10] Bruno A. Boley, " on the accuracy of the Bernoulli-Euler theory for beams of variable section ", J. Appl. Mech. 30, 373-378, 1963
- [11] Just, D. J., "plane frameworks of tapering box and I-section", Proc. ASCE Vol.103, No. ST1, 71-86, Jan., 1977.
- [12] Rutledge, W.D. and Beskos, D.E., "Dynamic analysis of linearly tapered beams", J. Sound & Vibrations, Vol. 79, No. 3, 457-462, 1981.
- [13] Resende and Doyle, "NONPRI-an effective non-prismatic three dimensional beam finite element". Compt. Struct., Vol. 14(1-2) 71-77, 1981.

- [14] Mumuni, I., "A finite element model for the analysis and optimal design of beams and plates with variable flexural rigidity". Thesis presented to Vanderbilt Univ., at Nashville, Tenn, 1983.
- [15] Kosko, E., "Uniform element modeling of tapered frame members", J. Structural Division, ASCE, Vol. 108, No. St1, 245-264, Jan., 1982.
- [16] Karabalis, D.L. and Beskos, D.E., "Static, Dynamic and Stability analysis of structures composed of tapered beams". Comput. Struct. Vol. 16, No. 6, 731-748, 1983.
- [17] Banerjee, J.R. and Williams, F.W., "Exact Bernoulli-Euler dynamic stiffness matrix for a range of tapered beams". International J. for Num. Methods in Engineering, Vol. 21, 2289-2302, 1985.
- [18] Arvind K. Gupta, "Vibration of tapered beams". J. Struct. Engg., Vol. 111, No. 1, Jan. 1985.
- [19] Hota V. S. Ganga Rao and C. C. Spyrakos. "Closed form series solutions of boundary value problems with variable properties". Comput. & Struct., Vol. 23, No. 2, 211-215, 1986.
- [20] Miyamoto, Y., Iwasaki, S. and Deto, H., "BEM Approach to Analysis of Bridge Structures". Boundary Elements VIII Conference, 1986.
- [21] Dimitrios Karamanlidis and Raja Jasti, "Geometrically nonlinear finite element analysis of tapered beams". Comput. & Struct. , Vol. 25, No. 6, 825-830, 1987.
- [22] Raymond R. Funk and Kai-tih Wang, "Stiffness of Non-prismatic members". Jr. Struct. Eng. Vol. 114 No 2, 489-494 Feb. 1988.
- [23] Sen Yung Lee, Huei Yaw Ke and Yee Hsiung Kuo., "Exact static deflection of a non-uniform Bernoulli-Euler beam with general elastic end restraints". Comput. & Struct., Vol. 36, No. 1, 91-97, 1990.
- [24] Nasreddin EI-Mezaini, Can Baikaya, and Ergin, "Analysis of Frames with Non prismatic Members". Jr. Struct. Engg. Vol. 117, No 6 June 1991
- [25] Sen Yung Lee and Shueei Muh Lin., "Exact vibration solutions for non-uniform Timoshenko beams with attachments"., AIAA Journal, Vol. 30, No. 12, 2930-2934, Dec., 1992.

- [26] Kathnelson, A. N., "High eigen frequency of non-uniform Bernoulli-Euler beams", Int. J. Mech. Sci. Vol. 34, No. 10, 805-808, 1992
- [27] Aristizabal-Ochoa, J.D., "Static, stability and vibrations of non-prismatic beams and columns", J. Sound and Vibrations, Vol. 162, No. 3, 441-455, 1993.
- [28] Kuo, Y. H. and Lee, S. Y., "Deflection of non-uniform beams resting on a nonlinear elastic foundation", Comput. & Struct. Vol. 51, No. 5, 513-519, 1994.
- [29] Reissner, M. E., "Remark on the theory of bending of plates of variable thickness", Journal of Mathematics and Physics, Vol. 16, 43-45, 1937.
- [30] Timoshenko, S. P. and Woinowsky-Krieger, S., "Theory of Plates and Shells". McGraw-Hill Kogakusha, Tokyo, 1959.
- [31] Rudolph Szilard, Dr. -Ing., PE., "Theory and analysis of Plates". Rainbow-Bridga Book Co., Ltd., 1974
- [32] Ugural, A. C., "Stresses in plates and shells". McGraw-Hill book company, 1981
- [33] Conway, H. D., "Symmetrically loaded circular plates of variable thickness", J. Appl. Mech. Vol. 15, 1-6, 1948.
- [34] Mansfield, E. H., "On the analysis of elastic plates of variable thickness", Quarterly Journal of Appl. Mech. and Appl. Mathematics, Vol. 15, 167-192, 1962.
- [35] Fertis, D.G. and Kozama, A., "Solution of the deflection of variable thickness plates by the method of equivalent systems". J. Industrial Mathematics, 12 (1), 1962.
- [36] Fertis, D.G. and Cunningham, H., "Equivalent systems for shear deflections of variable thickness members". J. Industrial Mathematics, 12 (1), 1962.
- [37] Demeter G. Fertis and Milos M. Mijatov, "Equivalent Systems for variable thickness plates". J. Engg. Mech. 115, No. 10 Oct. 2287-2300, 1989
- [38] Appl., F.C., and Byers, N.F., "Fundamental frequency of simply supported rectangular plates with varying thickness", J. Appl. Mech., Vol. 32, No. 1, 163-168, 1965.
- [39] Cheung, Y. K., "Finite strip method analysis of elastic slabs". Jr. Struct. Div., ASCE Vol. 94, 1365-1378, 1968.

- [40] Cheung, Y. K., "Finite strip method in the analysis of elastic plates with two opposite simply supported ends". Jr. Struct. Div., ASCE 7051, 1-7, 1968
- [41] Lord, H. W., and Yousef, S. S. "Elastic bending of circular plates of variable thickness : an analytical and experimental study"., Int. J. Mech. Sci., Vol. 12, No. 5, 417-434, 1970
- [42] Mukhopadhyay, M., "A semi-analytic solution for rectangular plate bending". Comput. struct. 9, 81-87, 1978.
- [43] Uko, C.E.A. and Cusens, A.R., "Application of spline finite strip analysis to variable depth bridges". Communications in applied numerical methods, Vol. 4, 273-278, 1988.
- [44] Fariborz, S. J. & Poubohloul, A., "Application of extended Kantorovich method to the bending of variable thickness plate". Comput. Struct. Vol. 31, No. 6, 1989.
- [45] Kerr, A. D., "An extension of Kantorovich method". Quart. Appl. Math. 26, 219-229, 1968.
- [46] Azad, A.K., Abdullah, M.K. and Baluch, M.H., "Analysis of radially tapered circular plate sectors by finite difference"., Proc., CIVIL-COMP-89, 103-108, 1989.
- [47] Singh, J. P. and Dey, S.S., "Variational finite difference approach to buckling of plates of variable stiffness"., Comput. & Stuct., Vol. 36, No. 1, 39-45, 1990.
- [48] Jaswon, M.A., and Maiti, M., "An integral formulation of plate bending problems", J. Engg. Math. 2, 83-93, 1968.
- [49] Stern, M., "Boundary integral equations for bending of thin plates". Progress in Boundary Elements Methods, Vol. 2, ed. C.A. Brebbia, Pentech Press, London; Springer-Verlag, New York, 158-181, 1983.
- [50] Danson, D.J., "Plate bending analysis using boundary element method". Technical Report, Computational Mechanics Center, Southampton, England, 1981.
- [51] Kamiya, N., and Sawaki, I., "Finite deflection of plates", Topics in Boundary Element Research-1, ed. C.A. Brebbia, Springer Verlag 204-224, 1984
- [52] Tottenham, H., "The boundary element method for plates and shells", Developments in Boundary Element Methods-1, eds. P.K. Banerjee and R. Butterfield, Applied Science Publishers 173-205, 1979.

- [53] Hartmann, F., Zotemantel, R., "The direct boundary element method in plate bending". *Int. J. Number. Methods Engg.* 23, 2049-2069, 1986.
- [54] Katsikadelis, J. and Armenakas, A., "A new boundary element solution to the plate problem". *J. Appl. Mech.*, 56, 364-374, 1989.
- [55] Ohga, M., Shigematsu, T. and Hara, T., "Structural analysis by a combined boundary element- transfer matrix method". *Comput. & Struct.* 24, 385-389, 1986.
- [56] Ohga, M. and Shigematsu, T., "Bending analysis of Plates with variable thickness by Boundary Element-Transfer Matrix method. *Comput. & Struct.* 28, No. 5 635-640 , 1988.
- [57] Sapountzakis, E. J. and Katsikadelis, J. T., "Analysis of plates with variable thickness by boundary element method". *J. Engg. Mech.* 117, No. 6 1241-1256, June, 1991.
- [58] Jianqiao Ye, " Large deflection analysis of axi-symmetric circular plates with variable thickness by the boundary element method"., *Appl. Math. Modeling*, Vol. 15, 325-328, June, 1991.
- [59] Cheung, M. S. and Wenchang Li, "Finite strip method combined with other numerical methods for the analysis of plates". *Comput. & Struct.* 45, No. 1 1-7, 1992.
- [60] Anant R. Kukreti, Jaleddin Farsa and Charles W. Bert, " Fundamental frequency of tapered plates by differential quadrature ", *J. Engg. Mech.* Vol. 118, No. 6, 1221-1238, June, 1992.
- [61] Shahab, A. A. S., " Finite element analysis for the vibration of variable thickness discs"., *Journal of Sound and Vibration* , Vol. 162, No. 1, 67-88, 1993.
- [62] Brebbia, C.A., *The boundary element method for engineers*, Pentech press,London, 1978.
- [63] Beskos, D. E., "Boundary Element Method in Structural Analysis" , ASCE, 1989.
- [64] Walker, "Approximate fundamental solutions and alternative formulations". *Boundary element methods*, Proc. Third international seminar, Irvine, California, July 1981, PP. 472-488.
- [65] Brebbia, C.A. and Dominguez, J., "Boundary elements an introductory course". *Computational mechanics publications*, Southampton, 1989, pp.-267-269.

[66] ICES-STRUDL, V3M1, 1977.

Vitae

Name : Mohammad Shebder Khan

Date of Birth : 20th September 1969

Education :

Higher Secondary : Obtained Intermediate Degree from Govt.
Pindiprolu Jr. College, Khammam, 1987

University : Obtained B. E in Civil Engineering from
Osmania University, India, 1991

: Obtained M. S in Structural Engineering
from KFUPM, Dhahran, KSA, 1995

Permanent Address : H. No. 8-1-120,
B. K. Bazaar, Bus Stand Road,
Khammam, A.P - INDIA - 507 001